

Sara Miguel Silva

**Action Mechanisms of Deflamin in
the Treatment of Colorectal Cancer**



UAlg

UNIVERSIDADE DO ALGARVE

DEPARTAMENTO DE CIÊNCIAS BIOMÉDICAS E MEDICINA

Oncobiology Master Thesis

Faro, 2021

Sara Miguel Silva

**Action Mechanisms of Deflamin in
the Treatment of Colorectal Cancer**

Master in Oncobiology - Molecular Mechanisms of Cancer

This work was done under the supervision of:

Marta Martins, PhD

Álvaro Tavares, PhD



UAlg

UNIVERSIDADE DO ALGARVE

DEPARTAMENTO DE CIÊNCIAS BIOMÉDICAS E MEDICINA

Oncobiology Master Thesis

Faro, 2021

Título:

“Action Mechanisms of Deflamin in the Treatment of Colorectal Cancer”

Declaração de autoria do trabalho

Declaro ser a autora deste trabalho, que é original e inédito. Autores e trabalhos consultados estão devidamente citados no texto e constam da listagem de referências incluída.

“I declare that I am the author of this work, that is original and unpublished. Authors and works consulted are properly cited in the text and included in the list of references.”

(Sara Miguel Silva)

Copyright © 2021 Sara Miguel Jesus da Silva

A Universidade do Algarve reserva para si o direito, em conformidade com o disposto no Código do Direito de Autor e dos Direitos Conexos, de arquivar, reproduzir e publicar a obra, independentemente do meio utilizado, bem como de a divulgar através de repositórios científicos e de admitir a sua cópia e distribuição para fins meramente educacionais ou de investigação e não comerciais, conquanto seja dado o devido crédito ao autor e editor respetivos.

Agradecimentos

Esta dissertação é fruto de um trabalho árduo e no qual tenho muito orgulho, mas que não teria sido possível sem o apoio incondicional de algumas pessoas, que merecem o meu mais sincero agradecimento.

Em primeiro lugar gostaria de agradecer à minha orientadora, Dra. Marta Martins, por todo o apoio e conhecimento que me transmitiu ao longo deste ano. Obrigada por todo o tempo que me dedicaste, presencialmente ou *online*, por todo o tempo de bancada que nos foi possível, pelos conselhos e amizade e, acima de tudo, pela confiança depositada em mim. À Dra. Ana Cavaco. Ana, obrigada por todos os momentos que passámos juntas, pelo afeto, apoio e acompanhamento, tanto no laboratório como fora. Ensinaste-me tudo o que necessitei com o maior rigor e precisão possível, sem nunca nos faltar uma boa gargalhada e um sorriso. Um obrigado, também muito especial, a todos os meus professores de mestrado, na Universidade do Algarve, por todo o conhecimento e ensinamentos transmitidos.

Em segundo lugar, um agradecimento enorme a todos os meus amigos: malta, sem vocês não tinha conseguido. Obrigada ao meu *Squad*, que me encorajou quando eu não tinha forças e que sempre acreditou no meu potencial. Às minhas *migas4ever*, por todos os desabafos que partilhámos nesta aventura coletiva: o que Évora uniu, ninguém separa. À Catarina Sapata, que me apoiou sempre e todos os dias, sem falhar, atendendo as minhas chamadas às duas da manhã. Às minhas colegas do Algarve, Alexandra e Alene, que apesar de longe sempre me apoiaram ao longo de todo o processo.

Gostaria também de agradecer à minha colega de casa, Marta, que me deu ombro, abraço e conforto: a espanhola mais portuguesa que já conheci e que nunca me deixou desistir. Amei morar e conhecer Lisboa contigo. Ao Miguel, que passou todos os dias comigo no laboratório e com quem pude privar sem medos. Obrigada por todo o teu apoio, ajuda e conhecimento. Ao meu namorado, Gonçalo Adrião: obrigada por estares sempre cá para mim, por toda a paciência que demonstras e por apoiares todas as minhas decisões, fazendo-me sempre ver do que sou capaz, não só ao longo deste ano, mas desde sempre. És imprescindível.

Por fim, agradecer àqueles sem os quais me teria sido impossível chegar aqui: os meus pais. Obrigada por todas as oportunidades fantásticas que me dão e por todo o apoio em alcançar os meus sonhos. Ao meu irmão, que mesmo longe e com poucas palavras, soube sempre como me confortar. Finalmente, à Paula, a irmã mais velha que sempre quis, obrigada por toda a paciência e apoio em todas as minhas escolhas.

Abstract

CRC is the third most common cancer in the world and the second leading cause of death worldwide, being its mortality associated with the dissemination to distant organs. For cancer to become invasive and metastatic it is necessary that a remodeling of the extracellular matrix occurs being the matrix metalloproteases (MMPs) the main molecules involved in this process. Since MMPs have major implications for migratory and angiogenic processes, promoting greater tumor malignancy, they are strong candidates to targeted therapies in order to delay malignant progression.

Deflamin is a 17 kDa oligomeric protein extracted from the white lupine seeds (*Lupinus albus*) with anti-inflammatory and MMP-2 and 9 inhibitory functions. Deflamin has been shown to induce an improvement of the colonic mucosa and inhibit the migratory activity in CRC cell lines. In *in vivo* studies previously developed in our lab, deflamin was shown to exert an anti-tumor and pro-apoptotic activity. In this context, my work aimed to clarify the mechanism of deflamin action using 3D and *in vivo* zebrafish xenotransplant models.

Overall, my results demonstrate that deflamin has an inhibitory role of the tumoral invasive process without significantly affecting proliferation of CRC cell lines. Regarding *in vivo* analysis, I found a trend towards less vessel infiltration in deflamin treated groups. Deflamin has also shown to be effective in reducing collagen degradation in the tumor microenvironment of zebrafish treated animals, indicating less extracellular matrix remodeling.

These results agree with results obtained previously in CRC lines and *in vivo* assays. Therefore, increasing our knowledge on the role of deflamin for CRC development has the potential to reveal a new nutritional therapeutic approach, with major implications for the health and well-being of CRC patients.

Keywords : Deflamin, matrix metalloproteinases, zebrafish, 3D spheroids

Resumo

O cancro colorretal (CRC) é a terceira neoplasia maligna mais comumente diagnosticada e a segunda causa de morte por cancro a nível mundial. O prognóstico dos pacientes é essencialmente estimado com base no estadio no qual a doença é detetada, sendo que em estadios iniciais a taxa de sobrevivência pode chegar até 90% e em estadios metastáticos apenas a 12%. Neste sentido, a mortalidade por CRC está amplamente associada à sua disseminação a órgãos distantes.

O CRC resulta de uma acumulação progressiva de alterações genéticas e epigenéticas em oncogenes e/ou genes supressores tumorais. Deste modo, e devido à elevada taxa mutacional, o epitélio normal transforma-se numa mucosa hiper-proliferativa e, subsequentemente, dá origem a um adenoma benigno que evolui para carcinoma e posteriormente metástase. Para que o cancro se torne invasivo e metastático, é necessário que ocorra, dentro dos principais mecanismos, uma reconfiguração da matriz extracelular por degradação dos seus substratos, sendo a principal molécula com ação degradadora da matriz as metaloproteases de matriz (MMPs).

As MMPs compreendem uma grande família de endopeptídasas capazes de degradar praticamente todos os componentes presentes na matriz extracelular, desempenhando um papel crucial na manutenção da homeostasia da matriz, bem como para o crescimento tumoral, invasão e metástase. Estas enzimas proteolíticas estão amplamente associadas com o desenvolvimento invasivo e metastático do CRC, sendo que a sua atividade é crucial para a remodelação do microambiente tumoral. Consequentemente, apresentam grandes implicações nos processos inflamatórios, migratórios e angiogénicos, promovendo uma maior malignidade do tumor, associada, por sua vez, a um pior prognóstico e a uma pior taxa de sobrevivência. Assim, devida a sua importância na progressão tumoral, as MMPs são fortes candidatas a estratégias terapêuticas voltadas para a sua inibição na tentativa de alcançar retardamento da progressão maligna, ou até mesmo para a prevenção do desenvolvimento displásico.

Estas estratégias terapêuticas de inibição da atividade das MMPs têm sido estudadas desde o início dos anos 90, com um grande investimento da indústria farmacêutica. A doxiciclina é, por enquanto, a única molécula sintética aprovada no mercado com propriedades inibidoras das MMPs. Atualmente a medicina tem permitido uma abordagem diferente para doenças inflamatórias que, ou não respondem ao tratamento tradicional, ou para doentes que não querem receber a terapia padrão. Neste sentido existem estudos que apontam que o uso de moléculas exógenas naturais é uma abordagem terapêutica a ser considerada. Vários estudos relativos a polipéptidos bioativos provenientes de leguminosas têm revelado ação anti-inflamatória, anti-migratória e ainda ação inibitória de MMPs, sendo considerados uma estratégia tanto na prevenção como na progressão de CRC.

Apesar de estudos sobre o tremço branco ainda serem insuficientes e limitados em testes clínicos e laboratoriais, a literatura disponível demonstra que fatores nutricionais do tremço, como Pis (inibidores de proteases), têm apresentado resultados quando se trata de doenças intestinais inflamatórias e no cancro colorretal. Análises utilizando apenas extratos proteicos demonstram que são capazes de diminuir significativamente a atividade enzimática da MMP-9, proliferação e migração em linhas de células de CRC (HT29).

A deflamina é uma proteína oligomérica de 17kDa, considerada inibidora de metaloproteases (MMPI), encontrada nas sementes de tremço branco (*Lupinus albus*) com um grande potencial anti-inflamatório e de ação inibitória tanto da MMP-9 como da MMP-2. Foi demonstrado que é capaz de induzir uma melhoria do perfil da mucosa colónica em processos de colites ulcerativas e, mais recentemente, promover a inibição da atividade migratória em linhas celulares de cancro colorretal, bem como inibição da atividade gelanólítica da MMP-2 e MMP-9. Em estudos *in vivo* desenvolvidos no nosso laboratório, a deflamina exerceu também uma atividade anti-tumoral e pró-apoptótica, diminuindo o tamanho de tumores xenotransplantados em modelos de *zebrafish* e aumentando a taxa apoptótica dos mesmos sem afetar a divisão celular. Neste sentido este trabalho teve como principal objetivo verificar a atividade da deflamina sobre linhas celulares de CRC, recorrendo a modelos celulares 3D, com o intuito de perceber se a sua atividade era replicável. Do mesmo modo, verificou-se a sua atividade anti tumoral em modelos *in vivo* com peixe-zebra (*Danio rerio*) através da análise de processos angiogénicos e de degradação da matriz extracelular.

Os resultados obtidos neste trabalho demonstram que a deflamina não exerce uma ação direta no ciclo celular nem induz apoptose em linhas de CRC tratadas com este agente, sugerindo assim a sua segurança como potencial estratégia terapêutica contra o CRC. Para as análises *in vitro* com modelos 3D de esferoides, a deflamina apresentou uma atividade inibitória do processo invasivo em matriz de colagénio para as linhas celulares HT29, HCT116 e SW480 ($p=0,0464$; $p=0,0482$ e $p=0,0130$, respetivamente), apesar de não ter afetado significativamente a proliferação celular das linhas HCT116 e SW480 ($p=0,8571$ e $p=0,1850$, respetivamente), o que reforça a sua atividade inibitória de invasão, previamente descrita em culturas celulares 2D.

Relativamente às análises com modelos *in vivo* em modelos de peixe-zebra, apesar da deflamina não afetar a formação de novos vasos sanguíneos, existe uma tendência observada para uma menor infiltração de vasos sanguíneos no centro da massa tumoral em peixes do grupo tratado ($100\mu\text{g/mL}$) quando comparados com o grupo controlo ($p=0,1093$). Além desta tendência, a deflamina mostrou-se eficaz na redução de degradação de colagénio no nicho tumoral em indivíduos tratados em relação aos controlos ($p=0,0168$), indicando assim uma menor remodelação da matriz extracelular.

Os nossos resultados mostraram-se de acordo com resultados obtidos anteriormente por o grupo de investigadores do ISA, bem como por experiências anteriores desenvolvidas pelo grupo LCosta do IMM. Deste modo, esta dissertação complementa os estudos previamente elaborados e explora mecanisticamente a ação que a deflamina exerce sobre o desenvolvimento e progressão de CRC.

Em estudos futuros, seria interessante investigar o papel que a deflamina exerce na atividade de metaloproteases, nomeadamente da MMP-9, em ensaios com modelos celulares 3D, bem como em ensaios *in vivo*. É também de extrema importância investigar os efeitos relativos à cito- e genotoxicidade da deflamina. Por atuar *in situ* e, aparentemente, não ser absorvida no sistema digestivo, a deflamina potencialmente contorna a maioria dos problemas relacionados aos MMPIs apresentados anteriormente em ensaios clínicos, associados a alta toxicidade e efeitos secundários sistémicos.

Aprofundar os conhecimentos já existentes sobre o papel desta proteína poderia revelar uma nova abordagem terapêutica nutricional, com importantes implicações para a saúde e o bem-estar dos pacientes com CRC. Além disso, foi proposto um enriquecimento nutricional de alimentos com deflamina, o que poderia ser uma estratégia para prevenir as doenças intestinais inflamatórias associadas ao cancro colorretal.

Palavras-chave: Deflamina, metaloproteases de matriz, peixe-zebra, esferoides 3D

Abbreviations

AKT	Protein kinase B
APC	Adenomatous Polyposis Coli tumor suppressor gene
BBIs	Bowman–Birk inhibitors
bFGF	Basic fibroblast growth factor
BSA	Bovine Serum Albumin
CAC	Carcinoma associated with colitis
CD	Crohn's disease
CHP	Collagen hybridizing peptide
CIMP	CpG island methylator phenotype
CIN	Chromosomal instability
CO ₂	Carbon dioxide
CRC	Colorectal cancer
CSRAs	Chemotherapy sensitive and resistant assays
DMEM	Dulbecco's modified eagle's medium
DMSO	Dimethyl sulfoxide
DNA	Desoxyribonucleic acid
ECM	Extracellular matrix
EDTA	Ethylenediaminetetraacetic acid
eGFP	Enhanced green fluorescent protein

EMT	Epithelial-mesenchymal-transition
ERK	Extracellular regulated kinase
FAP	Familial adenomatous polyposis
FBS	Fetal bovine serum
FGF	Fibroblast growth factor
GFP	Green fluorescent protein
h	Hours
HDI	Human development index
HGD	High-grade dysplasia
HIF-1	Hypoxia inducible factor-1
HIF-2	Hypoxia inducible factor-2
HNPCC	Hereditary non-polyposis colorectal cancer (Lynch Syndrome)
hpf	Hours post fertilization
hpi	Hours post injection
IBD	Inflammatory bowel diseases
IF	Intensity of eGFP fluorescence
iMM	Instituto de Medicina Molecular João Lobo Antunes
JPS	Juvenile polyposis syndrome
kDa	Kilodalton
KIs	Kunitz inhibitors

LGD	Low-grade dysplasia
LOH	Loss of heterozygosity
MAP	MUTYH-associated polyposis
MAPK	Mitogen activated protein kinase
MetOH	Methanol
MMPs	Matrix metalloproteinases
MMPI	Matrix metalloproteinase inhibitor
MMR	DNA mismatch repair
MLH1	mutL homolog 1 gene
mPDXs	Mouse patient-derived xenografts
MSI	Microsatellite instability
MSI-H	High microsatellite instability
MSS	Microsatellite stability
NaOH	Sodium hydroxide
P-AKT	Activated Protein kinase B
PBS	Phosphate-buffered saline
PDGF	Platelet-derived growth factor
PDXs	Patient-derived xenografts
Pen-strep	Penicillin-streptomycin
P-ERK	Activated extracellular regulated kinase

PHTS	Hamartoma tumor syndrome PTEN
PI3K	Phosphatidylinositol 3-kinase
PIs	Protease inhibitors
PJS	Peutz-Jeghers syndrome
PLAUR	Urokinase plasminogen activator surface receptor
proMMP	Latent matrix metalloproteinases
PTEN	Phosphatase and tensin homolog
PVS	Perivitelline space
RB	Retinoblastoma protein
ROS	Reactive oxygen species
RT	Room Temperature
SDS-PAGE	Sodium dodecyl sulfate polyacrylamide gel electrophoresis
SEM	Standard error of the means
TBS	Tris-buffered saline
TGF- α	Transforming growth factor-alfa
TGF- β	Transforming growth factor-beta
THBS1	Thrombospondin 1 gene
TIMPs	Tissue inhibitors of MMPs
TP53	Tumor protein 53 gene
TSG	Tumor suppressor genes

TSP-1	Thrombospondin-1
UC	Ulcerative colitis
VD	Vessel density
VEGF	Vascular endothelial growth factor
VEGF-A	Vascular endothelial growth factor-A
VI	Vessel infiltration
zPDXs	Zebrafish patient-derived xenografts

Index

Agradecimientos.....	v
Abstract.....	vii
Resumo.....	ix
Abbreviations	xiii
Index of figures.....	xxii
Index of tables.....	xxiv
1. Introduction	1
1.1. Incidence and epidemiology.....	1
1.2. Pathogenesis of CRC	3
1.3. CRC risk factors	4
1.4. Types of colorectal cancer.....	5
1.4.1. Sporadic CRC.....	5
1.4.2. Familial CRC.....	6
1.4.3. Hereditary CRC.....	7
1.4.4. Colorectal cancer associated with inflammatory bowel diseases (IBDs)	8
1.5. Tumor microenvironment (TME).....	9
1.6. Degradation of the extracellular matrix (ECM) in the development of CRC ...	12
1.7. Matrix metalloproteinases (MMPs).....	15
1.7.1. MMPs families.....	17
1.7.2. Gelatinases.....	17
1.7.3. Expression and inhibition of MMPs in CRC	19

1.8. Legumes as potential anti-cancer therapy	22
1.8.1. Deflamin, a therapeutical strategy against CRC	24
1.9. Use of <i>in vitro</i> 3D models	27
1.10. Zebrafish: a promising animal model	29
2. Objectives	35
3. Materials and methods	37
3.1. Biological materials	37
3.1.1. Vegetable protein extract	37
3.1.2. CCR human cell lines	37
3.1.3. <i>In-vivo</i> model	38
3.1.4. CHP preparation	39
3.2. Methods	39
3.2.1. Cell Culture	39
3.2.2. Western-Blot	40
3.2.3. Cellular apoptosis assay	42
3.2.4. Cellular viability assay	43
3.2.5. Viral infection of cell lines	44
3.2.6. Analysis of inhibitory activity of deflamin <i>in-vitro</i>	45
3.2.7. Analysis of deflamin activity <i>in-vivo</i>	48
3.3. Statistical analysis	52
4. Results and discussion	53
4.1. Analysis of deflamin activity in 2D cell culture systems	53
4.1.1. Cellular viability	53

4.1.2.	Cellular apoptosis	55
4.1.3.	Epithelial to mesenchymal transition.....	57
4.1.4.	Signaling Pathways.....	59
4.2.	Inhibitory activity of deflamin in <i>in-vitro</i> 3D models	60
4.2.1.	Spheroid proliferation in different CRC cell lines	61
4.2.2.	Spheroid invasion in different CRC cell lines	66
4.3.	Anti-tumoral activity of deflamin <i>in-vivo</i>	72
4.3.1.	Angiogenesis analysis in transgenic zebrafish model Tg(kdrl: eGFP)	74
4.3.2.	Degraded collagen analysis in wild-type zebrafish model.....	78
5.	Conclusion and future perspectives.....	82
6.	References.....	85

Index of figures

Figure 1.1: Worldwide cancer incidence and mortality in 2020	1
Figure 1.2: Incidence and mortality of cancer in Portugal, 2020.....	2
Figure 1.3: Malignant progression of CRC.....	4
Figure 1.4: Degradation of the extracellular matrix (ECM)	13
Figure 1.5: Structure of MMPs.....	16
Figure 1.6: Targets of MMP-2 and MMP-9 in the extracellular environment.....	18
Figure 1.7: Preventive and therapeutic potential of bioactive peptides from legumes as anti-cancer agents.....	23
Figure 1.8: Scheme of diverse 3D cell culture strategies.....	28
Figure 1.9: Experimental setup for generating zebrafish xenografts	32
Figure 3.1: Cleavage of the non-fluorescent Caspase Substrate by Caspase-3/7 to create the fluorescent Rhodamine 110..	43
Figure 3.2: AlamarBlue Assay Flow.	44
Figure 4.1: Analysis of cellular viability in the presence of three different concentrations of deflamin in CRC cell lines.	54
Figure 4.2: Analysis of caspases 3/7 activity in the presence of three different concentrations of deflamin in CRC cell lines.	56
Figure 4.3: Western-blot analysis.	57
Figure 4.4: Western-blot analysis.	59
Figure 4.5: Effects of deflamin on 3D cellular proliferation in human colorectal cancer HT29 cell line.....	62
Figure 4.6: Effects of deflamin on 3D cellular proliferation in human colorectal cancer HCT116 cell line.....	63
Figure 4.7: Effects of deflamin on 3D cellular proliferation in human colorectal cancer SW480 cell line.....	64
Figure 4.8: Effects of deflamin on 3D cellular invasion in human colorectal cancer HT29 cell line.	67

Figure 4.9: Effects of deflamin on 3D cellular invasion in human colorectal cancer HCT116 cell line.....	68
Figure 4.10: Effects of deflamin on 3D cellular invasion in human colorectal cancer SW480 cell line.....	69
Figure 4.11: Experimental setup for generating zebrafish xenografts and posterior analysis.....	73
Figure 4.12: Zebrafish vasculature analysis in HCT116 xenografts.....	74
Figure 4.13: Angiogenesis quantification in zebrafish HCT116 xenografts.....	75
Figure 4.14: Zebrafish CHP analysis in HCT116 xenografts.....	79
Figure 4.15: Degraded collagen quantification in zebrafish HCT116 xenografts.	80

Index of tables

Table 1: List of cell lines used.....	38
Table 2:List of primary antibodies used in Western Blot.....	42
Table 3: Example of spheroid formation solution for both invasion and proliferation spheroids, for any of the three cell lines	45
Table 4: Example of spheroid solution for invasion assay.....	46
Table 5: Glycine buffer preparation.....	49
Table 6: Blocking buffer preparation.....	50

1. Introduction

1.1. Incidence and epidemiology

Colorectal cancer (CRC) is the third neoplasia most commonly diagnosed and the second cause of death worldwide, being responsible for about 1.9 million new cases (10%) and approximately 940.000 deaths (9.4%) in 2020 (figure 1.1), according to globocan^[1]. In Europe is the second cancer with highest incidence (519.820, 11.8%) as well as the second cause of cancer-related mortality (244.824), considering both sexes^[1].

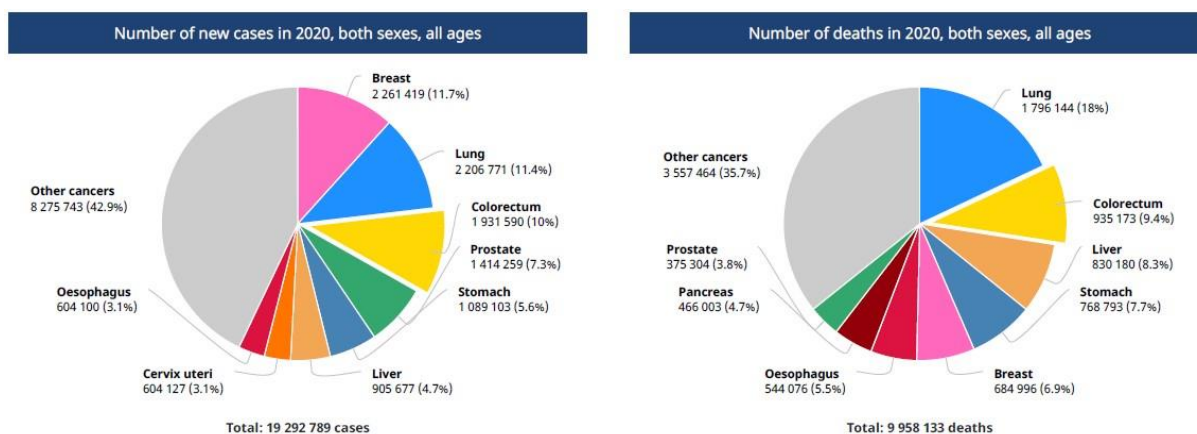
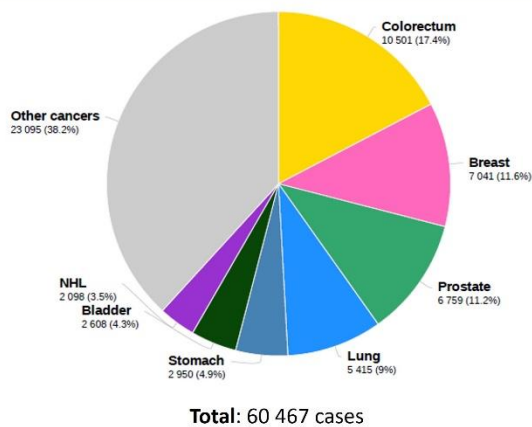


Figure 1.1: Worldwide cancer incidence and mortality in 2020. Retrieved from *Globocan*^[1]

In Portugal, statistics show that CRC appears as the most incident cancer (10.501, 17.4%) and the second with greatest mortality (4.320, 14.3%) (figure 1.2)^[1]. However, analyzing the feminine and masculine populations separately, CRC appears as second in incidence (4.083, 15.3% and 6.418, 19%, respectively) and mortality (1.759, 14,7% and 2.561, 14.1%, respectively), preceding breast and prostate cancer, respectively^[1].

The mortality and incidence rates relative to CRC may vary up to ten times worldwide^[2]. Studies show that in the last decades both rates are increasing rapidly in medium to low Human Development Index (HDI) countries, particularly in Eastern Europe, Asia and South America^[2,3]. In contrast, rates have stabilized or decreased in several countries with high HDI, due to improvements in perioperative care, as well as chemotherapy and radiotherapy^[2].

Estimated number of new cases in 2020, Portugal, both sexes, all ages



Estimated number of deaths in 2020, Portugal, both sexes, all ages

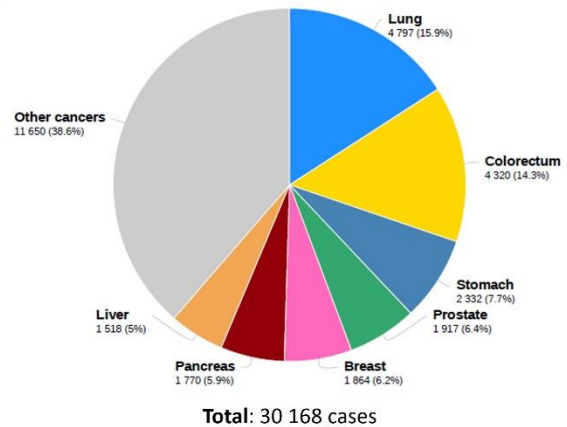


Figure 1.2: Incidence and mortality of cancer in Portugal, 2020. Retrieved from *Globocan*^[1]

Long term incidence rate has been shown to reduce in countries with a high HDI due to the removal of adenomatous polyps (CRC precursor lesions) through colonoscopies ^[2,4], as well as easy access to diagnostic tests and methods. Although 60% of deaths occur in countries with a high HDI, these have a stable or decreasing mortality rates when compared to countries with medium to low HDI, as they are characterized by better accessibility to screening services, especially endoscopic, early detection of injuries and specialized care ^[5].

Due to these large fluctuations in incidence and mortality rates between different countries, CRC is considered to be one of the best markers for a country's social and economic development, replacing infections-related cancers in countries undergoing rapid social and economic changes ^[2]. As the incidence varies according to the different regions, cancer development may be due to variations in the genetic heritage of different populations, vitamin D intake, local eating habits, among others ^[6].

The CRC represents 13% of all malignant tumors, presenting itself as the most common of the gastrointestinal tract ^[7]. The five-year survival rate of patients with CRC is highly variable, ranging from 65% in the United States, 55% in developed countries, 14% in Africa and 39% in developing countries ^[8]. However, these rates are significantly different when considering the tumor stage, ranging from 92% for stage I and 12% for stage IV ^[7,8]. Of the patients diagnosed with colorectal cancer, 90% are over 50 years old ^[3,7]. However, this pathology when diagnosed in younger patients is frequently more aggressive ^[7].

Although many factors have been proposed as prognostic in CRC, the stage of the tumor still plays a key role in assessing the clinical outcome, representing the operational basis for choosing the most appropriate therapy and for evaluating the effectiveness of different therapeutic methods by comparing the expected survival rates ^[9]. Thus, the prognosis of CRC is based on the classification Tumor, Nodules and Metastases, also known as TNM, to which are added other clinical and pathological factors, such as degree of differentiation, level of tumor invasion, number of lymph nodes involved in the tumor microenvironment, between others ^[9]. However, despite the great prognostic power based on these parameters, patients with a similar clinical profile and who are in the same stage, may have a different evolution, resulting in different clinical conditions ^[10].

1.2. Pathogenesis of CRC

The pathogenesis of CRC results from a complex process composed of multiple stages that progress from a neoplastic transformation of normal cells, invasion of tissue, intra and vascular leakage and, finally, metastasis in distant organs ^[10,11]. This progression implies a reprogramming of the cells with the potential to reverse their differentiation ^[10]. Thus, associated with a high degree of differentiation, there is a better prognosis ^[10]. This high degree of differentiation means that the neoplasm is morphologically similar to the native organ, while when little differentiated cells gradually lose their capacity for structural organization and begin to show less cohesion and all resemblance to the initial organ is lost ^[10,12]. As normal cells evolve progressively to a neoplastic state, they acquire a succession of hallmark capabilities ^[13,14], manifesting themselves as alterations in cell physiology that collectively dictate malignant growth ^[14].

During the development of colorectal adenocarcinoma, epithelial cells of the gastrointestinal tract acquire sequential genetic and epigenetic mutations in specific oncogenes and/or tumor suppressor genes (TSG), giving them a selective advantage in proliferation and self-renewal ^[15]. This was the model proposed in 1990 by Fearon and Vogelstein, where mutations occur in the tumor suppressor gene Adenomatous Polyposis Coli (*APC*) and, in later stages, in the *RAS* oncogene and tumor protein 53 gene (*TP53*) ^[16,17]. Due to genomic instability, the normal epithelium turns into a hyperproliferative mucosa and subsequently gives rise to a benign adenoma that progresses to carcinoma and subsequently metastases in approximately 10 years ^[15,16] (figure 1.3).

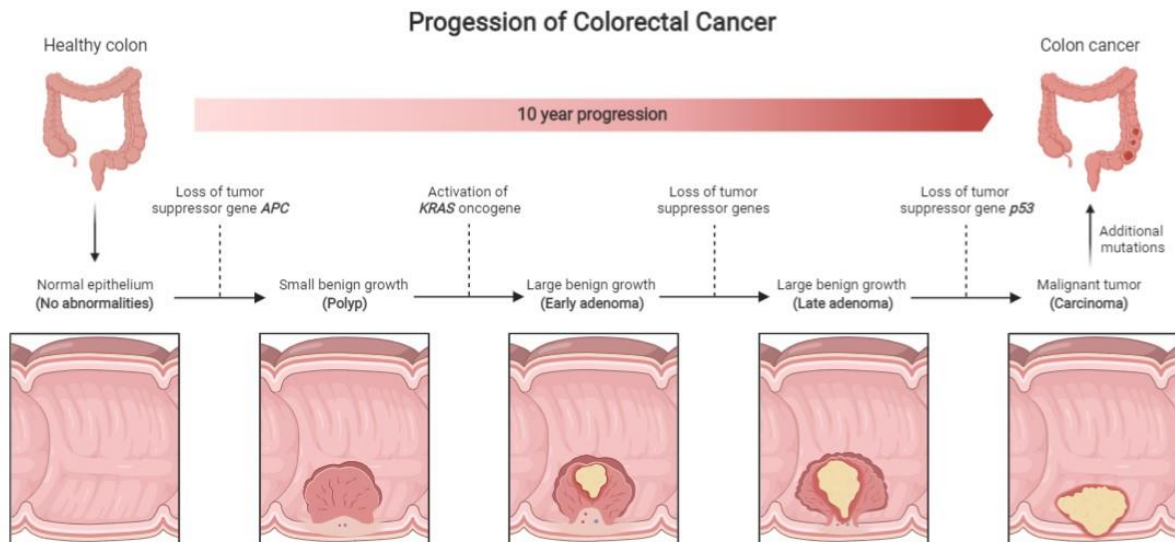


Figure 1.3: Malignant progression of CRC. In this process, the normal epithelium turns into a hyperproliferative mucosa and gives rise to a benign adenoma, also known as polyps. This early adenoma can progress to a carcinoma, where cells start to accumulate more mutations as well as loss of tumor suppressor genes and, subsequently, metastases in approximately 10 years. Adapted from *BioRender*^[133]

1.3. CRC risk factors

The risk of developing CRC is related to two types of factors: modifiable and non-modifiable. Among the modifiable factors are diet, lifestyle, and some socio-cultural factors. It was found that the risk of developing CRC increases after high consumption of meat and animal fats, due to the stimulation of insulin secretion, increased iron absorption and increased fat intake^[3]. There is also an increased risk associated with physical inactivity, as well as smoking and alcohol consumption^[3].

Regarding the non-modifiable risk factors, it can be found: sex, age, inflammatory bowel diseases (IBD), such as Crohn's disease and ulcerative colitis, adenomatous polyps and genetic factors, such as mutations and hereditary genetic syndromes^[3,7,8].

Up to 30% of patients with CRC have a family history of neoplasms, which means that there are probably predisposing germline mutations that have not yet been identified [8,15]. Patients with first-degree relatives who suffer from CRC are 2 to 4 times more at risk [8]. Hereditary CRCs are responsible for 7-10% of all cases and include hereditary colorectal cancer without polyps (HNPCC), adenomatous polyposis (FAP and MAP) and hamartomatous (PJS, JPS, PHTS) syndromes [15].

1.4. Types of colorectal cancer

There are three types of CRC that can be distinguished by different origins and modes of expression: the sporadic CRC, responsible for about 70% of all CRCs; familial CRC, a group of diseases for which no associated gene has been identified, making up to about 10–30% of cases; and hereditary CRC, accounting for 5-7% of cases, with two tumor variants that are distinguished by their predisposition to be related or not to the presence of adenomatous polyps [6,15].

At the molecular level, the various types of CRC can be considered as an heterogeneous group of diseases [15,18]. Loss of genomic integrity facilitates the accumulation of multiple mutations during their development and mechanisms such as chromosomal instability (CIN), methylation phenotypes in CpG islands (CIMP) and microsatellite instability (MSI), are involved in the transformation of colorectal epithelial cells, playing a significant role in tumor carcinogenesis [15,16,18].

1.4.1. Sporadic CRC

Sporadic CRCs occur in patients aged between 70-75 years, due to the accumulation of mutations in TSG and oncogenes, with approximately 70% beginning in the distal colon, with no previous existence of a significant family history or IBD [16,19,20]. There are three main genetic mechanisms responsible for sporadic CRC, namely chromosomal instability (CIN), microsatellite instability (MSI) and the methylation phenotype in CpG islands (CIMP) [20].

Most of these tumors develop along the CIN pathway, characterized by the accumulation of numerical or structural chromosomal abnormalities, resulting in aneuploid karyotypes, frequent loss of heterozygosity (LOH) in the TSG *loci* and chromosomal rearrangements [16,20].

Another important pathway is the MSI pathway, found in 15% of sporadic CRCs, caused by the dysfunction of MMR genes in DNA [20]. Tumors that have cells with an abnormal function of the MMR genes tend to accumulate mutations (insertions or deletions) in microsatellites located in DNA coding regions, generating frameshift mutations [16,20]. The deficiency in MMR genes is mainly due to the silencing of the genes, especially the *MLH1* gene (mutL homolog 1) (> 80% of cases), by hypermethylation of the promoter [16,20].

The third pathway, designated as CIMP, is characterized by methylation in CpG islands, with a gradual pattern of activation of oncogenes, such as *KRAS* and *c-MYC*, and inactivation of TSGs, such as the loss of the *APC* gene and *TP53* [16,20]. Approximately 30% to 40% of sporadic proximal CRCs are CIMP-positive [16,20]. In many cases, sporadic CRCs have high instability of microsatellites (MSI-H) due to methylation of the *MLH1* promoter, although more than 50% are CIMP microsatellites stable (MSS) [16]. CIMP-positive tumors based on the classic model can be divided into two types, namely, CIMP-high, related to *BRAF* mutations and *MLH1* methylation, and CIMP-low, related to *KRAS* and MSS mutations [16].

1.4.2. Familial CRC

Non-syndromic or familial CRC is a heterogeneous condition that includes patients with unrecognized hereditary syndromes and patients with apparently sporadic forms that aggregate into the families, accounting for nearly one third of CRC cases [21]. In these patients, the molecular mechanism has not yet been established, but it probably results from a combination of environmental and hereditary genetic factors, such as common genetic alterations of low penetrance [21,22].

There are also several studies that indicate that being first-degree relative with a CRC patient increases the risk of illness up to two to three times, when compared to the risk of the general population [22]. In these persons screening is particularly indicated, especially if the relative has been diagnosed under 50 years of age [22].

The heterogeneous nature of the non-syndromic CRC suggests that the variation in genetic risk is probably a consequence of the co-inheritance of multiple low-penetrance variants, some of which are common in the model proposed by Fearon and Vogelstein [17,21].

1.4.3. Hereditary CRC

Hereditary CRCs is responsible for 7-10% of all cases and can be distinguished by the presence, or not, of adenomatous polyps^[6,8]. Thus, they include hereditary non-polyposis colon cancer (HNPCC), classified as a malignant tumor with high risk for the development of non-digestive cancers; adenomatous polyposis (FAP and MAP) and hamartoma tumor syndromes (PJS, JPS, PHTS), characterized by the presence of multiple polyps in the colon of patients who, in the absence of preventive surgery, can become malignant around 40 years of age^[6,8].

The most common hereditary syndrome is HNPCC, currently known as Lynch syndrome, which accounts for 2–4% of all cases^[8]. Like most inherited syndromes, Lynch syndrome has a dominant pattern of inheritance. Patients exhibit an approximately 20% chance of developing CRC by age 50, and an approximately 50% chance of developing it by age 70^[8].

Familial adenomatous polyposis (FAP) is the second most frequent predisposing syndrome, although it is responsible for less than 1% of cases^[6,8]. FAP patients have thousands of pre-cancerous colorectal polyps growing by age 10–12 years^[8]. As these adenomas grow, the likelihood of carcinogenesis increases to an almost 100% risk of developing CRC at age 40^[6]. Meanwhile, *MUTYH*-associated polyposis (MAP) is less well defined at the clinical level and patients may or may not develop an exorbitant amount of polyps^[6,8]

Finally, conditions of hamartomatous polyps, such as Peutz-Jeghers syndrome (PJS), juvenile polyposis syndrome (JPS) and hamartoma tumor syndrome PTEN (PHTS) are rare and poorly studied but known to follow a progression different from adenomatous polyps^[6,8]. These polyps follow the "landscape effect", where the abnormal changes do not begin in the epithelium, as would be the case with adenomas, but in the slide below, the mucosa, eventually spreading to the epithelium^[6,8].

1.4.4. Colorectal cancer associated with inflammatory bowel diseases (IBDs)

Inflammatory bowel diseases (IBDs) are characterized by inflammation in the colon over long periods of time ^[8]. This inflammation results in the abnormal release of growth cytokines, excess blood flow, free radicals and other factors that predispose to carcinogenesis, making patients with chronic IBDs at an increased risk of developing CRC ^[8].

Crohn's disease (CD) and ulcerative colitis (UC) are chronic inflammatory bowel diseases characterized by recurrent episodes of inflammation of the intestinal mucosa ^[23]. This chronic inflammation of the mucosa has several potential consequences, one of which is the occurrence of colorectal cancer associated with colitis ^[23–25]. More recently, it has also been shown that patients with IBD have an increased risk of developing extraintestinal malignancies, probably as a consequence of immunosuppressive therapies and an underlying inflammatory state ^[26]. There are also some risk factors that have been consistently identified, such as the age of onset of colitis, extent, duration and severity of the disease, inflammatory complications and family history of CRC ^[23–25].

CRC-associated ulcerative colitis is characterized by inflammation and ulcers in the large intestine ^[24]. Although there are some limitations as a prognostic marker, it is hypothesized that it develops from multifocal dysplasia where the inflamed colonic mucosa undergoes molecular changes associated with cancer before there is any histological evidence of dysplasia ^[8,24]. Crohn's disease, also known as an autoimmune and partially hereditary inflammation of the colon, presents with a deeper penetrating inflammation and an absence of intestinal ulcers ^[8].

Thus, the carcinogenesis of CRC in IBDs follows a sequential progression from absence of dysplasia to low-grade dysplasia (LGD) and then high-grade dysplasia (HGD), bridging in invasive CRC ^[25,27]. However, this model is not absolute, and the CRC may appear in patients without a history of dysplasia and in cases that go from LGD to carcinoma ^[25,28].

The genetic abnormalities most commonly identified in carcinoma associated with colitis (CAC), such as chromosomal instability (CIN) and microsatellites (MSI) are also found in CRC, occurring with the same frequency [23,25]. However, there are some differences with regard to the dysplasia-carcinoma sequence of some CAC mutations, activations and inactivation, namely mutations in p53, which can occur earlier in cases of colitis, since these mutations are seen more frequently in dysplasia associated with colitis than among sporadic polyps, reaching an occurrence of 85% [23–25]. Mutations in the *APC* and *KRAS* genes, which are known to occur much earlier in the sporadic CRC adenoma-carcinoma sequence, are seen less frequently when associated with colitis and are believed to appear much later in the dysplasia-carcinoma sequence [24,25]. Changes in *KRAS* appear to keep the NF-κB signaling pathway active, allowing for continued cytokine production, neovascularization and tumor growth [23,24,28,29].

1.5. Tumor microenvironment (TME)

Solid tumors are not defined exclusively by malignant cells and their characteristics. They are complex entities, characterized by the coexistence of cancer cells and their microenvironment, composed of various cell types, including fibroblasts, adipocytes, endothelial cells, bone marrow-derived immune cells, and the extracellular matrix (ECM) [30], as well as vasculature and other matrix-associated molecules [31]. All these components that comprise the tumor microenvironment (TME) and interact with malignant cells have a direct impact in the tumorigenic process.

In CRC, the multistep process from normal colonic epithelium to an adenomatous polyp and ultimately to an invasive colon carcinoma is associated with or supported by the TME [31]. Transformed epithelial cells modulate the functions of stromal cells with the overall purpose of facilitating their own growth, survival, invasion, and metastasis [31,32]. This dependence or “addiction” of the cancer cells to the stromal components opens novel avenues for the development of potential therapeutic agents [31].

Cancer cells have developed multiple functional capabilities, also known as the cancer hallmarks, that allow them to proliferate, survive and disseminate. These functions, such as evading growth suppressors, inducing angiogenesis, resisting cell death, avoiding immune destruction, among others, are acquired in different tumor types via distinct mechanisms and at various times during the course of multistep tumorigenesis ^[13].

A major contributor to the tumor microenvironment is inflammation and inflammatory mediators ^[31]. The recognition of chronic inflammation as the seventh trait acquired by tumor cells necessary for survival, growth, and metastasis has intensified studies on the role of intratumoral inflammatory cells and proinflammatory cytokines in cancer progression ^[31]. Chronic inflammation is now recognized as both a tumor initiator and promoter, and it has been studied in relation to proinflammatory prostaglandins, for example, in colon cancer ^[31].

Colon carcinomas, similar to most other solid tumors, are infiltrated by different cells such as tumor-associated macrophages (TAMs), myeloid derived suppressor cells (MDSCs), mast cells, cancer associated fibroblasts (CAFs), monocytes, neutrophils, CD8 and CD4 T-cells, dendritic cells (DCs), natural killer (NK) cells, endothelial cells, endothelial progenitor cells (EPCs), platelets, and mesenchymal stem cells (MSCs) ^[31,33]. The role of these immune cell types in tumor evolution and growth is diverse and is tightly linked to their inherent functions and to the cytokines they express (e.g., or inhibitory ligands) ^[31,32].

Some immune cells often demonstrate plasticity in the TME, showing both tumor-promoting and tumor-inhibiting potential ^[32]. For example, some macrophages (M1) mainly produce pro-inflammatory cytokines that potentiate the anti-tumor immune response ^[32,34]. By contrast, other immune cells, such as tumor promoting macrophages (M2) can favor fibroblast proliferation, ECM deposition and immunosuppression ^[32,33,35].

Importantly, the total composition of immune cells in the TME is not a binary ‘anti-tumor’ or ‘pro-tumor’ environment, but rather a mixture of all these cell types ^[32]. The overall phenotype is determined by the interactions of the immune cells with each other and with non-immune cells ^[32].

The induction of angiogenesis is an important early event in the development of most cancers and is an integral part of tumor growth and survival ^[31]. Like normal tissues, tumors also require sustenance in the form of nutrients and oxygen to support their growth ^[32]. During tumor progression, an “angiogenic switch” is almost always activated and remains on, causing the grow of new vessels that help to sustain neoplastic growth ^[36].

The well-known examples of angiogenesis inducers and inhibitors are vascular endothelial growth factor-A (VEGF-A, coded by the gene *VEGFA*) and thrombospondin-1 (TSP-1, coded by the *THBS1* gene), respectively ^[14]. The *VEGFA* gene encodes ligands involved in the formation of new blood vessels ^[14]. VEGF ligands can be sequestered in the extracellular matrix in latent forms that are subject to release and activation by extracellular matrix-degrading proteases (e.g., MMP-9) ^[13]. TSP-1, a key counterbalance in the angiogenic switch, also binds transmembrane receptors displayed by endothelial cells and thereby evokes suppressive signals ^[37].

The limited success achieved by only targeting tumor cells highlights the importance of understanding the role of the tumor microenvironment and its precise contribution to carcinogenesis ^[31]. In the past decade, therapeutic development has improved survival rates for patients with metastatic CRC, and many more treatment options exist for advanced disease ^[31,32]. However, the fact that metastatic CRC remains incurable prompts investigators to explore a deeper understanding of the factors underlying cancer progression ^[31,32].

The advancements in understanding the TME have led, in recent years, to the development of efficacious therapies to treat advanced cancer ^[31,32]. In-depth characterization of each of the cellular components in cancer has shed light on the convoluted network of interactions between the numerous components within a tumor mass ^[32]. The treatment of thousands of cancer patients with monoclonal antibodies targeting inhibitory receptors expressed by immune cells (immune checkpoint blockade) has yielded remarkable response rates in several types of solid and hematologic malignancies ^[32]. In this context, the analysis of the TME has become fundamental to predict response to treatment.

1.6. Degradation of the extracellular matrix (ECM) in the development of CRC

In all tissues, the extracellular matrix provides a structural and biochemical framework for cell support and scaffolding, with a range of functions important for regulating both inter- and intra-cellular signaling, and for cellular differentiation, adhesion and invasion ^[11,31,38,39].

The ECM is a complex network of noncellular components, including structural proteins (predominantly collagens), matricellular proteins, glycoproteins, proteoglycans, and polysaccharides ^[11,30,38,39]. These molecules contribute to the deposition and arrangement of ECM and modulate cell-matrix interaction through their distinct biochemical and physical properties ^[30,40].

In addition to its structural function, the ECM is highly dynamic and versatile, being an essential part of the tissue environment, governing crucial aspects of cell biology ^[30,41]. In this context, disruption of the tightly controlled production, degradation and remodeling of the major components, disorganizes the ECM, promoting abnormal cell behavior, tumor-associated angiogenesis and inflammation (figure 1.4), and finally leads to generation and progression of cancer microenvironment ^[30,42]. Remodeling of the ECM is characterized by the increased synthesis and deposition of collagens and upregulation of matrix metalloproteinases (MMPs) ^[11,30]. These enzymes process matrix components, such as collagens, leading to the production and release of bioactive fragments mainly from non-fibrillar collagens ^[30].

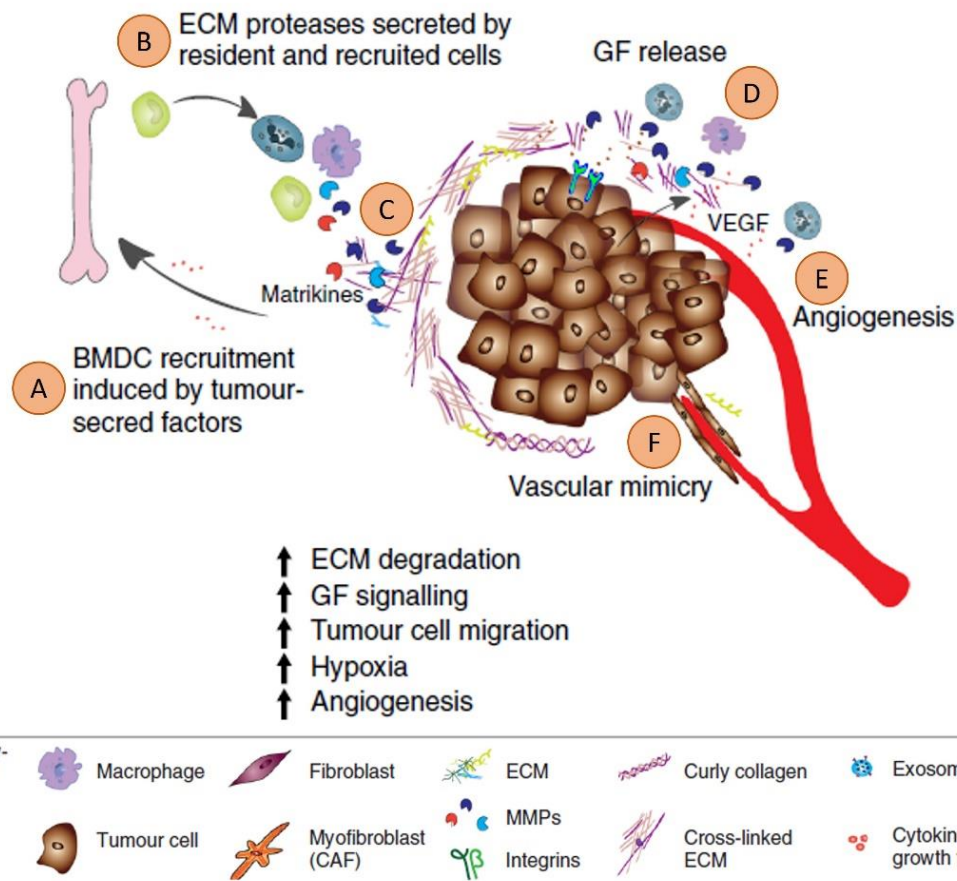


Figure 1.4: Degradation of the extracellular matrix (ECM). (a) To sustain a tumorigenic microenvironment, tumor cells and resident immune cells secrete cytokines, chemokines, and growth factors (GFs), which differentiate and recruit bone marrow-derived cells (BMDCs); (b) The BMDCs, cancer-associated fibroblasts (CAFs) and tumor cells secrete ECM-degrading proteases, including MMPs, which are cell surface-bound (e.g., MT1-MMP) or secreted (e.g., MMP-9); (c) Proteolytic ECM degradation generates bioactive matrikines and (d) releases matrix-bound GFs. These factors induce pro-tumorigenic ECM signaling that promotes tumor proliferation, migration, invasion, and angiogenesis; (e) These combined changes to the ECM create a hypoxic environment. Neutrophils secrete potent MMP-9 that degrades ECM and releases matrix-bound VEGF that forms a concentration gradient for new angiogenic sprouting; (f) Stimulated by dense ECM, the tumor cells may gain endothelial-like functions and mimic the vasculature that connects to blood vessels. Adapted from Winkler, J. et al. (2020)^[134]

MMP-derived changes in the tumor microenvironment typify tumor prognosis, supporting the function of structural remodeling of the ECM in the progression of many cancers, such as colorectal cancer^[30]. MMPs target a wide range of ECM and other extracellular proteins^[30,39]. MMP-3 and -10, for instance, target proteoglycans, fibronectin, and laminin, whereas MMP-8 and -13 selectively target collagen I and II, respectively^[41]. In addition, both MMP-2 and -9 degrade denatured collagen (gelatin)^[41].

In the last decades, an increased interest around the ECM and its potential role in cancer tumorigenesis has arisen^[30,32,42]. The ECM, with its distinctive biochemical and biomechanical properties, is one of the proximal structures that tumor cells of epithelial origin must destroy in order to permit invasion and cell migration^[11,38,42]. The ECM structure and composition became disorganized during cancer progression, promoting itself cellular transformation, and, consequently, metastasis^[42].

Undeniably, the ECM microenvironment, or niche, plays an important role in regulating cell behavior^[41], once several components participate in cancer progression, such as fibroblasts that synthesize growth factors, chemokines, and adhesion molecules, but also inflammatory cells, specially T cells and myeloid suppressor cells, which fail to exercise antitumor effector functions, and co-operate with cancer cells to promote tumor growth^[42,43].

Adding to fibroblasts and inflammatory cells, transforming growth factor-beta (TGF- β) and hypoxia also play a role in the tumor microenvironment and degradation of the ECM via MMP. TGF- β is a pleiotropic factor with several different roles in health and disease^[44]. In cancer, TGF- β plays a paradoxical role, since it represses epithelial tumor development in the early steps of tumorigenesis, while in advanced stages it can stimulate tumor progression, once carcinoma cells acquire resistance to the proliferative inhibition and apoptosis induced by TGF- β ^[44]. TGF- β also regulates MMPs expression in both cancer cells and tumor stroma-associated cells, while in the tumor microenvironment MMPs activate the latent secreted TGF- β , producing a harmful cycle facilitating the enhancement of tumor progression^[44].

In addition, hypoxic cancer cells also show increased proteolytic activity, as a result of increased expression of urokinase plasminogen activator surface receptor (*PLAUR*)^[45]. *PLAUR* promotes cell invasion by altering the interactions between integrins and the ECM^[45]. Therefore, hypoxia is also associated with an increase in the expression of MMP-2 and MMP-9 *in vitro*, via a HIF1-dependent mechanism^[45].

Together, deregulation of ECM dynamics can facilitate cellular dedifferentiation and cancer stem cell expansion ^[41], disrupting tissue polarity and promoting tissue invasion. As a result, epithelial cells are directly affected by deregulated ECM dynamics, leading to cellular transformation and metastasis ^[41].

Nowadays, the recent methodological advances have made possible to isolate and analyze biological healthy and tumoral acellular matrixes with preserved 3D tissue architecture, providing a new tool for a more complex patho-physiological *in vitro* cancer model ^[42]. In conclusion, tumor stroma could appear to be a good candidate target for cancer treatment, since it promotes cancer progression, growth, and aggressiveness ^[42].

1.7. Matrix metalloproteinases (MMPs)

Most cases of colorectal cancer are diagnosed at an advanced stage, when the cancer has metastasized to distant organs and is usually not curable ^[46]. To produce metastases, cancer cells require degradation of extracellular matrix (ECM) and/or basement membrane by protease enzymes ^[46]. Proteins comprising the ECM play critical roles in cell proliferation and migration, and different proteases control different processes ^[11,46]. Among the different proteinases, matrix metalloproteinases (MMPs) seem to be primarily responsible for the degradation of the ECM, being studied extensively as key mediators of ECM degradation and in the processing of other bioactive molecules ^[11,46].

Proteolytic enzymes are major players in the breakdown and reconstitution of ECM in a variety of physiological and pathological processes, such as tissue remodeling, wound repair, inflammatory responses, angiogenesis, destructive diseases, as well as tumor invasion and metastasis ^[47]. The activation and release of proteolytic enzymes has also been related to a variety of non-neoplastic pathological conditions, some of which involve acute as well as chronic inflammation and/or tissue degradation, such as degenerative diseases, asthma or several other infectious disorders ^[47].

The four categories of proteolytic enzymes (cysteine-, serine-, aspartic-, and metalloproteinases) are named and classified according to the essential catalytic component (usually an amino acid) in their active site ^[47].

MMPs comprise a large family of 25 zinc-dependent endopeptidases capable of degrading all components of the ECM, playing a crucial role for tumor growth, invasion and metastasis, being categorized primarily by their structural features as gelatinases, collagenases, membrane-type, stromelysins and matrilysins [11,46–51].

MMPs have a common domain structure including a pro-peptide, a catalytic domain, a hemopexin-like C terminal domain, and a hinge region that links the catalytic site with the hemopexin domain (figure 1.5) [11,48,51,52]. They are synthesized as secreted or membrane-associated inactive zymogens (proMMP) and must be proteolytically processed to an active state [11,46,51]. This processing involves removal of a cysteine residue that interacts with zinc ions from the active site, thereby resulting in MMP activation [11,46,48,52].

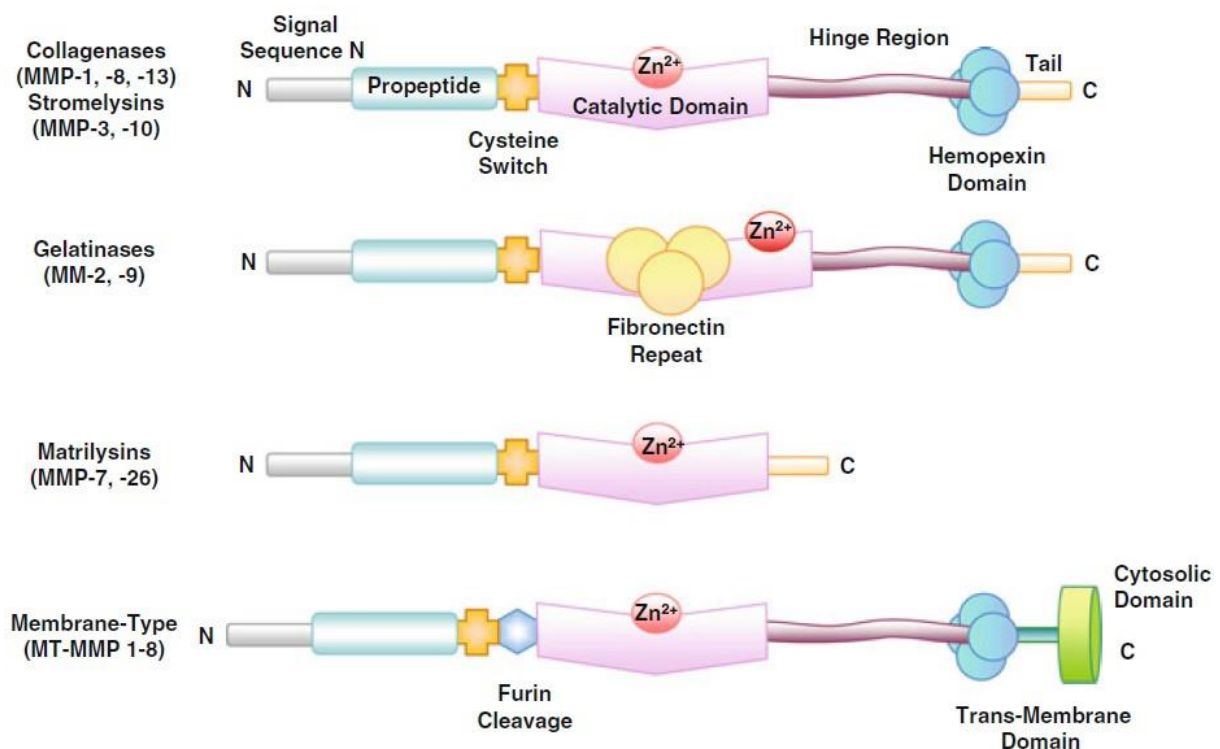


Figure 1.5: Structure of MMPs. Typically, MMPs consist of a propeptide of about 80 amino acids, a catalytic metalloproteinase domain of about 170 amino acids, a linker peptide (hinge region) of variable lengths, and a hemopexin domain of about 200 amino acids. Matrilysins are exceptions as they lack the linker peptide and the hemopexin domain. Membrane-bound MMPs (MT-MMPs) have a furin-like proprotein convertase recognition sequence at the C-terminus of the propeptide. Retrived from Benjamin, M. M., & Khalil, R. A. (2012)^[135]

MMPs are responsible for important physiological processes such as tissue repair, wound healing, hair follicle growth, organogenesis, embryogenesis, ovulation and angiogenesis [49,53]. In this regard, their activity plays a pivotal role in tumor growth and the multistep processes of invasion and metastasis, including proteolytic degradation of ECM, alteration of the cell–cell and cell–ECM interactions, migration and angiogenesis [49,53,54].

1.7.1. MMPs families

MMPs can degrade the majority and minority components of the extracellular matrix [48]. With a few exceptions, namely MMP-11 and MMP-23, most of these enzymes have broad substrate specificity, not only breaking down extracellular matrix components, but also acting as activators for biologically important molecules [55]. However, since they present a wide range of substrates and different functions, many of these are similar but have a different biological function that has yet to be clarified [56].

Besides that, the MMP family can be divided into at least six subfamilies: (1) collagenases (MMP-1, MMP-8 and MMP-13); (2) gelatinases (MMP-2 and MMP-9); (3) stromelysins (MMP-3, MMP-10, MMP-11 and MMP-12); (4) matrilysins (MMP-7 and MMP-26); (5) MMP membrane-type (MT)-MMPs (MMP-14, MMP-15, MMP-16, MMP-17, MMP-24 and MMP-25), and (6) other MMPs (MMP-12, MMP-19, MMP-20, MMP-21, MMP-22, MMP-23 and MMP-28) [51,56].

Nevertheless, this classification, as mentioned above, provides only a rough framework, as the substrate specificities of different MMP subtypes may overlap [51].

1.7.2. Gelatinases

MMPs are an enormous set of zinc-containing endopeptidases, which play crucial function in the destruction of all types of extracellular matrix components [48,49,51]. Among them are the gelatinases, which consist of MMP-2 (gelatinase A, 72 kDa) and MMP-9 (gelatinase B, 92 kDa) [10,11,46,57,58].

MMP-2 and MMP-9 are considered to be the key enzymes for tumor invasion and metastasis, due to their ability to degrade type IV collagen, which is a major component of the basement membrane ^[46]. Likewise, they also share proteolytic activity against other extracellular matrix molecules (figure 1.6).

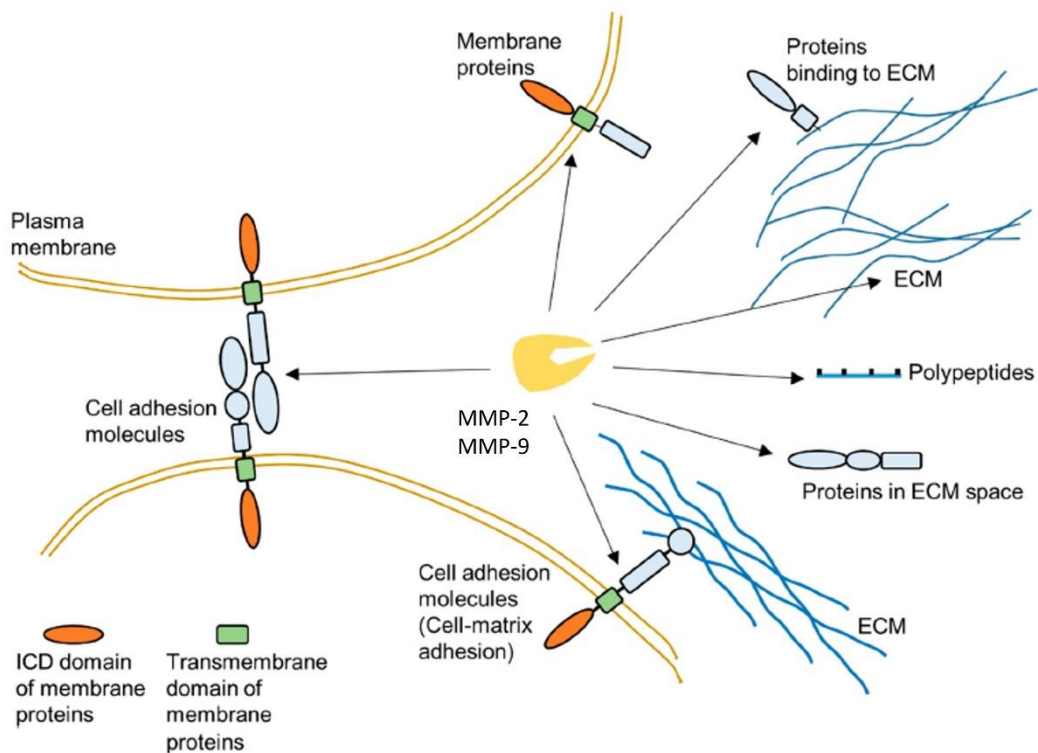


Figure 1.6: Targets of MMP-2 and MMP-9 in the extracellular environment. Besides the capability to degrade type IV collagen, gelatinases also show proteolytic activity against other proteins from the matrix, as well as disintegration of the adherent and tight junctions in cell-cell and focal adhesions in cell-matrix adhesions. Adapted from *Huang H. (2018)* ^[125]

Gelatinases are expressed and secreted as inactive proenzymes ^[58]. Its expression is regulated by growth factors, cytokines, cell-matrix and cell-cell interactions, while the enzyme activity is regulated extracellularly and mainly based on the balance between proenzyme activation and inhibition by tissue inhibitors of MMPs (TIMPs) ^[58]. Multiple signaling pathways play a role in the activation of gelatinases ^[11]. SMAD proteins are involved in TGF- β signaling and function in cell cycle regulation, differentiation, and apoptosis ^[11]. For example, SMAD4 binds to receptor-regulated SMADs and suppresses colon cancer cell migration by regulating MMP-9 activity ^[11].

Some studies in CRC have shown that MMP-2 binds to intact collagen to prevent autolytic inactivation^[55]. In addition to gelatin and other forms of denatured collagen, MMP-9 cleaves a number of other physiological substrates^[55]. Therefore, anti-cancer therapies focused on MMP-2 and MMP-9 should be considered in order to develop effective therapies against colorectal cancer^[58,59].

1.7.3. Expression and inhibition of MMPs in CRC

From inhibition and activation of latent MMPs, through the regulation of secretion molecules and inhibition by tissue inhibitors of metalloproteinases (TIMPs), MMPs are regulated at many levels^[55].

Various proteases are involved in cancer progression and metastasis. As mentioned above, MMP-2 and MMP-9 have been implicated in colon cancer progression and metastasis in animal models and patients^[49,58]. Metastatic capacity of colorectal cancer cells and elevated levels of gelatinases in tumors have often been considered to be due to enhanced MMP production by the malignant cells^[58].

This relationship between elevated metastatic capacity and increased MMP expression has been shown indirectly in *in vitro* experiments^[58]. For example, serum-free culture media of both poorly and highly metastatic murine colon carcinoma cells, both containing MMP-2 and MMP-9, showed that amounts of MMP-2 were markedly higher in the highly metastatic cell lines^[58,60]. Inhibition of gelatinases by synthetic MMP inhibitors has been considered to be an attractive approach to block cancer progression. However, despite promising results in animal models, clinical trials with MMP inhibitors have been disappointing so far^[58].

The role of MMPs in angiogenesis is also of great interest^[55,56], specially due to its dual role in tumor vasculature, acting both as positive and negative regulators of angiogenesis, depending on the time point of expression during tumor angiogenesis as well as the availability of the substrates^[49]. The relevance of these enzymes as positive regulators has largely been demonstrated^[55]. Multiple MMPs, including MMP-2, -9, and -14 can degrade the basal lamina of capillary vessels and have been implicated in tumor cell extravasation^[61].

Several pro-angiogenic factors such as vascular endothelial growth factor, basic fibroblast growth factor or transforming growth factor are induced or activated by MMPs, triggering the angiogenic switch during carcinogenesis and facilitating vascular remodeling and neovascularization at distant sites from a tumor ^[55,56].

The pro- and anti-angiogenic effects of MMPs participate in crucial steps as the ability to degrade ECM or cleave several substrates ^[55,56]. Specifically, MMP-2 and MMP-9 give rise to the modulation of the dynamic remodeling of ECM (editing aggrecan, collagens, elastin, fibronectin, laminins, and glycosaminoglycans, and latent signaling proteins), activating and deactivating by proteolytic cleavages releasing biological activities that induce cellular regulation ^[56].

Proteolytic degradation of components of the basement membrane and extracellular matrix are essential steps in tissue invasion ^[55]. Since metastases are the principal cause of death in cancer patients, a greater understanding of the process of tumor invasion and metastasis is essential in leading to the identification of new therapeutic targets ^[55].

Given the robust experimental and clinical evidence associating MMPs with tumor progression and poor prognosis, several MMPis were synthesized and trialed from the late 1980s into the early 2000s for various cancer types ^[61], attempting to control their enzymatic activity ^[49]. Yet, and although they have been around for almost 25 years now, none have reached clinical utility ^[62,63].

One of the first drugs developed was batimastat, a small peptidomimetic molecule designed to mimic the most common MMP substrate, collagen ^[61]. Batimastat showed broad-spectrum inhibition of virtually all MMP family members and preclinical data indicated a promising antitumor effect of the drug ^[61]; however, early trials showed that its water insolubility resulted in low oral bioavailability^[61,64]. Although several phase I studies showed efficacy with direct injection of the drug into the pleural or peritoneal space of patients with malignant effusions or ascites, significant toxicity, including pain, pyrexia, transaminitis, dyspnea, cough, and nausea, was observed ^[61,64]. Therefore, further testing was not pursued, given the development of a more readily orally bioavailable drug, marimastat ^[47,48].

Marimastat was developed as a next-generation oral analogue with a similar mechanism of action as batimastat ^[61]. It too showed much promise in the preclinical setting and reached phase II and III clinical trials in the metastatic setting for multiple solid tumor types including colorectal cancer ^[61,65]. Despite the breadth of these trials, they failed to demonstrate a survival benefit. Many patients also had a negative impact on their quality of life due to a debilitating "musculoskeletal syndrome" consisting of joint pain, stiffness, and inflammation, which forced the discontinuation of the drug in several patients ^[61,66].

Besides these two inhibitors, more drugs were developed in order to overcome the barriers imposed, such as tanomastat, a small-molecule inhibitor of MMP-2, -3, -8, -9, and -13, prinomastat, which inhibits MMP-2, -3, -9, -13, and -14, and rebimastat, an inhibitor of MMP-1, -2, -3, -8, -9, -13, -14 ^[61,67]. Although they were more specific and would avoid inhibition of ADAM-10 and -17, the trials failed to demonstrate a positive effect on survival. While musculoskeletal toxicity was seen less often with these inhibitors, some studies still reported significant joint pain and swelling, as well as bone marrow suppression and venous thromboembolism ^[61].

The one compound approved for clinical use because of its ability to inhibit MMPs, Periostat™ (CollaGenex Pharmaceuticals, New York, NY) for periodontal inflammation, is a low-dose doxycycline formulation ^[62]. This drug is currently the only MMPI approved by the US FDA and is used as an adjunct therapy in chronic periodontitis ^[68], not exhibiting clinical relevance for cancer treatment.

Our knowledge of the biochemistry and biology of MMPs has grown considerably in the 15 years since the clinical trials of MMPIs were halted ^[61]. Detailed analyses of MMP molecular structures have provided accurate information of the determinants of their substrate specificity, paving the path to the design of novel, highly selective and potent MMPIs based on differing mechanisms of action ^[61,69]. Next generation MMPIs have to be highly specific, function topically and preferably inhibit a single MMP function^[69]. These features can circumvent not only the potentially deleterious inhibition of protective MMPs but also avoid the onset of the musculoskeletal syndrome ^[61].

Thus, it is important to regulate the activity of this family of enzymes in an extremely delicate way ^[69]. Such advances could help us to overcome the limitations that potentially caused the failure of the clinical trials, and reconsider MMPI treatment of metastatic cancer in a new light ^[61,69].

In the light of today's knowledge that some MMPs have antitumor effects in some types of cancers, considerable effort is being put into the design of MMPIs that are highly selective and possibly inhibit only deleterious functions of specific, tumor-associated MMPs ^[61,69]. In CRC, many studies reveal a correlation between increased MMP-2 and MMP-9 expression and worse outcome ^[11], thus being considered a good and attractive target for bioactive compounds in cancer therapy as important key-players in the degradation of extracellular matrix proteins during inflammation ^[10].

1.8. Legumes as potential anti-cancer therapy

Legumes have been cultivated for thousands of years and have played an important role in the traditional diets in many areas of the world, namely Asia, America and the Middle East ^[70-72]. Regarded as “poor man’s meat”, legumes such as peas, beans, lentils, chickpeas and soybeans are not only rich in protein, but also significant sources of dietary fiber, resistant starch, folate, vitamin E, B-vitamins such as pyridoxine and folic acid, selenium, saponins, protease inhibitors, lectins, phytates and isoflavones with potential anticancer effects ^[70-74].

In recent decades, several experimental, epidemiological, and clinical studies have shown that legume consumption helps in reducing the incidence of several types of tumors ^[70,71,74-78] and case-control studies have provided evidence that it can specifically decrease the risk of CRC ^[70,71,74,79-81].

Supporting this information, The World Cancer Relief Fund/American Institute for Cancer Research Committee recognized the potential of legume consumption to decrease cancer risk and emphasized the need for additional research in this area ^[79]. Naturally-occurring plant protease inhibitors are being investigated for their potential in the prevention and/or treatment of a diverse set of human pathologies, including cancer, neurodegenerative and cardiovascular diseases, muscle atrophy and inflammatory processes (figure 1.7) ^[78].

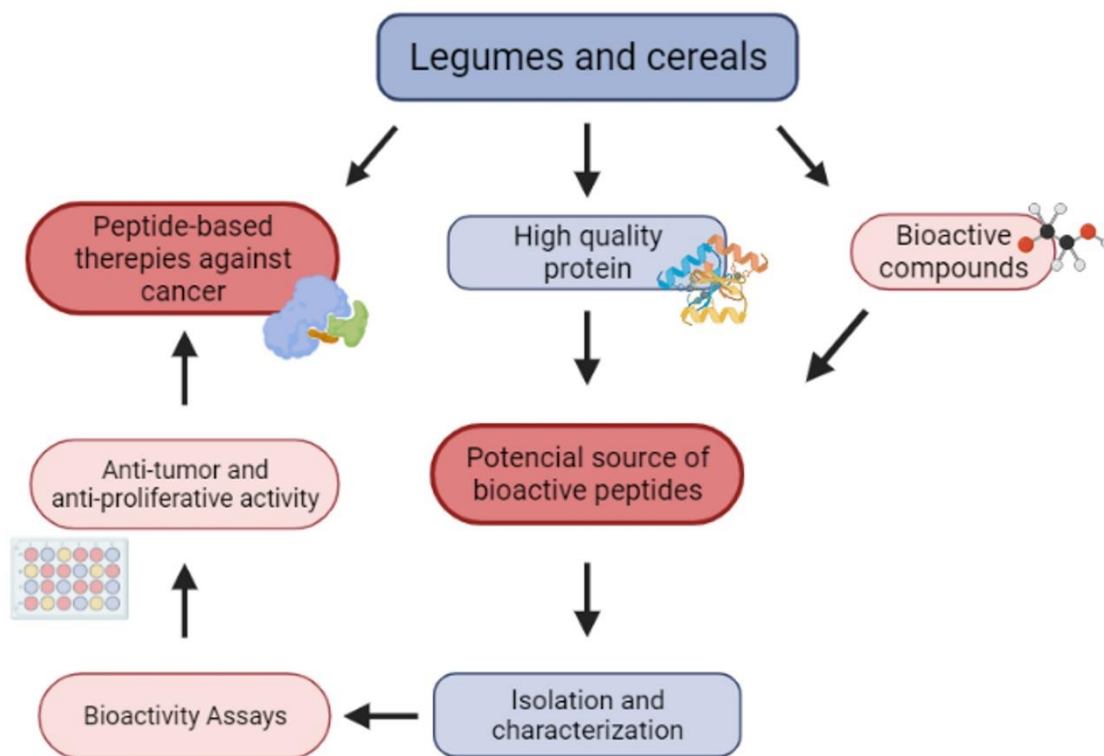


Figure 1.7: Preventive and therapeutic potential of bioactive peptides from legumes as anti-cancer agents. Adapted from *Ortiz-Martinez (2014)* ^[136]

Legume seeds are known to contain several natural protease inhibitors (PIs), classified into various families, such as the PIs of the Bowman–Birk class (BBIs), with molecular masses of 8–10 kDa, or the Kunitz classes (KIs), with molecular masses of 20 kDa ^[79,82,83]. It is known that some of these PIs are resistant to heat-denaturation and proteolysis, as well as to the extreme conditions of the gastrointestinal tract ^[78,79]. The potential of these PIs as cancer-suppressing agents has been demonstrated for both *in-vitro* and *in-vivo* model systems for a few species, such as soya, fava bean and pea ^[79,84].

Being protease inhibitors, it is likely that these anticancer activities may derive from MMP-9 or MMP-2 inhibition ^[79]. It has been shown, in animal models, that dietary intake of PIs from some legumes can prevent inflammatory processes within the gastrointestinal tract ^[78,79]. Nevertheless, the effect of legume PIs on gelatinases has been largely neglected. Furthermore, given the wide range of legume seeds consumed throughout the world and the observation that phenotypic differences may dictate their anticancer potential ^[75,78], it is likely that differences in specific PIs can also result in different MMP inhibitory activities ^[79].

Protease inhibitors of the Bowman-Birk family show considerable variation between and within legume species where seed and vegetative isoforms may be distinguished [78]. The expression of distinct genes, together with the post-translational modifications of primary gene products, which mainly occurs during seeds desiccation, is responsible for the wide array of inhibitors reported for different legume species [78].

Therefore, assessing MMP inhibition by PIs from different legume species is deemed important to quantify and compare functional components, as well as to select proper legume-based anti-cancer diets [79]. This may be particularly important for legumes used in recognized healthy diets, such as the Mediterranean diet, which comprises for example lupins, chickpea and other species that seem to have been largely forgotten in anticancer studies [79].

1.8.1. Deflamin, a therapeutical strategy against CRC

Legumes have been a key food for many civilizations around the world being thought to be one of the first crops cultivated by people [85]. The legume lupin is a seed of the domesticated *Lupinus* species of the genus *Lupinus*, belonging to the Fabaceae family of legumes [85]. They have been consumed since the ancient Egyptian as a snack food around the Mediterranean and in the Americas, usually pickled to reduce the bitterness [85,86].

Legume seeds, including lupin seeds, have been recognized to contain a big variety of protease inhibitors, including matrix-metalloproteinases inhibitors (MMPIs)^[50,78]. Although studies on white lupine are insufficient and limited in clinical, epidemiological and laboratory tests, the available literature demonstrates that the nutritional factors of lupine exhibit effects on the physiological condition of the human body, including diabetes, hypertension, obesity, cardiovascular diseases, lipid concentration, glycaemia, appetite, insulin resistance, and colorectal cancer [86].

However, although the presence of MMPIs of natural occurrence may be considered ubiquitous in plant tissues, virtually all PIs suffer from at least one of the following limitations, disadvantages or weaknesses when considering their possibility of clinical and/or nutraceutical application: toxicity; chemical inactivation (e.g. denaturation) or destruction (e.g. proteolysis) during the digestive process; absorption into the blood stream, with or without triggering immunogenic (i.e. IgG) or allergenic (i.e. IgE) responses; destruction during boiling (e.g. during cooking); low water solubility and the lack of a specific, low-cost and efficient method of isolation, that could also be efficiently up-scaled to an industrial level [46,50,87,88]. This certainly explains, for the most part, why there is not yet a single, plant derived biological compound which found successful application in the realms of human health and nutrition at the level of MMP inhibition [50].

Up to now, a considerable number of MMPIs have also been synthesized, some of which have been used as potential therapeutic agents to limit tumor progression [89]. However, only a few of these entered the clinical stage, and although they showed signs of some success in patients [90], because of MMP's ubiquity, most trials were hampered by dose-limiting toxicity, insufficient clinical benefits, and severe side-effects, due to their lack of specificity and inhibition of normal physiological processes [59].

One way to surpass these setbacks would be to discover MMPIs capable of acting directly *in loco*, without affecting MMP intracellular expression and therefore avoiding generalized side-effects [59,89,90]. This could be of particular interest in the case of gastrointestinal cancers, which are undoubtedly the most diet-linked types of cancer [59].

Previous studies, performed by Ricardo Ferreira's group (Lima *et al.* 2016) tested several edible legume seeds to detect if any inhibitory activity against MMP-9 was present [53,79]. Nonetheless, not all the legume species exhibited activity, and for the species with positive results, the activity was present at significantly different levels. Standing out amongst all specimens, *Lupinus albus* exhibited the greatest inhibitory potential against MMP-9, which is known to be implicated in the process of cell invasion [46,59].

The albumins from *L. albus* were able to dramatically decrease both MMP-9 and -2 activities, and concomitantly to inhibit cell proliferation and cell migration ^[79]. *L. albus* had never been reported as a source of MMPs inhibitors before, and these results suggested that it is very plausible that a diet rich in lupin can be more useful for CRC reduction and prevention than are other usually suggested legume foods, such as soybeans ^[79]. As such, this lupin was further tested and a oligomeric protein responsible for this strong MMPI activity was subsequently isolated ^[50].

Findings in *Lima et al.* ^[79] provided a new alternative to natural therapeutical agents, when they discovered a new MMPI, isolated from the edible seeds of sweet lupin *L. albus*. This MMPI, named deflamin (patent WO/2018/060528), is a small oligomeric protein, with approximately 17 kDa ^[50,53,59,63,79] and one of the few proteins derived from vital foods that is nontoxic and effectively reduces MMP-2 and -9 activities *in-vivo* ^[50,79].

As it acts *in-situ* and, presumably, is not absorbed in the digestive system, passing through it without exerting any apparent side-effects, due to its ability to withstand low pH levels, deflamin bypasses most problems related to previous MMPIs shown in clinical trials, associated to high toxicity and systemic secondary effects ^[50,53]. Deflamin also presents itself being water-soluble and withstanding high temperatures, meaning that products containing this oligomeric protein can be cooked without losing their bioactivity ^[53].

Because of the promising results in laboratory assays, deflamin was tested *in-vivo*, in animal models of colitis, where these bioactivities were confirmed. Through all these studies, deflamin has shown to have great anti-inflammatory potential by being a potent MMPI. Apart from the great inhibition of gelatinase activity shown ^[79], deflamin has other characteristics that makes this protein fraction ideal to be used as a nutraceutical ^[53]. The discovery of this non-toxic, digestion-resistant oligomeric protein is an exceptional attribute to add value to this as yet little-known crop, being of great interest to further study the effects of deflamin in other different models, allowing to better understand its effect on colorectal cancer.

Being a food component, with a potentially high anti-tumor function, deflamin could be used as a nutraceutical, a functional food or as a nutritional complement for colorectal cancer (CRC) patients ^[59].

1.9. Use of *in vitro* 3D models

2D cultures

For many decades, 2D *in vitro* cultures, in which cells grow in a monolayer, have been used as a tool to evaluate the biological performance of bioactive molecules under investigation for use as therapeutics for different diseases like Parkinson's, HIV, diabetes or cancer [91,92]. The easy handling, cost-effectiveness, good reproducibility and ability to grow a myriad of different cell types made 2D cultures one of the most employed pre-clinical *in vitro* methodologies for drug development [91]. In addition, this type of cell culture system has also contributed to reduce the use of laboratory animal models, as an initial screening preceding preclinical animal studies and human clinical trials, determining the initial 'stop/go' decisions on the progressing of the development of a drug [91].

From 2D to 3D cell culture

However, as cell lines grown on 2D plastic surfaces, they are unable to reproduce the real complexity and 3D structure found in the human body, especially in the solid tumors, where monolayer cell cultures are unable to mimic the structure and drug resistance conferred by elements of the tumor microenvironment and its 3D organization [43,91,93,94]. These limitations include the lack of cell–cell and cell–extracellular matrix (ECM) signaling that occurs *in vivo* environment where such signals are essential to cell differentiation, proliferation, and a range of cellular functions [43,91,92]. All these aspects are responsible for the inaccurate assessment of the biological performance of therapeutics [93].

3D cell cultures

Three-dimensional cultures are *in vitro* cultures where immortalized cell lines are placed within hydrogel matrices that mimic *in vivo* cell environments [91,92]. 3D aggregates, known as multicellular tumor spheroids, have been developed to overcome limitations of 2D cultures [94,95], much better recapitulating the *in vivo* situation of tumors than cell monolayers, as they are composed of proliferating, non-proliferating, well-oxygenated, hypoxic, and necrotic cells [91]. Furthermore, 3D growth of cells in spheroids influences cell behavior, cell shape, polarity, gene expression, proliferation, cell motility, differentiation and drug sensitivity as well as radiation resistance [91,92,94,95].

Cells are embedded in a hydrogel matrix, that resembles the extracellular matrix (ECM), and left to proliferate, resulting in the formation of a sphere if the cells are normal, or a distorted structure if malignant ^[92]. The spheroids are thus improved models for cell migration, differentiation, survival, and growth ^[92,95,96].

Nowadays, different methods are currently available to assemble 3D cell cultures which are categorized in two main classes: (i) scaffold-based 3D cell cultures (hydrogels and inserts) and (ii) non-scaffold based 3D cell cultures (figure 1.8) ^[91]. In scaffold-based 3D cultures, cells grow anchored to 3D platforms that mimic the extracellular matrix (ECM) architecture ^[91,93]. These platforms may be comprised by natural (e.g., collagen), semi-synthetic (e.g., chitosan) or synthetic (e.g., polycaprolactone) biomaterials ^[91]. In contrast, the ECM present in non-scaffold-based 3D cell cultures is composed of proteins produced by cells during the formation of the culture ^[91,93].

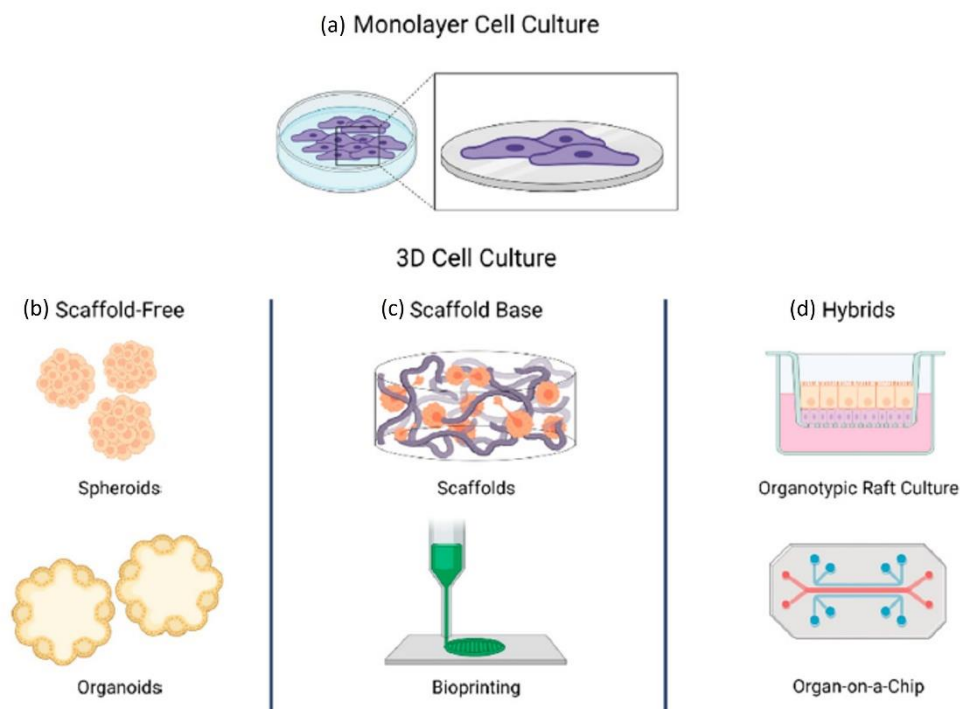


Figure 1.8: Scheme of diverse 3D cell culture strategies. (a) In monolayer cell culture, cells grow attached to a plastic base; (b) In scaffold-free systems, cells aggregate as occurs in natural processes of organogenesis; (c) Scaffold-based systems use structures that mimic the extracellular matrix and (d) Hybrids use a matrix or a scaffold to support scaffold-free systems. Adapted from *Dios-Figueroa, 2021*^[126]

Although the advantages of multicellular spheroids have been widely recognized, challenges involved in the tedious procedures required for spheroid culture are still holding back the biological community from adapting the well-validated spheroid tissue models for studying drug delivery. Challenges associated with the use of spheroid models includes forming and maintaining spheroids of uniform size with small numbers of cells and making tissue-like spheroids with multiple cell types ^[95].

3D spheroids are becoming increasingly used for the analysis of different therapeutic agents and other pharmaceutical molecules in many research laboratories ^[91,93]. To accomplish this, spheroid assembly is currently being optimized using low cost techniques that allow their production at a large scale under reproducible conditions (controlled morphology and size), as well as in a faster and automated way ^[93]. Therefore, when drug candidates are being tested using cell-based assays, the culture methods used should mimic the most natural *in vivo* representative form possible. The most natural, tissue-mimicking method of cell growth for drug discovery applications is, arguably, 3D ^[91].

1.10. Zebrafish: a promising animal model

Although *in vitro* systems can be highly effective for studying primary tumor behavior, connected organ systems are needed to understand metastasis ^[97]. Several *in vitro* cell culture chemotherapy sensitive and resistant assays (CSRAs) have been developed to fulfil the needs to predict the response to a given treatment, but they have very limited success ^[98]. Due to the lack of predictiveness, these assays are not recommended in oncology practice, mainly due to some limitations of the 2D assays, such as relying only on indirect viability assays (ATP or MTT or EDRA or ChemoFx) ^[99] and/or the absence of a 3D architecture ^[98,99]. Moreover, these *in vitro* assays rely on several passages in culture for amplification, subjecting cells to a strong selection pressure ^[98]. Therefore, a tendency towards targeted therapy and combination therapy has been facilitated by testing in various animal models *in vivo*.

The murine model has been routinely used as a pre-clinical model organism in cancer research under the basis that they are a mammalian species, with the same organ systems as humans as well as the genetic similarities to human ^[97,100]. It has proved to be an invaluable model, fundamental for drug discovery, development of new drug combinations and biomarker studies ^[98]. Although genetically modified animals do spontaneously develop tumors, the introduction of human tumor cells into other species, xenografting, is a pre-clinical vital tool that enables researchers to study tumor metastasis and evaluate drug responses ^[97].

Patient-Derived Xenografts (PDXs), also called cancer “Avatars”, are generated by the implantation of human primary tumor cells or tissues, obtained from surgery or biopsy, into a host animal ^[98]. Xenografts provide greater experimental control and can provide a direct translational link to the patient, particularly when the developmental origin of cancer remains unknown ^[97]. However, within a mouse, metastatic spread from xenografts often occurs in a later stage, well after the primary deposit has become distressing to the animal ^[97,101]

Therefore, one of the biggest disadvantages of mice for cancer research is that it is basically impossible to study early tumor dissemination and changes in the tumor microenvironment at the cellular level, not being suitable for large-scale small molecule screening ^[100]. Another drawback of the murine model, specifically for PDX, is the fact that the tumor graft needs to be transplanted into an immunocompromised adult recipient ^[100].

The latency period until tumor establishment and expansion in the mouse is also a major constrain for the use of mPDXs to aid decision making for first clinical choices ^[98]. Generally, there is a period of 3 to 4 weeks since the initial diagnosis until start of treatment, and mPDXs take months to be established, not being compatible with the time frame needed for first clinical decisions ^[98]. This is of extreme relevance, since postponing an effective treatment allows disease progression and tumor evolution as well as resistance ^[98], while patients are subjected to unnecessary toxicities such as chemo- and radiotherapy . Finally, the establishment of mPDXs is costly and resource-intensive, with limiting statistical power, not to mention the ethics implications of using an adult animal model ^[98].

Thus, the zebrafish model is emerging as a complementary and alternative model to mouse model. Many of the obstacles posed by mPDXs could be partially overcome by zPDXs followed by whole-animal high-throughput small molecule screening ^[100]. Fish, as non-mammalian vertebrate models of cancer, are not new to the field. Their advantages for biomedical research are the low-cost maintenance at high numbers of animals, the large number of progeny, among others ^[97,100]. Therefore, the zebrafish as a tool in human cancer xenotransplantation studies could overcome some of the drawbacks previously mentioned of the murine model.

The zebrafish (*Danio rerio*) is a tropical bony fish which for over 30 years has been increasingly used in developmental biology and human disease modelling as it contains almost all human organ systems ^[97,102]. Importantly, the development of human tumors and their response to chemotherapeutic treatment in zebrafish embryos is comparable to that observed in mouse xenograft assays ^[97,103]. Additionally, while mouse xenograft models require immunodeficient mice to prevent immune-rejection of the human cancer cells, the lack of a mature adaptive immune system within zebrafish embryos up to 14days-post-fertilization (dpf) allows analysis of human cancers without rejection ^[97].

Zebrafish has gained the most attention for studying development and disease (figure 1.9) due to its cost-effective maintenance, high fecundity, fast external development, optical clarity, and small size of the embryos as well as adults, thus becoming a popular model organism for developmental biology ^[97,98,100,102,104]. Thanks to the transparency of zebrafish embryos and larvae it is possible to visualize tumor cell growth and dynamics at early stages of cancer development *in vivo* ^[100,102,104]. Further, the efficiency and simplicity of genetic manipulation makes zebrafish a versatile animal for disease modeling ^[100].

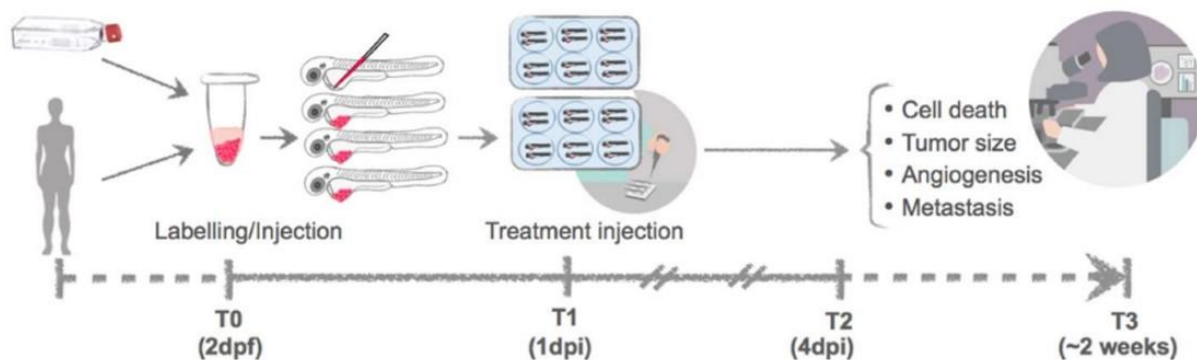


Figure 1.9: Experimental setup for generating zebrafish xenografts. Cells derived from in vitro culture or primary human cells are labelled and microinjected in the peri-vitelline space (PVS) of 2dpf larvae. One day after injection, larvae are screened for successful injection and distributed in groups for testing biological therapies. Three days after treatment, larvae are fixed and processed for immunofluorescence for analysis such as proliferation, cell death, angiogenesis, and metastatic potential. dpi: days post injection. Adapted from *Costa et al, 2020*^[97]

Recently, zebrafish has been developed as a promising experimental model for cancer research due to its strikingly similar molecular features between fish and human ^[102,105]. The zebrafish genome is sequenced, sharing 70% of homology with humans, namely in crucial pathways involved in vertebrate development and cancer and it is also reported that 82% of disease-causing human proteins have an ortholog in zebrafish ^[98,100,104–107].

There are well-established zebrafish transgenic lines with fluorescently labeled tissues available, such as the *Tg(fli:1a)* and *Tg(mPeg1)*, as well as mutants without pigmentation, such as the casper line, that offer new insights into cancer cell growth, dissemination, implantation, migration, and tumor microenvironment in real-time ^[98,100,104,108,109]. Aspects of human disease can be recapitulated and followed *in vivo* in zebrafish at the molecular level because of its highly evolutionarily conserved genes and signaling pathways ^[102,105]. Another advantage is the reduced number of tumor cells (~500 cells) necessary for successful transplantation ^[98]. Since much less human material is required to generate a xenograft, establishing zPDXs using tumor biopsy samples can be more feasible than in mice ^[98].

In the last decade, human cancer cell xenotransplantation into zebrafish has been developed, as previously mentioned. The possibility to maintain high numbers of larvae at one place and time makes zebrafish a convenient model for small molecule screening in drug discovery ^[100,103,110,111]. This is of high importance in the emerging field of PDX small molecule screening. Zebrafish accelerates the pre-clinical development process as its embryos are suitable for large-scale whole animal screening ^[100].

Zebrafish have also been used to study the tumor microenvironment, such as tumor-induced angiogenesis. Tumor neovascularization is promoted by cancer cells that release angiogenic growth factors into the tumor environment, being an important element in tumor growth and metastatic spread ^[100]. Zebrafish embryos enable real-time *in vivo* visualization of the first steps of tumor neovascularization ^[100].

Recently, *Fior et al.* developed zebrafish xenografts to screen therapeutic options in advanced CRC ^[103]. They also shown that zebrafish xenografts can be used to screen for cancer driven angiogenesis and metastatic potential ^[103,111]. This is only possible because the majority of cancer-associated human genes, as well as signaling pathways that control cell proliferation, migration, death, and differentiation, are conserved in zebrafish, as previously mentioned ^[103]. Such conservation enables the study of different cancer hallmarks.

The main benefits of zebrafish are most prominent when using embryonal stages for xenotransplantation ^[98]. The small-sized transparent embryos lacking a mature immune system makes them a good model to transplant and track high numbers of animals ^[97,100]. This fact is a powerful reason for the utilization of zebrafish as a pre-clinical screening model which could lead to patient-derived cancer cell xenotransplantation and to new options for personalized medicine ^[98,100,107]. Most of the recent transplantation studies in zebrafish use embryonal stages of 48 hours post fertilization (hpf) as the stage for transplantation, when the embryos are capable on independent feeding ^[97,100].

Like other animal and *in-vitro* models, such as mice and spheroids, zebrafish also have some disadvantages. One of the major drawbacks of the zebrafish xenografts is that engraftment efficiencies vary significantly, not allowing the successful establishment of a zPDX from every single sample available [98]. This may happen due to innate immune rejection of the inoculated tumor cells or bad quality of the samples [98]. To overcome this, some chemicals and irradiation have been employed in certain studies; however, these can ultimately lead to misleading results [98].

Another obstacle to the use of this model is the different incubation temperatures. Since zebrafish are typically reared at 28–29°C, and human cells thrive at 37°C, the compromise usually adopted is to raise zebrafish xenografts at 33–35°C, which can have an impact on the physiology of the fish and the biology of the tumor cells [98]. Lastly, another limitation of the zebrafish could be the pharmacokinetics and pharmacodynamics of some drugs [98]. Although it has been demonstrated that larvae have the ability to perform metabolic reactions, and that drug distribution, metabolism, and excretion are similar to humans, these fields are still scarcely explored in zebrafish [98].

Zebrafish has proven to be reliable for modeling and visualizing human cancer cell biology and dynamics, including metastases or tumor tissue neo-angiogenesis, *in vivo* [100]. The availability of transgenic and mutant models, as well as the possibility to transplant cancer cells into zebrafish, provides a wide array of options for studying human cancer [112]. Although zebrafish is a non-mammalian model organism, it has striking evolutionary conservation of disease-related genes and pathways with humans [100]. Screening for targeted treatment in zebrafish xenografts could provide new opportunities for anticancer personalized therapy in the future as recent research has shown that zebrafish studies are reliable in modeling human cancer [100,112].

2. Objectives

CRC is a very common malignant disease, being the third most frequently diagnosed cancer and the second main cause of cancer death worldwide. The current knowledge about target therapies toward the inhibition of MMPs is still very limited, primarily because most MMPs inhibitors showed to have a dose-limiting toxicity in the clinical trials, not allowing its synthesis as an anti-tumoral drug. Several legume polypeptides showed an inhibitory action of MMPs, without revealing cytotoxic effects for cells, being considered a potential strategy against the malignant progression of colorectal cancer. Since previous studies have shown that deflamin has great anti-inflammatory and MMP-9 inhibitory potential, it is of great interest to study it as a promising pharmaceutical drug. Thus, the main objective of this dissertation is to better understand the mechanism of action of deflamin through:

1. An *in vitro* approach:
 - a. Evaluate the role of deflamin on cell proliferation and invasion in different CRC cell lines using 2D and 3D cellular models.

2. An *in vivo* approach:
 - a. Assess the effect of deflamin on the angiogenic process of CRC cell line xenotransplanted into the zebrafish larvae.
 - b. Understand how deflamin affects the degradation of the extracellular matrix in CRC tumors using the zebrafish xenograft model.

3. Materials and methods

3.1. Biological materials

3.1.1. Vegetable protein extract

The plant material used in this dissertation was purified from white lupine (*Lupine albus* sp.) at Professor Ricardo Ferreira's Lab in Instituto Superior de Agronomia, as a powder of deflamin extract. For laboratory use as an experimental compound, the deflamin extract is diluted in 1x PBS to a final concentration of 1mg/mL.

3.1.2. CCR human cell lines

For this study, the following cell lines were used: SW480, HCT116 and HT29, and purchased at ATCC as described in table 1.

All lines were maintained in culture in DMEM medium (Gibco Dulbecco's Modified Eagle Medium) supplemented with 10% FBS (fetal bovine serum) and 1% penicillin-streptomycin in a humidified atmosphere at 37°C with 5% CO₂.

In order to ensure that the cultured lines did not accumulate in-vitro mutations after a few passages, cell lines were maintained at low passage (P<20) and cryopreservation stocks were made. Thus, at passages 2 to 4, the cells were frozen in DMEM with 5% DMSO (Dimethyl sulfoxide).

Table 1: List of cell lines used.

Cell line	Tissue	Tumor grade	Origin	Description
SW480	Colon	Grade IV (stage II)	American Type Culture Collection (ATCC, Virginia, USA)	Isolated line of a primary tumor of a 50-year-old Caucasian man. Classified as poorly differentiated colon adenocarcinoma
HCT116	Colon	Non-specified	American Type Culture Collection (ATCC, Virginia, USA)	Line obtained from a colorectal carcinoma of an adult male.
HT29	Colon	Grade I (stage I)	American Type Culture Collection (ATCC, Virginia, USA)	Obtained from a primary tumor of a 44-year-old Caucasian woman. Characterized as a well differentiated colon adenocarcinoma.

3.1.3. *In-vivo* model

At 48h post-fertilization (hpf) Zebrafish larvae (*Danio rerio sp.*), both wild-type and the transgenic model Tg(kdrl:eGFP) with blood vessel marked with eGFP, were used.

3.1.4. CHP preparation

The Collagen Hybridizing Peptide (CHP) is a synthetic peptide that can specifically bind to denatured collagen strands through hydrogen bonding, both in histology, *in vivo*, and *in vitro* (3D cell culture). CHP is an extremely specific probe for unfolded collagen molecules: it has negligible affinity to intact collagen molecules due to the lack of binding sites; it is also inert towards non-specific binding because of its neutral and hydrophilic nature ^[113].

The CHP was prepared by dissolving 60µg of the powder in 400µL of sterile 1x PBS, to get a stock solution with a CHP concentration of 50µM, according to the manufacturers guide (3Helix).

3.2. Methods

3.2.1. Cell Culture

Cell culture is one of the most important tools used in molecular biology, providing systems to study the majority of diseases. The cell lines used are described in section “CRC cell lines”.

All cell lines were routinely cultured on 75cm² or 25cm² flasks and maintained on an incubator at 37°C and 5% of CO₂ under a humidified atmosphere. Culture medium was changed every 2 to 3 days (10mL for a 75cm² flask and 5mL for a 25cm² flask). Cells were split at 80% confluence. For that, the medium was aspirated to avoid any serum residues once it inactivates trypsin due to the presence of protease inhibitors, such α 1-antitrypsin and α 2-macroglobulin. After removing the medium, the flask is washed twice with PBS 1x, to remove residual DMEM. Two mL of a trypsin/EDTA (GIBCO) solution was added. Cell's flasks were placed at the incubator during five minutes for detachment. The trypsination was stopped with serum-complemented medium and cells were counted using the Neubauer chamber. According to the cell number, about 0,5-1mL of the suspension was added to new flasks.

Thawing Cell

For long term storage, cells were frozen at -80°C in cryovials in cell culture medium containing 5% of Dimethyl-sulfoxide (DMSO) (Sigma-Aldrich). DMSO acts as a cryoprotective agent. Cells were thawing by placing the cryovials in a 37°C water-bath for 2min and the cell suspension was transfer to a 75cm² containing DMEM supplemented with 10% of FBS and 1% penicillin-streptomycin. The medium was replaced only the day after, in order to allow the cells attachment to the flask and remove the residual DMSO. All processes were performed under sterile conditions.

3.2.2. Western-Blot

The protein levels were assessed using the western-blot (WB) technique, commonly used to separate and identify proteins. It consists of three main stages, the proteins separation according to their molecular weight in a sodium dodecyl sulfate polyacrylamide gel electrophoresis (SDS-PAGE); the transfer to a solid support, normally a nitrocellulose membrane and, lastly the detection by using specific primary and secondary antibodies ^[114].

Protein extraction

For this analysis, control and deflamin treatment conditions (50µg and 100µg/mL) of HCT116, SW480 and HT-29 were cultured in a 6-well plate and grown until 80% of confluence. The total protein extracts were prepared by lysing the cells in 250µL of lysis buffer (25mM Tris pH 7.5 (Sigma-Aldrich), 500mM EDTA (Sigma-Aldrich), 1% Triton X-100™ (VWR), 25nM TCEP (Sigma-Aldrich) and in the presence of protease inhibitor cocktail (Roche) and phosphatase inhibitor cocktail 2 (Sigma-Aldrich)). After 10min on ice and with the aid of a scraper, cells were released from the well and transferred to an Eppendorf for centrifugation at 8000Gs for 10min at 4°C. Supernatants were transferred to a new Eppendorf and stored at -20°C for further use.

Protein quantification

For western blotting purposes, protein concentrations of all samples were normalized to the equal amounts (10µg) using the Quick Start™ Bradford Protein Assay (Bio-Rad) accomplished by measurement of absorbance at 590nm.

This is a colorimetric protein assay based on the absorbance shift of Coomassie Brilliant Blue, being a rapid and sensitive method [115]. The concentration of the samples was then determined by comparing to a standard curve of known Bovine Serum Albumin (BSA) concentrations: 50µg/mL, 100µg/mL, 200µg/mL, 400µg/mL, and 500µg/mL. The samples were then added to a 96-well plate and the absorbance was measured in the Infinite 200 Plate Reader (Tecan). Using the absorbance and our linear standard curve, we calculated our protein concentration and calibrated our samples at the same concentration.

SDS-PAGE

Sample Buffer, containing Tris (1M, pH 6.8), SDS (2%), glycerol (10%), Bromophenol blue (0.0006%) and H₂O was then added to the total protein extract and denatured for 5min at 90/95°C. This will confer a negative charge to the proteins so they can be separated by size. Samples were loaded into a 10% polyacrylamide gels. The electrophoresis was performed in SDS-Page running buffer using the BIO-RAD WB power source initially at 90V until proteins reach the running gel and then at 120V. This step will allow us to separate the proteins based on their molecular weight.

Protein detection and transference

It was then performed a dry transfer onto nitrocellulose membranes using the iBlot® Dry Blotting System (Life Technologies). Following, we blocked the membrane in 5% non-fat dry milk (Nestlé, Portugal) diluted in TBS 0,1% Tween20 for one hour and incubated with the specific primary antibodies (table 2) overnight at 4°C using a roller mixer (Stuart).

Next day, the membranes were washed three times for five minutes with TBS 0.05% Tween20 followed by one-hour incubation at room temperature with the corresponding secondary antibody (donkey anti-mouse or goat anti-rabbit (1:5000) both from Santa Cruz Biotechnologies). All membranes were washed three times for 5min.

Proteins were detected using Amersham ECL Western Blotting Detection Reagent (GE Healthcare Life Sciences), according to manufacturer's instructions. Signal was detected on radiographic film (Fujifilm), using Curix60 (AGFA).

Table 2:List of primary antibodies used in Western Blot.

Antibody	Dilution	Antibody Dilution Buffer	Source
Anti-Vimentin Rabbit Monoclonal Antibody	1:1000	5% w/v Milk, 1X TBS, 0.1% Tween	Cell signaling® Vimentin (D21H3) Rabbit mAb
Anti-E-cadherin Mouse Monoclonal Antibody	1:1000	5% w/v BSA, 1X TBS, 0.1% Tween	Cell signaling® E-Cadherin (24E10) Rabbit mAb
Anti-N-cadherin Rabbit Monoclonal Antibody	1:1000	5% w/v BSA, 1X TBS, 0.1% Tween	Cell signaling® N-Cadherin (D4R1H) Rabbit mAb
Anti-phospho- p42/44 MAPK (ERK1/2) (T202/Y204) Rabbit Monoclonal Antibody	1:1000	5% w/v BSA, 1X TBS, 0.1% Tween	Cell signaling® Phospho-p44/42 MAPK (Erk1/2) (T202/Y204) (197G2) Rabbit mAb
Anti-phospho-AKT (S473) Rabbit Monoclonal Antibody	1:1000	5% w/v BSA, 1X TBS, 0.1% Tween	Cell signaling® Phospho-AKT (S473) (736E11) Rabbit mAb
Anti-β-Actin Mouse Monoclonal Antibody	1:25000	5% w/v Milk, 1X TBS, 0.1% Tween	Abcam Anti-beta Actin antibody [mAbcam 8226] (ab8226)

3.2.3. Cellular apoptosis assay

For apoptosis analysis, cells were seeded at a density of $1-2 \times 10^4$ in 96-well plates. 24h after seeding cells were treated with control and three treatment conditions, 25µg/mL, 50µg/mL, and 75µg/mL of deflamin for 48hr. Measurement of caspase 3/7 activity was performed using the Apo-ONE® Homogeneous Caspase-3/7 Assay kit (#G7790, Promega) following manufacture instructions.

Caspases 3 and 7, members of the cysteine aspartic acid-specific protease (caspase) family, play key effector roles in apoptosis in mammalian cells as they will cleave multiple target proteins and, as a result, lead to cellular apoptosis.

This assay consists in the addition of a substrate, rhodamine 110, that is non-fluorescent prior to the assay. Once added to the sample, and when in the presence of caspase 3/7, it is cleaved and emits an intensely green fluorescence (figure 3.1)^[116]. The amount of fluorescent product generated is proportional to the amount of caspase 3/7 cleavage activity present in the sample. The fluorescence was measured at an excitation wavelength of 499nm and an emission of 530nm.

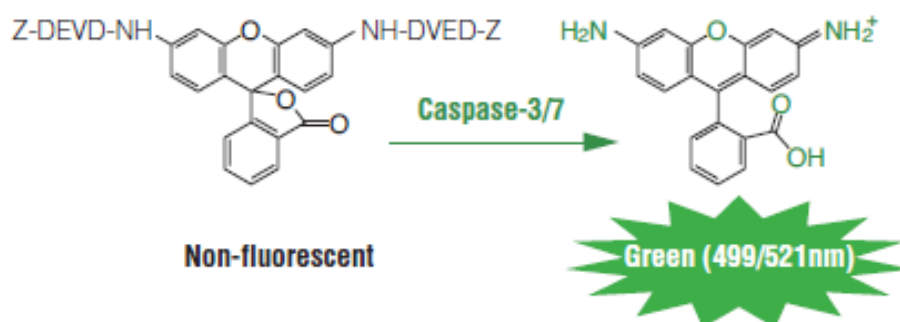


Figure 3.1: Cleavage of the non-fluorescent Caspase Substrate by Caspase-3/7 to create the fluorescent Rhodamine 110. Retrieved from *Promega*^[116].

3.2.4. Cellular viability assay

For cell viability, cells were seeded at a density of $1-2 \times 10^4$ in 96-well plates. 24hr after seeding cells were treated with control and three treatment conditions, $25 \mu\text{g/mL}$, $50 \mu\text{g/mL}$, and $75 \mu\text{g/mL}$ of deflamin. Every day, for 5 days, 1:10 of AlamarBlue reagent (Invitrogen) was added to three wells of cells.

AlamarBlue is a proven cell viability indicator that uses the natural reducing power of live cells to convert resazurin to the fluorescent molecule, resorufin^[117]. The active compound of AlamarBlue (resazurin) is a non-toxic, cell permeable compound that is blue in color and virtually non-fluorescent. Upon entering cells, resazurin is reduced to resorufin, which produces a very bright pink/red fluorescence^[118]. Viable cells continuously convert resazurin to resorufin, thereby generating a quantitative measure of viability.

Fluorescence was measured 2 hours after incubation with Alamar blue, for five consecutive days (excitation 560nm; emission 590nm) in the Infinite 200 Plate Reader (Tecan) (figure 3.2).

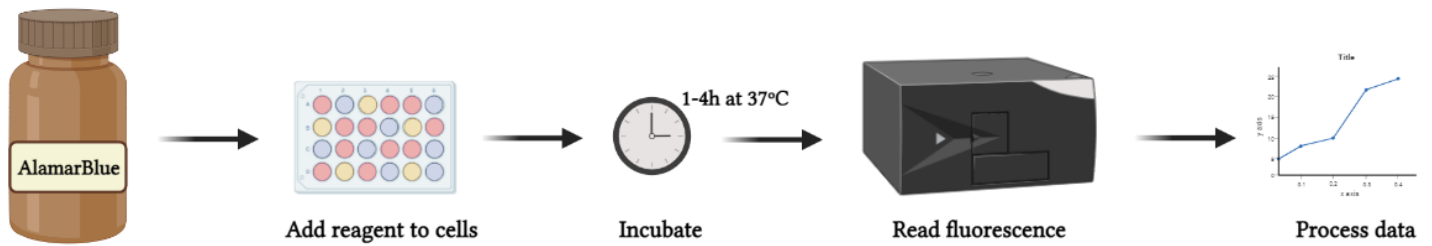


Figure 3.2: AlamarBlue Assay Flow. To start the assay, the AlamarBlue compound is added to the cells. The cells are then placed in an incubator at 37°C and 5% of CO₂ under a humidified atmosphere. The amount of fluorescence is proportional to the number of living cells and corresponds to the cell's metabolic activity. Damaged and non-viable cells have lower innate metabolic activity and thus generate a proportionally lower signal than healthy cells. After incubation, the fluorescence of the cells can readily be measured in the Infinite 200 Plate Reader (Tecan). Finally, the results are analyzed by plotting fluorescence intensity versus compound concentration. Adapted from *BioRender*^[133], *AlamarBlue Assay Protocol*^[118].

3.2.5. Viral infection of cell lines

Lentiviruses are a key tool in today's field of biology as they provide a reliable way to achieve stable over-expression of a gene in the cells of interest.

HCT116, HT-29 and SW480 cells were seeded into 6-well plates for 24 hours, until they reach about 70 to 80% of confluency. After that, the medium was replaced by fresh medium containing 5µg/mL of polybrene (Sigma-Aldrich) and 10µL of FUDtTW lentiviral particles (1*10⁶ particles/mL from Champalimaud Foundation).

Lentiviral transduction is an efficient method for the delivery of transgenes to mammalian cells and unifies the ease of use and speed of transient transfection with the robust expression of stable cell lines^[119].

Selection of a stable transfected culture started 7 days after infection by FACs sorting of dtTomato cells. Infected cells were confirmed by fluorescence microscopy using a Zeiss LSM710 confocal microscope.

3.2.6. Analysis of inhibitory activity of deflamin *in-vitro*

3.2.6.1. Spheroid formation (3D cellular model)

The formation solution of spheroids was obtained by combining 1/4 of the final volume of methylcellulose (6 mg/mL), 10% FBS, 20 to 40 μ g/mL of collagen (3mg/mL) (according to the cell line), 1 μ g/mL of mitomycin (only for the case of invasion spheroids) and adding DMEM medium until the desired final volume is filled. Cancer cells were then resuspended into this solution considering that each spheroid is composed of 500 cells (Table 3). The solution was plated in a non-adherent 384-well plate at a final volume of 50 μ L per well. The plate was then placed in an incubator for 24h to allow formation of individual spheroid per well.

Table 3: Example of spheroid formation solution for both invasion and proliferation spheroids, for any of the three cell lines. Here, we take as an example the formation of 27 spheroids (50 μ L per well). This value considers pipetting errors, normally associated with the preparation of small amounts of solutions. Thus, the final volume of the solution is prepared for the formation of three extra spheroids. Here, we also take as an example a cell concentration of 50 000 cells per mL, so that we call fill the table according to the final concentrations and respective volume. **Note:** collagen concentration varied for better formation of spheroids according to the cell line in use. For example, for the cell line SW480 we used a concentration of 40 μ g/mL (18 μ L), while for the lines HT29 and HCT116 we used a concentration of 20 μ g/mL (9 μ L).

Components (final concentration)	Invasion spheroids solution (μL)	Proliferation Spheroids solution (μL)
Methylcellulose (1/4 of total volume)	337,5	337,5
FBS (10%)	135	135
Collagen (20 to 40 μ g/mL)	18	18
Mitomycin (1 μ g/mL)	13,5	-----
DMEM	576	589,5
Cells (500 cells per mL)	270	270
Final Volume (μL)	1350	1350

3.2.6.2. 3D cell invasion assay

For the 3D invasion assay, the spheroids were embedded in a collagen matrix to evaluate the invasion of cells. This matrix resembles and mimics an *in-vivo* 3D extracellular matrix situation where cells migrate from a small cluster in order to form micro-metastasis. In order to form the collagen gel, 30 μ L to 40 μ L of the spheroid solution was removed from each well, without removing or destroying the spheroid. For control condition, the spheroid was embedded in 7 μ L of a gelatinous collagen matrix mixture consisting of two parts of collagen (3mg/mL), 15% FBS, 1 μ g/mL of mitomycin, 2% of NaOH (1M) and fulfilling with DMEM until the final volume is achieved. For both treatment conditions, 50 μ g/mL, and 100 μ g/mL, deflamin was added within the 7 μ L final volume (Table 4).

Table 4: Example of spheroid solution for invasion assay, for any of the three cell lines. Here, we take as an example the preparation of a solution for six spheroids (7 μ L per spheroid), considering the pipetting errors associated with the preparation of small volume solutions. Thus, the final volume of the solution is prepared for the formation of two extra spheroids (this is, only to four wells the solution will be applied).

Components (final concentration)	Control solution (μ L)	Deflamin treatment (50 μ g/mL)	Deflamin treatment (100 μ g/mL)
FBS (15%)	6,3	6,3	6,3
Collagen (2/3 of total volume)	28	28	28
Mitomycin (1 μ g/mL)	0,42	0,42	0,42
DMEM	6,44	5,14	3,84
NaOH (2%)	0,84	0,84	0,84
Deflamin (0, 50 or 100 μ g/mL)	0	1,3	2,6
Final Volume (μL)	42	42	42

After one hour of incubation for solidification, imaging of the spheroids was performed by fluorescence microscopy in a Zeiss LSM710 confocal microscope, allowing different cross-sections at different optical planes of a z-stack. This time point was accounted as 0h. Following, the gels were covered with 10 μ L of DMEM with 10% FBS and incubated again. The next images were taken at the time points of 24h, 48h and 72h.

Images were analyzed by counting the number of invading cancer cells using the FIJI/ImageJ software. Invasive cells were considered as the ones who present themselves between the inner perimeter, spheroid border, and the outer perimeter, furthest invasive cell.

3.2.6.3. 3D cell proliferation assay

For the proliferation assay and to measure the growth of the spheroid, no collagen was added to the medium, in order to avoid cellular migration and keep the integrity of the spheroid. Therefore, about 30 to 40 μ L of the spheroid formation solution was removed from each well, without removing or destroying the spheroid. For control condition, the spheroid was embedded in 30 μ L of DMEM with 10% of FBS. For both treatment conditions, the volume of deflamin was added in order to perform a final concentration of 50 μ g/mL and 100 μ g/mL.

After one hour of incubation, imaging of the spheroids was performed by fluorescence microscopy in a Zeiss LSM710 confocal microscope, allowing different cross-sections at different optical planes of a z-stack. This time point was considered as 0h. The next images were taken at the time points of 24h, 48h and 72h.

For the analysis of images and quantification of spheroid growth, a peripheral area of the spheroid was outlined at 0, 24, 48 and 72h, using the FIJI/Image J software. These areas allow quantifying the spheroid growth every 24h, by comparison with the 0h area.

3.2.7. Analysis of deflamin activity *in-vivo*

3.2.7.1. Animal care and handling

In vivo experiments were performed in the zebrafish (*Danio rerio sp.*), which was maintained, handled, and treated in accordance with European Animal Welfare Regulations and standard protocols.

3.2.7.2. Cellular preparation for xenograft

For injection, HCT116 cells were grown in 75cm² flasks at 37°C in DMEM medium containing 10% of fetal bovine serum (FBS) and 1:100 penicillin-streptomycin (pen-strep) until they reach 80% confluence. The medium was then aspirated, and the cells were washed with 1x PBS to avoid any residues. After that, the cells were incubated in 2mL of trypsin/EDTA for 5min at 37°C for detachment. The trypsination was stopped with serum-complemented medium. The cells were centrifuged for 4 min at 1200 rpm. The supernatant was then aspirated, leaving the cell pellet. Following, cells were resuspended and washed twice in 8-10mL of 1x PBS, through centrifugation at 1200rpm for 4min. After discarding the supernatant, the cells were resuspended in culture medium to a final concentration of 2,5x10⁵ cells/mL.

3.2.7.3. Xenograft in zebrafish (*Danius rerio sp.*)

The HCT116 cell line, previously infected with a plasmid expressing the fluorescent dtTomato (red) tag, was injected at the desired concentration (approximately 800 cells per injection) in the perivitelline space (PVS) of the larvae, 48hpf (hours post fertilization) under anesthetics Tricaine 1x (Sigma-Aldrich).

For injection, 5 to 10µL of the cell suspension were loaded into an injection needle and the needle was mounted onto the micromanipulator. The tip of the needle was broken off to obtain the ideal tip opening diameter (5-10µm²).

After the injection, the larvae were transferred to an incubator at 34°C until the end of the experiment. At 24hpi (hours post injection) the zebrafish larvae were screened for the presence or absence of tumor mass and discarded the ones with cells in the yolk sac, cell debris, edema, or the non-injected ^[103].

3.2.7.4. Treatment conditions

The xenografts successfully injected were separated into three groups: a control group treated with 1x PBS; two groups of treatment with deflamin, at concentrations of 50µg/mL and 100µg/mL, respectively. The compound was introduced into the medium E3 at 24hpi, at a concentration of 50µg/mL or 100µg/mL. Over a period of three consecutive days, the medium was changed and new deflamin was added to the treatment conditions as well as new medium and 1x PBS to the control group. After this period, only animals with tumors were analyzed.

3.2.7.5. Fixation and immunofluorescence of zebrafish larvae

The animals selected for this study were fixated in a solution of 4% paraformaldehyde overnight, after the three days of treatment, and stored at -20°C in 100% methanol.

For the transgenic Tg(kdrl:eGFP) larvae, after fixation, the samples were re-hydrated in a series of 75%, 50% and 25% MetOH and incubated for 7min in acetone at -20°C for permeabilization. The larvae were then washed with a glycine buffer solution (1x PBS, 0.5% Tween20, 0.5% TritonX and 100Mm Glycine) (Table 5) for 1h at RT, in order to bind free aldehyde groups (that otherwise may bind the antibody). After the wash, they were incubated in a blocking buffer solution, PBDX_GS (1x PBS, 1% BSA, 1% DMSO, 1% TritonX and 1.5% FBS) (Table 6), for 1h at RT and then with the diluted primary antibody (eGFP, 7,5µL/mL) for 1h at RT and overnight at 4°C.

Table 5: Glycine buffer preparation for a final volume of 15mL.

Components (final concentration)	Glycine Buffer
PBS (1x)	14,8 mL
Tween20 (0,5%)	75 µL
TritonX (0,5%)	75 µL
Glycine (100Mm)	0,113 g
Final Volume (mL)	15

Table 6: Blocking buffer preparation for a final volume of 25mL.

Components (final concentration)	Blocking Buffer
PBS (1x)	24,4 mL
BSA (1%)	0,25 g
DMSO (1%)	250 μ L
TritonX (1%)	12,5 μ L
FBS (1,5%)	375 μ L
Final Volume (mL)	25

In the next day the samples were incubated for 1h at RT and overnight at 4°C with the secondary antibody (Alexa Fluor® 488, 1:400) and DAPI (1:1000) and, on the third day zebrafish were mounted with Vectahield mounting media without DAPI (Vectorlabs) on the slides and stored at 4°C for further analysis.

For the wild-type zebrafish larvae, the samples were re-hydrated in a series of 75%, 50% and 25% MetOH and incubated for 7min in acetone at -20°C for permeabilization. The larvae were then washed in PBS 1x and incubated overnight with the collagen hybridizing peptide (CHP), at a final concentration of 20 μ M. In the next day, the samples were incubated for 1h at RT with DAPI (1:1000) and mounted with Vectahield mounting media (Vectorlabs) on the slides and stored at 4°C for further analysis.

3.2.7.6. Angiogenesis analysis

All images were obtained through fluorescence microscopy, using a Zeiss LSM710 confocal microscope, with a Z-stack with a 7 μ m interval. The images were then analyzed, and quantification was done using the FIJI/ImageJ software.

For angiogenesis analysis, two parameters were measured: vessel density (VD) and vessel infiltration (VI). The difference between vessel density and vessel infiltration relies on the difference between the vessels that are fully formed and those that manage to infiltrate the tumor. That is, when we talk about density, we talk about the vessels that are on the surface of the tumor as well as those that infiltrate. When we talk about infiltration, we talk about the tumor core, that is, the central nucleus of the tumor and the vessels that manage to reach there to supply oxygen and nutrients to these cells, which are initially in a more hypoxic state.

Vessel density and vessel infiltration were assessed throughout z-projections of corresponding images using ImageJ Z-Projection tool and the percentage of eGFP fluorescent per tumor was quantified. To analyze the vessel infiltration, the superficial slices of the images were not considered (about 40% of total stacks).

$$VD = \frac{eGFP\ area}{tumour\ area}, VI = \frac{eGFP\ area}{core\ of\ the\ tumour}.$$

3.2.7.7. Degraded Collagen analysis

To determine a potential effect of deflamin on the degradation of the extracellular matrix and its main components, we decided to analyze the degraded collagen in zebrafish xenografts. Collagen is one of the main components of the ECM as well as one of the main targets of MMP-2 and 9. So, it is expected that, by inhibiting gelatinases, an inhibition of ECM remodeling occurs as well as less degradation of its main targets, namely collagen.

All images of the zebrafish xenografts were obtained through fluorescence microscopy, using a Zeiss LSM710 confocal microscope, with a Z-stack with a 9µm interval. The images were then analyzed, and quantification was done using the FIJI/ImageJ software.

For degraded collagen analysis, all images from the control and treatment situations were measured. To start, in each image, we measured the total tumor area so that we can operate and measure the CHP signal only in the tumor. This was just an auxiliary measurement. Using the total tumor area, we applied it on top of the CHP channel (this allows to detect only the CHP signal that is coming from the actual tumor cells). Next, we removed the background noise from the CHP channel and measured the intensity of eGFP fluorescence (IF) per tumor, using z-projections of corresponding images with ImageJ Z-Projection tool. This measure corresponds to the integrated density. Three randomly selected areas of the background were also measured, for each image, and the mean gray value was used to correct and normalize the real value of intensity of fluorescence.

$$IF = \text{Integrated Density} - (\text{Total area eGFP} \times \text{Mean fluorescence of background readings})$$

3.3. Statistical analysis

GraphPad Prism version 9.0.0 for windows (GraphPad Software) was used to perform statistical analysis. This software allowed to perform the statistical analysis of all the experiments performed, making possible to perceive whether or not the results obtained were statistically significant, when compared with a control situation.

For this, the statistical paired t-test was chosen. The paired sample t-test is a statistical procedure used to determine whether the mean difference between two sets of observations is zero. Common applications of the paired sample t-test include case-control studies or repeated-measures designs.

In vitro assays regarding spheroid proliferation and invasion were performed in quadruplicate and the error bars on the graphics represent the standard error of the means (SEM). Comparisons of means were done with repeated-measures paired t-test and the level of statistical significance was set at $*p < 0,05$ and $**p < 0,01$. Experiments were repeated at least four times to ensure reproducibility of the assays.

In regard to the *in vivo* assays, paired t-test was used to compare differences among different groups and the statistical significance was set as $*p < 0,05$. The data is expressed as scatter charts and error bars represent the standard error of the means (SEM).

4. Results and discussion

4.1. Analysis of deflamin activity in 2D cell culture systems

4.1.1. Cellular viability

The measurement of cell viability plays a fundamental role in all forms of cell culture, providing a more accurate understanding of the number of healthy cells in a sample. Previous results obtained by Lima *et al.*, 2016^[79] group showed that HT29 CRC cell proliferation was reduced when protein fractions of *L. albus* were added to the growth medium. More recent studies published earlier 2021, performed by the same group, revealed that the cellular viability of HT29 cell line was not significantly affected when cells were exposed to different concentrations of deflamin, ascertaining the deflamin extract's safety for food purposes^[59]. Thus, it is important to assess, albeit preliminary, whether deflamin may exhibit cytotoxic effects on cells that could translate into potential adverse side effects in human colon cancer cells. In this context, we sought to investigate further the role of deflamin in cellular viability of a panel of CRC cell lines: HT29; HCT116; and SW480.

For that, we exposed CRC cell lines to three different concentrations of deflamin (25µg/mL, 50µg/mL, and 75µg/mL) and compared it to untreated control group, performing an Alamar blue viability assay. Non-fluorescent Alamar blue (oxidized) is reduced into a pink fluorescent dye in the medium due to cell activity^[117]. The fluorescence signal was measured 2h after Alamar blue incubation, for 5 consecutive days, at an excitation wavelength of 560nm and an emission of 590nm.

Our results indicate that the viability of all different cell lines is not affected by any of the concentrations of deflamin, when compared to the control group, suggesting that deflamin is neither involved in the cell cycle regulation nor shows any cytotoxic effects to the cell populations (figure 4.1). Since the objective would be to use deflamin, a natural compound, as a pharmaceutical drug in the treatment of colorectal cancer, albeit as an adjuvant, it is extremely important that it does not present any general cytotoxic effects.

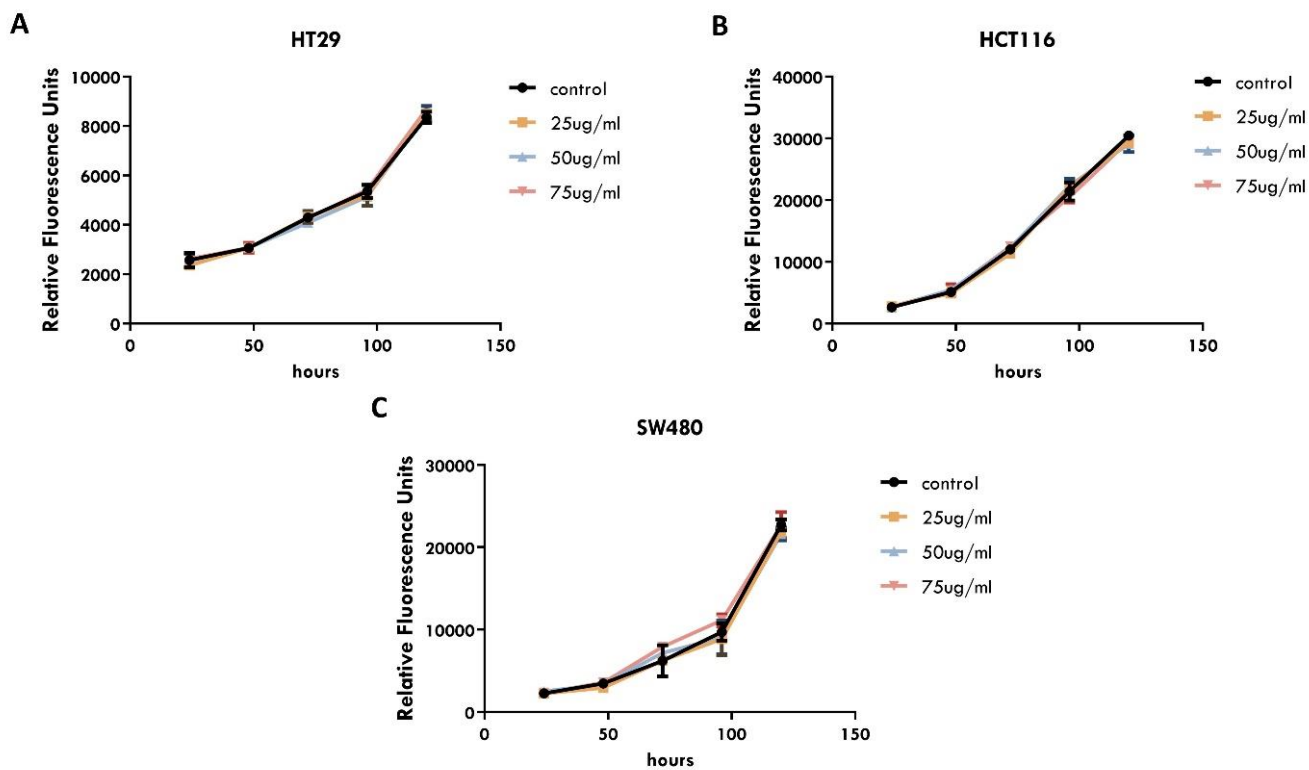


Figure 4.1: Analysis of cellular viability in the presence of three different concentrations of deflamin in CRC cell lines. The AlamarBlue™ assay was used to determine the growth response of CRC cell lines to deflamin (25 – 75µg/mL) for 5 days. (a) Cell growth of HT29 cell line (b) Cell growth of HCT116 cell line; (c) Cell growth of SW480 cell line. (Three independent experiments are represented, n=3).

4.1.2. Cellular apoptosis

Apoptosis is the cell's natural mechanism for programmed cell death that can be triggered by several factors, such as therapeutic agents, namely chemotherapeutic. This process is characterized by the activation of caspases, such as caspase 3, 6 and 7. These cysteine proteins will cleave multiple target proteins and, as a result, lead to cellular apoptosis.

With the goal to evaluate if deflamin could provoke cellular damage, we measured the levels of activity of caspase 3/7 in three different cell lines (HT29, HCT116 and SW480) at increasing concentrations of deflamin (25 μ g/mL, 50 μ g/mL, and 75 μ g/mL), using Apo-ONE® Homogeneous Caspase-3/7 Assay kit (#G7790, Promega).

This assay consists in the addition of a substrate, rhodamine 110, that is non-fluorescent prior to the assay. Once it is added to the sample, and when in the presence of caspase 3/7, it is cleaved and emits an intensely green fluorescence. The amount of fluorescent product generated is proportional to the amount of caspase 3/7 cleavage activity present in the sample. The fluorescence was measured at an excitation wavelength of 499nm and an emission of 530nm.

Our results show that the activity of caspase 3/7 is similar between all the different treatment conditions, as well as to the control group, in all cell lines (figure 4.2). This indicates that there is no induction of apoptosis by deflamin, suggesting that it does not play a direct role in inducing cellular apoptosis.

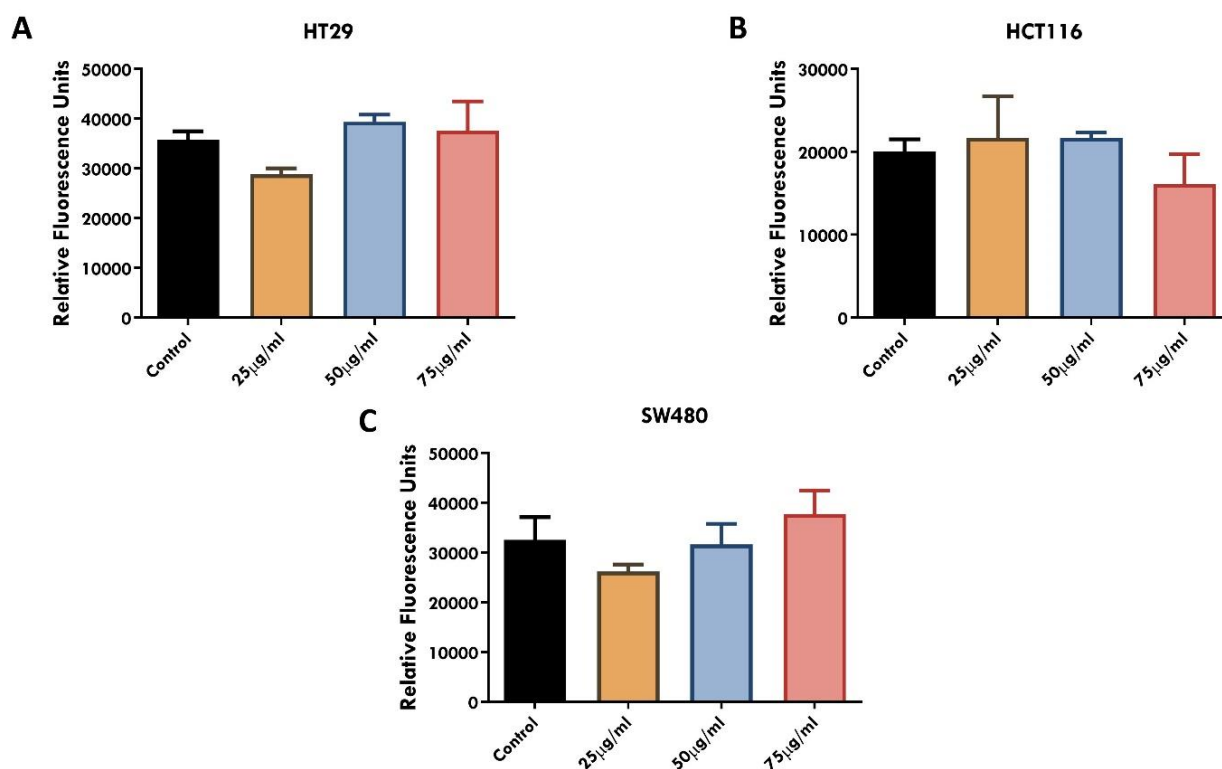


Figure 4.2: Analysis of caspases 3/7 activity in the presence of three different concentrations of deflamin in CRC cell lines. The Apo-ONE® Homogeneous Caspase-3/7 Assay kit was used to determine the activity of caspases 3/7 of CRC cell lines to deflamin (25 – 75 µg/mL). Activity of caspase 3/7 in (a) HT29, (b) HCT116 and (c) SW480 cell lines.

As previously seen, deflamin plays an inhibitory role on MMPs in the ECM, namely MMP-2 and MMP-9. Adding, previous and unpublished results from LCosta Lab at IMM, also showed anti-tumoral activities of deflamin based on the inhibition of MMPs. However, we wondered if it could also have an action mechanism of tumoral inhibition by inducing cellular damage and, consequently, cellular apoptosis, as many chemotherapeutic agents currently do. Many new drugs are available for use in the treatment of colorectal cancer, resulting in improved prognosis, but also more frequent and severe side-effects [120].

These results suggest that deflamin does not induce the activity of the main apoptosis caspases. Since it does not play a role in apoptosis or cell viability, we can infer that deflamin could be a good nutraceutical and a great candidate to become a valuable anti-tumoral agent, as well as a powerful asset for the treatment and prevention of inflammatory diseases such as IBD.

4.1.3. Epithelial to mesenchymal transition

The epithelial-to-mesenchymal-transition (EMT) implies the acquisition of mesenchymal features by epithelial cells, such as CRC cells. The events occurring during EMT include (1) the loss of adherents junctions and the downregulation of cytokeratins and E-cadherin, epithelial specific markers, (2) the increase of mesenchymal markers, such as fibronectin, N-cadherin, and vimentin, and (3) the gaining of a fibroblastic invasive phenotype [121].

In 2016, Lima *et al.* group [79] reported that the HT29 cell line was less invasive when in the presence of the albumin fraction of *L. albus*, indicating that a protein fraction of this species was inhibiting cellular migration in 2D cultures. Later, in 2019, Bianca Basso, a master student developing her thesis in LCosta group at IMM, showed that two different concentrations of deflamin, 40µg/mL and 80µg/mL, inhibited the 2D migratory activity of three CRC cell lines, namely HT29, HCT116 and SW480 (data not published). Since the migratory capacity of tumor cells is directly associated with EMT, we wondered whether deflamin could play a role in the EMT process of cancer cells.

Therefore, we compared the protein levels of epithelial and mesenchymal markers, such as E-cadherin, N-cadherin, and vimentin of CRC cell lines SW480, HCT116 and HT29, treated with two different concentrations of deflamin (figure 4.3).

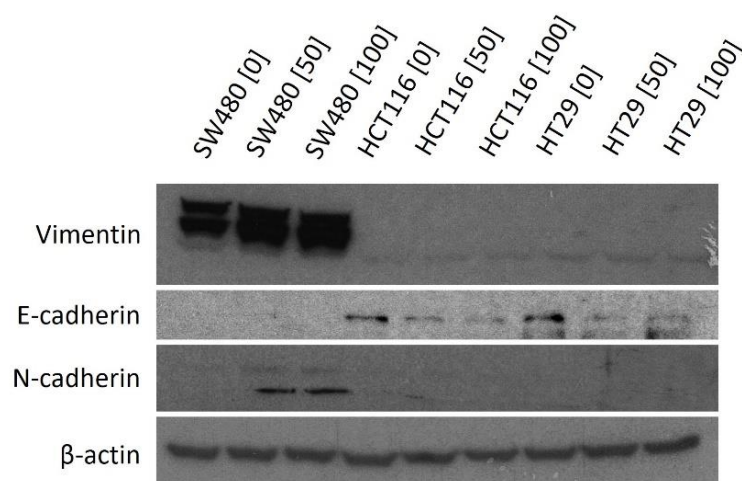


Figure 4.3: Western-blot analysis. Effect of deflamin (0, 50 and 100µg/mL) in EMT markers for the CRC cell lines SW480, HCT116 and HT29, respectively.

In our panel of cells, we can observe that vimentin was slightly increased by the treatment of SW480 cells with deflamin. For the cell lines HCT116 and HT29, vimentin was barely detected probably because these cell lines are highly epithelial. Regarding the expression of E-cadherin, it was not detected for the SW480 cell line, however, HCT116 and HT29 cell lines showed a decrease in E-cadherin expression with increasing deflamin concentration, when compared to untreated controls. Finally, and in agreement with the previous results SW480 cell line showed an increase of N-cadherin for both deflamin concentrations (50µg/mL and 100µg/mL) when compared to non-treated cells. Again, N-cadherin was not detected in HCT116 and HT29 cell lines, neither after deflamin treatment.

It is worth to mention that while E-cadherin is an epithelial marker, and that its loss leads to cells with a greater invasive and migratory capacities, as they lose their cell-cell adherents junctions, N-cadherin and vimentin are mesenchymal markers. Overall, our results seem to indicate that deflamin treatment leads to a more mesenchymal phenotype, both in cancer cells already expressing mesenchymal markers, such as SW480 cell line, or in CRC cell lines more epithelial such as HCT116 and HT29.

The results suggest that the presence of deflamin in the medium can lead the cells to a phenotype with mesenchymal-like characteristics. This result is unexpected given the previous *in vitro* and *in vivo* results of an anti-tumoral role of deflamin, therefore more experiments are needed in order to explore the impact that deflamin has on EMT and cancer associated development.

4.1.4. Signaling Pathways

We went further to investigate if deflamin could alter the regulation of intracellular signaling pathways involved in proliferation and apoptosis, such as MAPK and the PI3K-AKT pathways^[122,123]. When activated, these pathways can lead to excessive and uncontrolled proliferation as well as an inhibition of apoptosis, which in turn is associated with tumor aggressiveness^[122,123].

In our panel of CRC cell lines, neither P-ERK nor P-AKT was affected by any of the deflamin's concentrations (figure 4.4), when compared to the control situation, indicating that deflamin does not play a role regulating these pathways. These results complement and agree with the results obtained for cell proliferation and apoptosis, where it is verified that deflamin does not appear to interfere with intracellular processes, but rather exhibits its anti-tumor action in extracellular processes, such as ECM degradation.

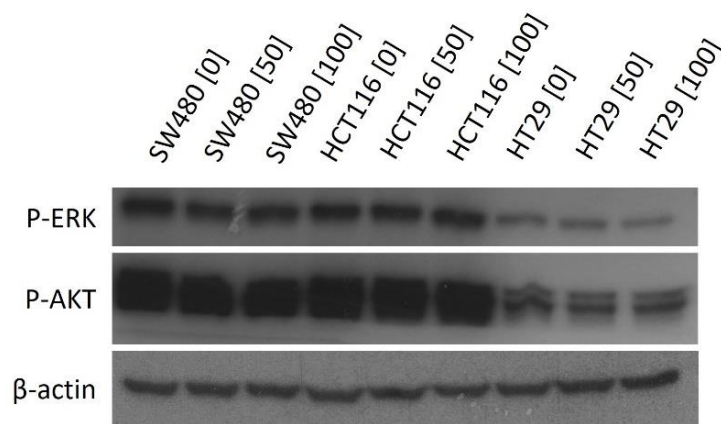


Figure 4.4: Western-blot analysis. Effect of deflamin (0, 50 and 100 μ g/mL) in MAPK and PI3K/AKT pathways for the CRC cell lines SW480, HCT116 and HT29, respectively.

4.2. Inhibitory activity of deflamin in *in-vitro* 3D models

Previous studies on the activity of deflamin have shown that this oligomeric protein had an inhibitory effect on the activity of MMP-9, both in inflammatory bowel diseases as well as in the HT29 cell line of CRC [50,59,79]. In this sense, further studies were carried out by our lab, LCosta, at IMM, to better understand the activity of deflamin on other CRC cell lines, namely in verifying its anti-tumor activity in *in vivo* models with zebrafish. The results were very promising for some of the seven cell lines studied (HT29, SW480, HCT116, SW48, SW837, CACO2 and LOVO), specifically for the lines HT29, HCT116 and SW480, where a clear inhibition of the migratory activity in 2D cellular cultures was observed [63]. In addition, zymographic analyzes were also performed to test the gelatinolytic activity of the total extract of MMPs, and specifically of the gelatinases MMP-2/9, in all cell lines [63]. The results indicated that, for the cell lines SW480 and HT29, deflamin was capable of reducing the gelatinolytic activity of the total MMP extract as well as for MMP-2 and MMP-9, reinforcing its previously mentioned activity against the metalloproteinases in the extracellular matrix.

Thus, and in order to explore further the work already developed, we proposed to better understand the MMP inhibitory activity of deflamin using 3D models. Therefore, we tested the role of deflamin in cellular proliferation and invasion of HT29, HCT116 and SW480 cell lines using the 3D spheroid model.

As described earlier in the section “1.9. Use of *in vitro* 3D models”, 3D cultures are *in vitro* techniques where immortalized cell lines are placed within hydrogel matrices [92,124]. This multicellular tumor spheroids have been developed to overcome limitations of 2D cultures [94,95], mainly as the growth of cells in spheroids influences cell behavior, cell shape, polarity, gene expression, proliferation, cell motility, differentiation and drug sensitivity as well as radiation resistance [92,94,95,124].

This 3D cell model allows a better approach to carry out our tests with potential anti-tumor drugs, such as deflamin, since it more reliably represents the natural environment *in vivo*. The presence of abundant cell-cell/cell-ECM intercommunications within 3D spheroids leads to a substantial difference compared to 2D cultured cells, allowing a better, more trustworthy analysis of cell migration, growth, survival, and differentiation.

4.2.1. Spheroid proliferation in different CRC cell lines

In order to assess the effect of deflamin on tumor development, we used a 3D model of spheroid formation. Spheroids were formed in 384-well plates where, in each well, a spheroid-forming solution with approximately 500 cells is applied. The plate is then placed in a humid atmosphere, at 37°C, for 72h, for the formation of the spheroids. After 72h, the medium where the spheroids were formed was changed to a new medium, prepared for the three conditions: control, without deflamin; 50µg/mL and 100µg/mL of deflamin, respectively. After gel formation (about 1 hour), the spheroids are observed under a confocal microscope, every 24 hours, for 72 hours, in order to determine the growth rate.

Starting with the HT29 cell line, there is no significant difference seen between the control and the 50µg/mL deflamin group for any of the time points (24hr, $p=0,1230$; 48hr, $p=0,2369$; 72hr, $p=0,2187$). However, when comparing the control group with spheroids treated with a deflamin concentration of 100µg/mL, there is a statistical significance in spheroid size reduction for all time points (24hr, $p=0,0331$; 48h, $p=0,0164$, 72h, $p= 0,0080$) (figure 4.5B).

According to the results, there is a tendency to an inhibitory effect of deflamin on cell proliferation in spheroid models of the HT29 line, but only significant for a treatment condition of 100µg/mL of deflamin. Thus, we also assessed the 3D proliferation of cell lines HCT116 and SW480, for both concentrations of deflamin, in order to verify if the same would happen.

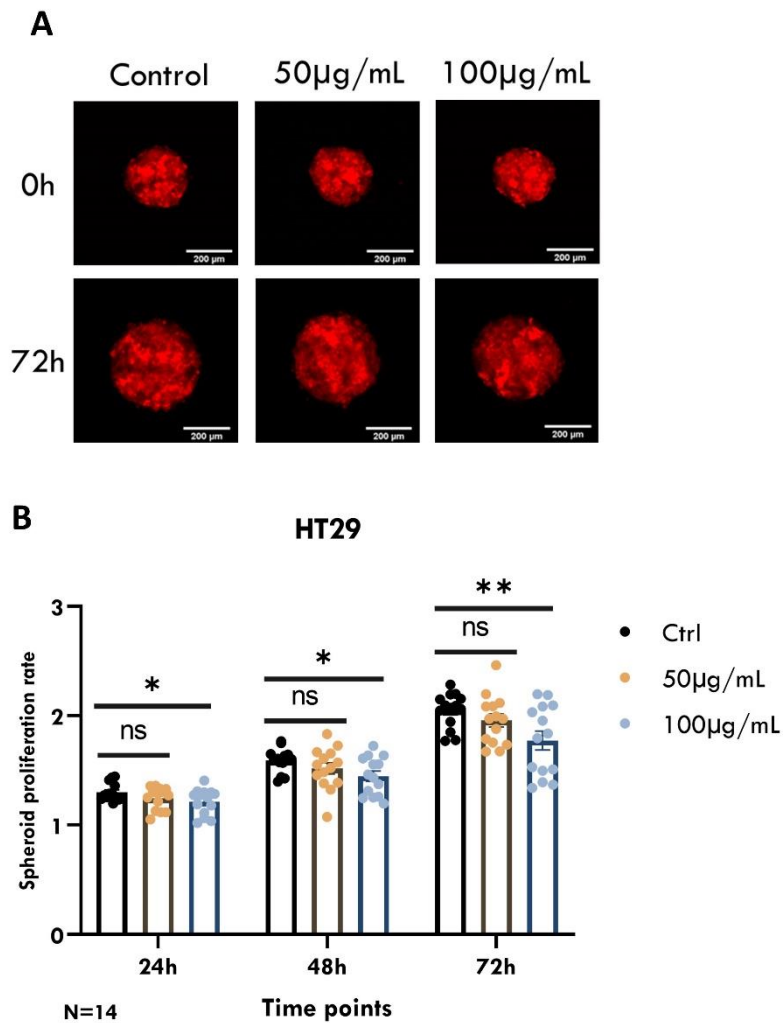


Figure 4.5: Effects of deflamin on 3D cellular proliferation in human colorectal cancer HT29 cell line. (A) Representative image of cellular spheroids for the time points 0h and 72h, for control, 50 μ g/mL, and 100 μ g/mL of deflamin. (B) Quantification of cellular proliferation rate for the time points 24h, 48h and 72h, for control, 50 μ g/mL, and 100 μ g/mL of deflamin. Data are present as means \pm SEM. The number of spheroids analyzed is indicated in the representative images and each dot on the graphic represents one cellular spheroid. Statistical analysis was performed using an unpaired t-test. Statistical results: (ns) >0.05 , * $p\leq 0.05$, ** $p\leq 0.01$. Scale bars represent 200 μ m.

Regarding the HCT116 cell line, there is no significant difference between the control group and a deflamin concentration of 50 μ g/mL at the time point of 24h ($p=0,4009$), nor for 48h ($p=0,5786$) or 72h ($p=0,1708$). The same was observed when comparing the control group with the treatment of 100 μ g/mL deflamin, where there is no statistical significance for 24h ($p=0,6731$), 48h ($p=0,3994$) or 72h ($p=0,8571$) (figure 4.6B).

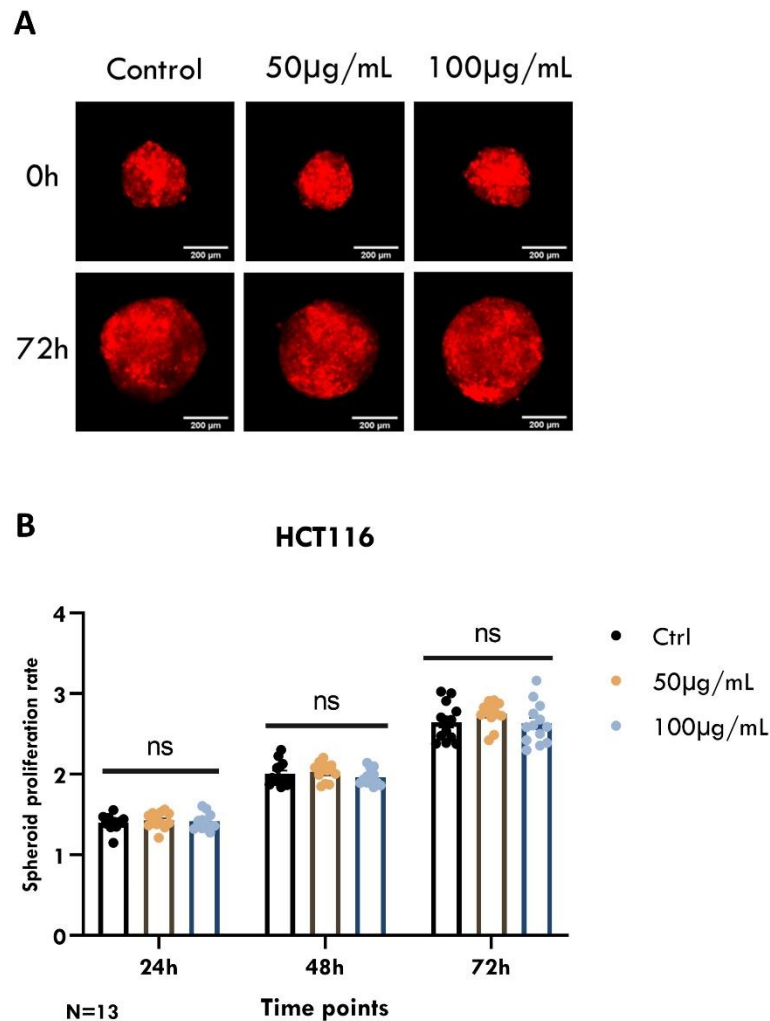


Figure 4.6: Effects of deflamin on 3D cellular proliferation in human colorectal cancer HCT116 cell line. (A) Representative image of cellular spheroids for the time points 0h and 72h, for control, 50 μ g/mL, and 100 μ g/mL of deflamin. (B) Quantification of cellular proliferation rate for the time points 24h, 48h and 72h, for control, 50 μ g/mL, and 100 μ g/mL of deflamin. Data are present as means \pm SEM. The number of spheroids analyzed is indicated in the representative images and each dot on the graphic represents one cellular spheroid. Statistical analysis was performed using an unpaired t-test. Statistical results: (ns) >0.05 . Scale bars represent 200 μ m.

The SW480 cell line also does not show significant differences between the control group and a deflamin concentration of 50 μ g/ml at the time point of 24h ($p=0,9601$), nor for 48h ($p=0,8807$) or 72h ($p=0,6769$). When comparing the control group with the treatment of 100 μ g/mL deflamin, we observe that there is no statistical significance for 24h ($p=0,2778$), 48h ($p=0,2815$) or 72h ($p=0,1850$) (figure 4.7B).

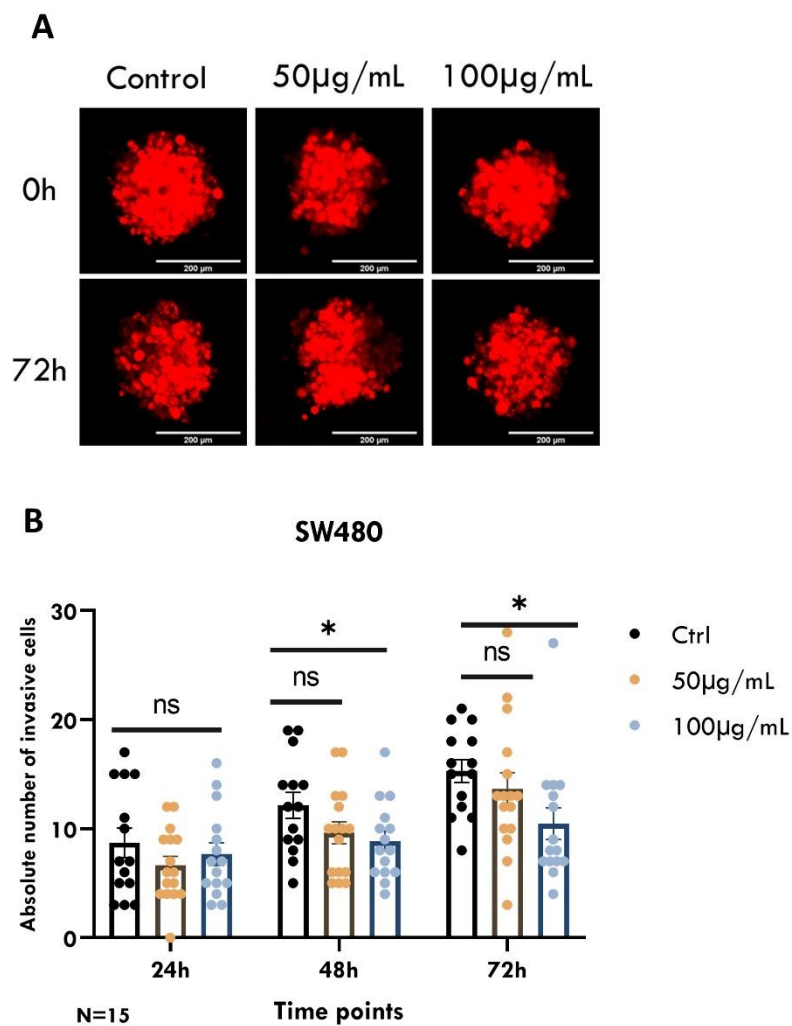


Figure 4.7: Effects of deflamin on 3D cellular proliferation in human colorectal cancer SW480 cell line. (A) Representative image of cellular spheroids for the time points 0h and 72h, for control, 50 μ g/mL, and 100 μ g/mL of deflamin. (B) Quantification of cellular proliferation rate for the time points 24h, 48h and 72h, for control, 50 μ g/mL, and 100 μ g/mL of deflamin. Data are present as means \pm SEM. The number of spheroids analyzed is indicated in the representative images and each dot on the graphic represents one cellular spheroid. Statistical analysis was performed using an unpaired t-test. Statistical results: (ns) >0.05 . Scale bars represent 200 μ m.

The results obtained indicate that deflamin did not significantly alter the growth rate for the cell lines HCT116 and SW480, at any of the time points, for any of the concentrations (50µg/mL and 100µg/mL).

In general, the results obtained for the 2D vs 3D cell proliferation assays are in concordance, with the exception of the HT29 line, for which deflamin seems to play a relevant role when observing the 3D results. Considering the proliferation curves obtained in 2D for this line (figure 4.1a), it can be seen that the growth of HT29 cells is much slower than that of the other lines. This fact can determine HT29 cell line higher sensitivity towards deflamin treatments, which would result in a lower proliferation rate when subjected to deflamin.

However, it is necessary to bear in mind that results obtained in 2D cannot be extrapolated to 3D models. Cells in 2D monocultures, in addition to growing on a plastic surface, do not show the same characteristics or interactions as cells in 3D models, suspended in a hydrogel matrix, where the environment more remarkably resembles the ECM. Likewise, it is not entirely unexpected to observe a difference between 2D and 3D assays, since on 2D plastic surfaces cells are unable to reproduce the real complexity and 3D structure expected. Adding up, the MMP effect on the ECM and upon other proteins besides collagen, like e-cadherin, growth factors, TGF-β, among others, may differ when considering 2D vs 3D models.

Nevertheless, it was not expected to see a difference in proliferation rates between different cell lines. Since the three cell lines do not show exorbitant differences from each other, nor do they have relevant mutations that cause them to have a different phenotype, it would not be expected that deflamin would affect the proliferation of a single cell line.

Considering the results obtained for cell proliferation of the HT29 line and the fact that they differ from the other lines, it would be necessary to carry out more studies in order to understand these discrepancies. An assay on spheroid apoptosis could be performed, at different concentrations of deflamin, using cell markers such as caspase 3, to assess whether the observed results are due to a lower proliferation rate or to an apoptotic rate. This because spheroids tend to develop a necrotic center, similar to tumors, due to oxygen constriction and lack of nutrients. This apoptotic rate could be masked, in a way, by a lower proliferative rate. We could also do a flow cytometry assay, where we would stain the DNA with a cell cycle reagent and sort the cells by cell cycle phase, as deflamin might not have an effect on the cell cycle in a 2D monolayer but can exhibit an effect on a 3D model. This assay would create a histogram of the DNA content distribution across the steps of the cell cycle, and we could see if deflamin is interfering with proliferation.

4.2.2. Spheroid invasion in different CRC cell lines

In order to access the effect of deflamin on cellular invasion, we used a 3D model of spheroid formation. Spheroids were formed in 384-well plates where, in each well, a spheroid-forming solution with approximately 500 cells is applied. The plate is then placed in a humid atmosphere, at 37°C, for 72h, for the formation of the spheroids. After 72 hours, the medium where the spheroids formed is changed. For invasion assays, a collagen matrix is formed, with mitomycin in order to ensure that the observed results are due to invading cells and not spheroid cell proliferation, which is applied to each well in order to test the invasiveness of each cell line. This medium is prepared for the three conditions: control, without deflamin; 50µg/mL and 100µg/mL of deflamin, respectively. After gel formation (about 1 hour), the spheroids are observed under a confocal microscope, every 24 hours, for 72 hours, in order to determine the number of invasive cells.

Our results indicated that, relative to the HT29 cell line, there was a significant inhibition of cell invasion at the time points of 48h ($p=0,0228$) and 72h ($p=0,0464$) but not at 24h ($p=0,1213$), when comparing the control group with a treatment of 100µg/mL deflamin. There was also no statistically significant inhibition when comparing control vs 50µg/mL at any of the time points (24h, $p=0,4647$; 48h, $p=0,0642$; 72h, $p=0,1295$) (figure 4.8B), although there is a clear tendency in reduction of the number of invasive cells in treatment conditions.

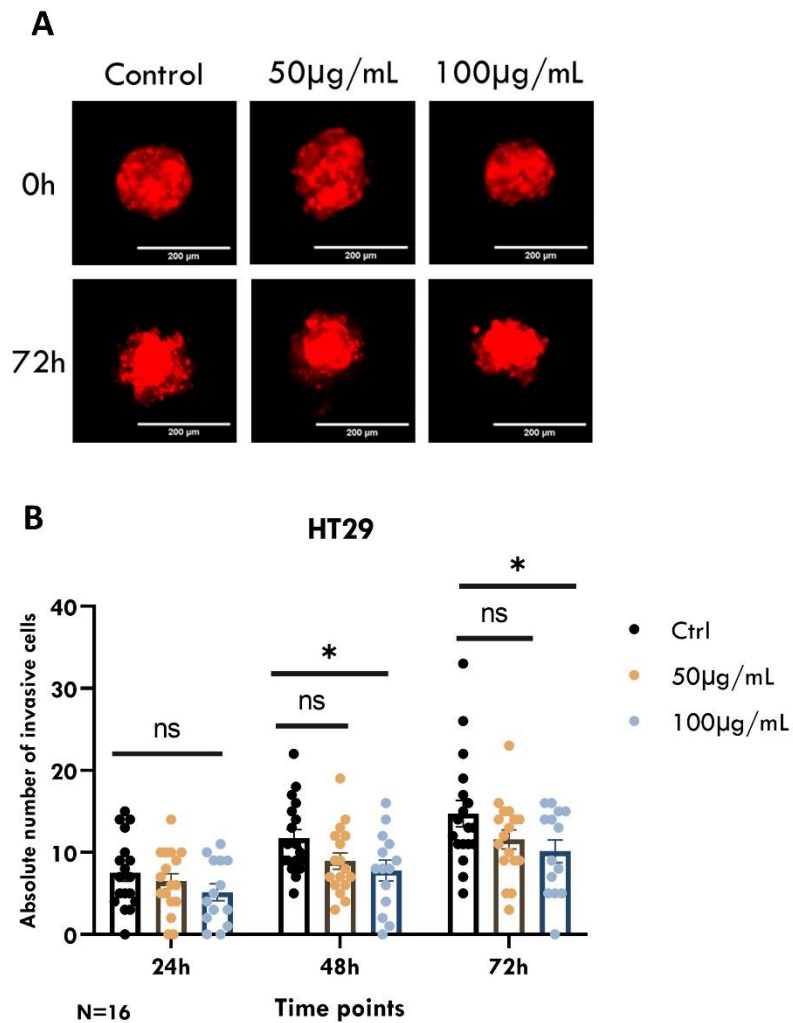


Figure 4.8: Effects of deflamin on 3D cellular invasion in human colorectal cancer HT29 cell line. (A) Representative image of cellular spheroids for the time points 0h and 72h, for control, 50 μ g/mL, and 100 μ g/mL of deflamin. (B) Quantification the absolute number of invasive cells for the time points 24h, 48h and 72h, for control, 50 μ g/mL, and 100 μ g/mL of deflamin. Data are present as means \pm SEM. The number of spheroids analyzed is indicated in the representative images and each dot on the graphic represents one cellular spheroid. Statistical analysis was performed using an unpaired t-test. Statistical results: (*ns*)>0.05. Scale bars represent 200 μ m.

Concerning the HCT116 cell line, despite showing inhibition of cell invasion when compared to the control group vs 50µg/mL, this difference is not significant for any of the time points (24h, $p=0,2939$; 48h, $p=0,1201$;72h, $p=0,1976$). However, when comparing the control group with the treatment of 100µg/mL deflamin, we see a constant inhibition of invasion that is shown to be significant for 24h ($p=0,0445$), 48h ($p=0,0468$) and 72h ($p=0,0482$) (figure 4.9B).

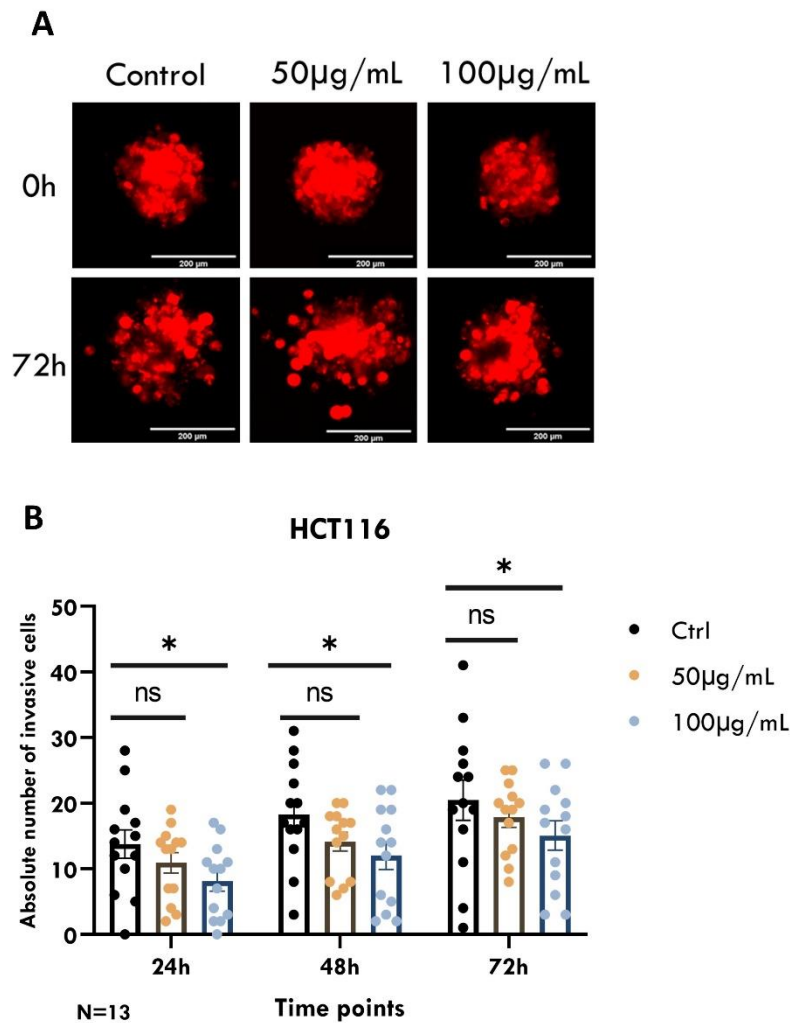


Figure 4.9: Effects of deflamin on 3D cellular invasion in human colorectal cancer HCT116 cell line. (A) Representative image of cellular spheroids for the time points 0h and 72h, for control, 50µg/mL, and 100µg/mL of deflamin. (B) Quantification the absolute number of invasive cells for the time points 24h, 48h and 72h, for control, 50µg/mL, and 100µg/mL of deflamin. Data are present as means \pm SEM. The number of spheroids analyzed is indicated in the representative images and each dot on the graphic represents one cellular spheroid. Statistical analysis was performed using an unpaired t-test. Statistical results: (ns) >0.05 . Scale bars represent 200µm.

Lastly, the SW480 line also showed a statistically significant and ascending inhibition when compared to the control group vs treatment of 100µg/mL, for the 48h ($p=0,0365$) and 72h ($p=0,0130$) time points, but not for the 24h ($p=0,5100$). Similar to previous cell lines, the concentration of 50µg/mL of deflamin did not significantly inhibit cell invasion for any of the time points (24h, $p=0,1861$; 48h, $p=0,1145$; 72h, $p=0,3895$) (figure 4.10B).

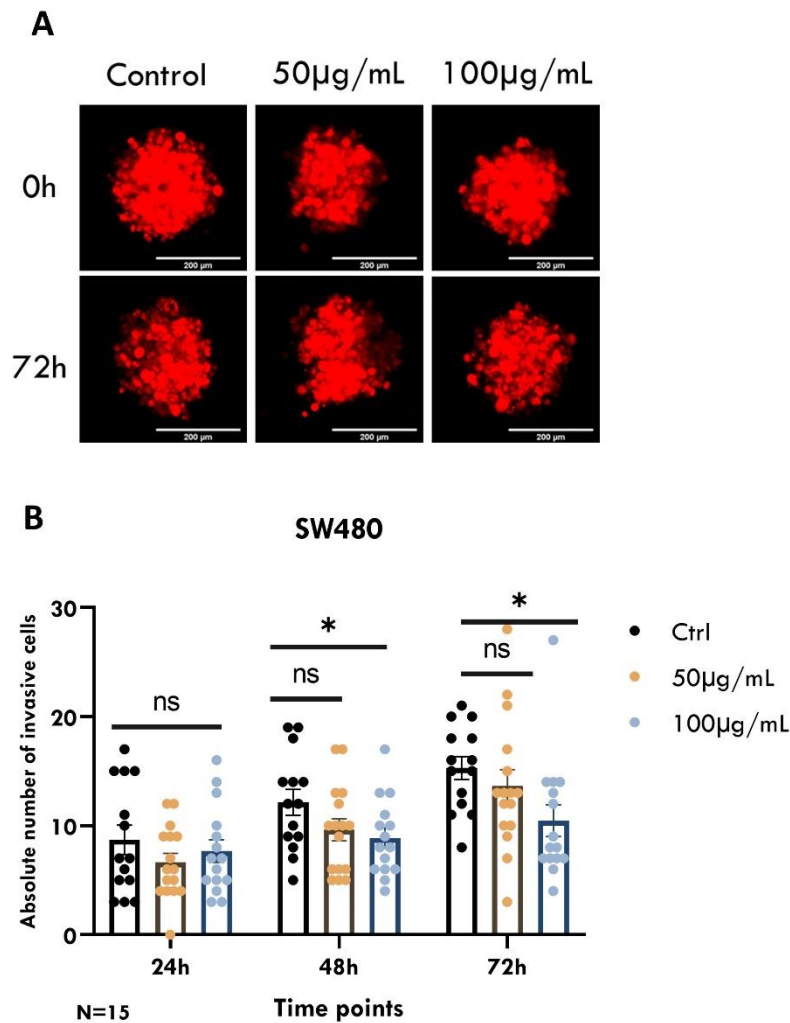


Figure 4.10: Effects of deflamin on 3D cellular invasion in human colorectal cancer SW480 cell line. (A) Representative image of cellular spheroids for the time points 0h and 72h, for control, 50µg/mL, and 100µg/mL of deflamin. (B) Quantification the absolute number of invasive cells for the time points 24h, 48h and 72h, for control, 50µg/mL, and 100µg/mL of deflamin. Data are present as means \pm SEM. The number of spheroids analyzed is indicated in the representative images and each dot on the graphic represents one cellular spheroid. Statistical analysis was performed using an unpaired t-test. Statistical results: (ns) >0.05 . Scale bars represent 200µm.

According to the results obtained in our panel of CRC cell lines, there is a clear inhibition of the migratory activity of cells when in the presence of 100µg/mL of deflamin in the spheroid formation solution. As regards the HT29 and SW480 lines, this inhibition is observed for all time points but only significant for 48h and 72h ($p<0,05$), while for the HCT166 line there is a significant inhibition for all time points tested.

As previously stated, cancer cells are able to remodel the extracellular matrix through the activation of a complex system of proteases. Among these enzymes are metalloproteinases 2 and 9, previously described as good therapeutic targets in CRC to limit cell migration and invasion and, consequently, decrease metastasis. These proteases act mostly upon the degradation of type IV collagen, which is the main target to be broken down during tumor invasiveness ^[125].

The scaffold-based systems used in 3D cell cultures are structures that mimic the extracellular matrix (ECM) composition to simulate the native acellular microenvironment ^[126]. In our experiments, we used human collagen, which is the most prevalent embedding material used to create an artificial matrix, as it is both a component of the ECM, and is upregulated within a tumor microenvironment ^[127].

As previously verified *in vitro*, deflamin showed an inhibitory activity on 2D cellular migration as well as an inhibition on the gelatinolytic activity of both metalloproteinases 2 and 9 for several CRC cell lines ^[63]. This inhibition of MMP activity leads to a decrease in extracellular matrix degradation and remodeling, which, in turn, promotes less cell migration and invasion. Since MMP-2 and MMP-9 are shown to be degrading enzymes of type IV collagen, the main component of the ECM *in vivo*, promoting cell invasion, and that deflamin is reported to have an inhibitory activity on the gelatinolytic activity of these gelatinases, we hypothesized that deflamin could exert an inhibitory action of gelatinases in 3D *in vitro* assays, leading to the inhibition of cellular invasion. Our results go in line with our hypothesis since a clear inhibition of invasion is seen when deflamin is present at a higher concentration in the formation solution. A possible explanation for the results obtained in 3D assays is that deflamin, by inhibiting MMP-2/9, inhibits the degradation of the ECM, in this case of collagen, thus preventing the migration and cell invasion of the cells that make up the spheroid.

This inhibitory activity of cell invasion may take more or less time to occur, depending on the cell line being analyzed and its characteristics. Line HT19 (ATCC®-HTB-38™) is a cell line originating from a stage I/grade I primary tumor of the colon while SW480 (ATCC®-CCL-228™) is a cell line originating from a primary tumor, stage II/grade IV also from the colon. The HCT116 line (ATCC®-CCL-247™) was isolated from a patient with advanced metastatic disease. These differences between tumor and cell line grade and stage may account for the temporal differences found for significant inhibition of cell invasion observed in 3D spheroid models.

Although the results in 3D spheroid models present themselves as very promising and appearing to have a potential anti-tumor effect of deflamin on various colorectal cancer cell lines, there are some limitations to this study. For example, specific labeling for MMP-2 and MMP-9 were not performed in order to compare their activity between the control group and the treated groups, and to understand if there is any inhibition of gelatinolytic activity in 3D *in vitro* models. Also, zymography of the spheroid formation media were not performed, which would be very useful to understand and corroborate inhibitory activity of deflamin on the gelatinolytic activity of MMPs. Although there are several studies, already mentioned, that correlate deflamin with an inhibitory role of MMP-2 and MMP-9, there are still no studies that access this activity in 3D *in vitro* models.

4.3. Anti-tumoral activity of deflamin *in-vivo*

As previously mentioned, prior studies to this dissertation were performed regarding the anti-inflammatory activities of deflamin in *in vivo* models of colitis using mice ^[50]. These studies revealed that mice treated with deflamin showed reduced signs of colon inflammation, corroborating the anti-inflammatory activities of deflamin *in vitro*.

Later, in 2019, the inhibitory and anti-tumoral activity of deflamin in *in vivo* models using zebrafish was accessed by Bianca Basso at iMM ^[63]. According to the results obtained, it was found that deflamin revealed anti-tumor activity, interfering with the cellular growth (treated tumors were almost four times smaller when compared to the control group) and apoptotic rates (four times increased rate when compared to control) in tumors of the HCT116 cell line ^[63]. To better understand the effect of deflamin on the proliferative process of tumor cells, the number of mitotic spindles was also accessed but no significant differences were observed between the treated and control group ^[63], suggesting once more that deflamin does not interfere with cellular cycle or cell viability.

Despite the evidence that deflamin has an anti-tumoral activity, there are action mechanisms of deflamin that have not yet been proven or demonstrated, requiring different experiments that access other aspects of the inhibitory action of deflamin. Therefore, we wondered whether MMPs inhibition induced by deflamin could affect ECM remodeling and have an impact on angiogenesis. For that, we decided to access two of those principles: 1. The effect of deflamin on angiogenesis and vascular remodeling, and 2. The effect of deflamin on type IV collagen degradation, the main target of gelatinases.

In order to evaluate a possible anti-tumoral action and a potential therapeutic role of deflamin in an *in vivo* model, we xenotransplanted the HCT116 CRC cell line into the perivitelline cavity of zebrafish larvae at 48hpf. 24hpi, the xenografts successfully injected were separated into three groups: a control group treated with 1x PBS, and two groups of treatment with deflamin, at concentrations of 50 μ g/mL and 100 μ g/mL, respectively into E3 medium (figure 4.11). Over a period of three consecutive days, the medium was changed and new deflamin was added to the treated groups as well as new medium to the control group. After this period, only animals with tumors were analyzed.

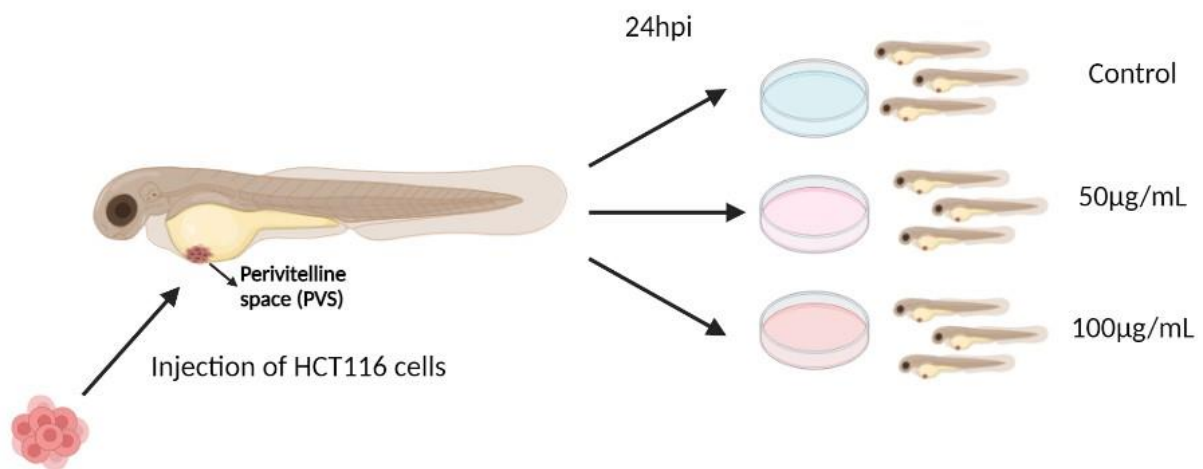


Figure 4.11: Experimental setup for generating zebrafish xenografts and posterior analysis. Cell line HCT116, derived from *in vitro* culture and previously labelled with dtTomato are microinjected in the PVS of 2dpf larvae. One day after injection, larvae are screened for successful injection and distributed in three different groups: untreated control and two treatment groups, 50 μ g/mL, and 100 μ g/mL of deflamin, respectively.

4.3.1. Angiogenesis analysis in transgenic zebrafish model Tg(kdr1:eGFP)

In order to understand whether the inhibitory effects of deflamin on MMPs have consequences for angiogenesis and new blood vessel formation, the zebrafish model Tg(kdr1:eGFP) was used. This model has the blood vessels labeled with GFP fluorescence, which allows us to see new vessel formation under confocal microscopy. The cells used were fluorescently labeled with dtTomato and an immunofluorescence was performed using DAPI to label cell nuclei (figure 4.12). Using this model, our analyzes allowed us to determine two parameters: (1) the total vessel density and (2) the vessel infiltration.

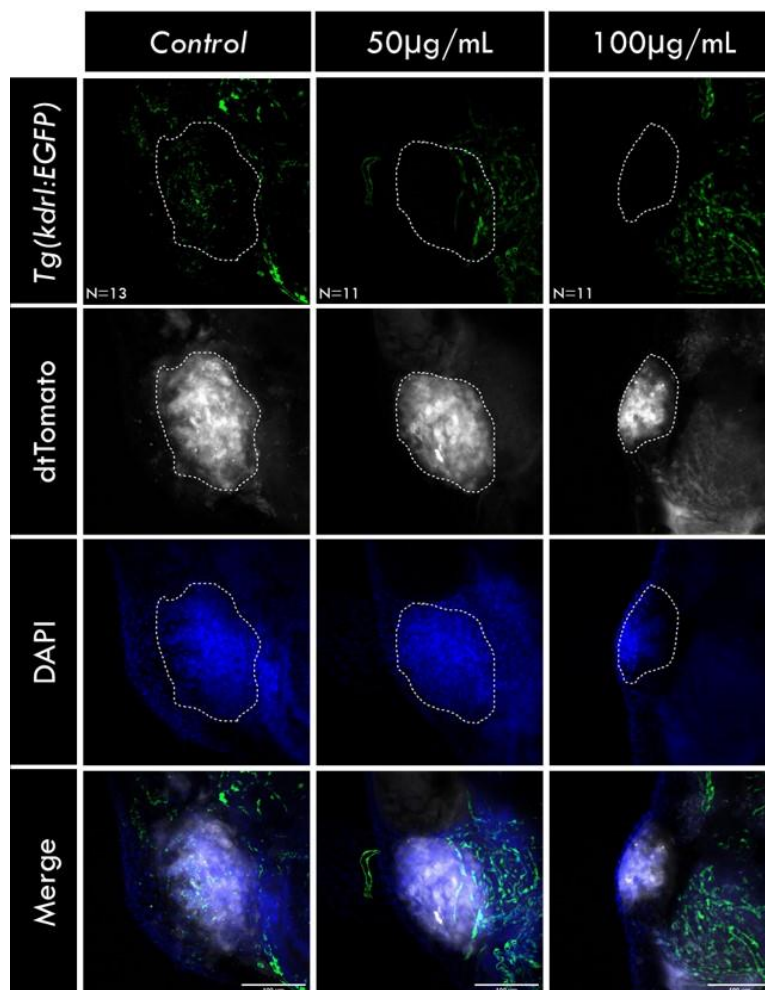


Figure 4.12: Zebrafish vasculature analysis in HCT116 xenografts. Human cancer cell line HCT116 was fluorescently labeled with dtTomato (in white) and injected into the PVS of 2dpf Tg(kdr1:eGFP) zebrafish larvae. Zebrafish xenografts were treated *in vivo* with deflamin (50µg/mL and 100µg/mL) and compared with untreated controls. Zebrafish xenograft vasculature was imaged by confocal microscopy (in green). The number of zebrafish analyzed is indicated in the representative images. Scale bars represent 100µm.

Regarding vessel density, and according to the analysis of the results, there is no significant difference between the control group and both treated groups, 50 μ g/mL ($p=0,1209$) and 100 μ g/mL ($p=0,8623$), indicating that deflamin does not affect the formation of new blood vessels (figure 4.13A). Concerning the vessel infiltration there is also no significant difference between the control and treated groups, 50 μ g/mL ($p=0,9867$) and 100 μ g/mL ($p=0,1093$), indicating that deflamin does not interfere, at least significantly, when it comes to regulating the infiltration of the new blood vessels (figure 4.13B). However, there is a trend to lower infiltration of blood vessels for higher concentration of deflamin without, however, being statistically significant.

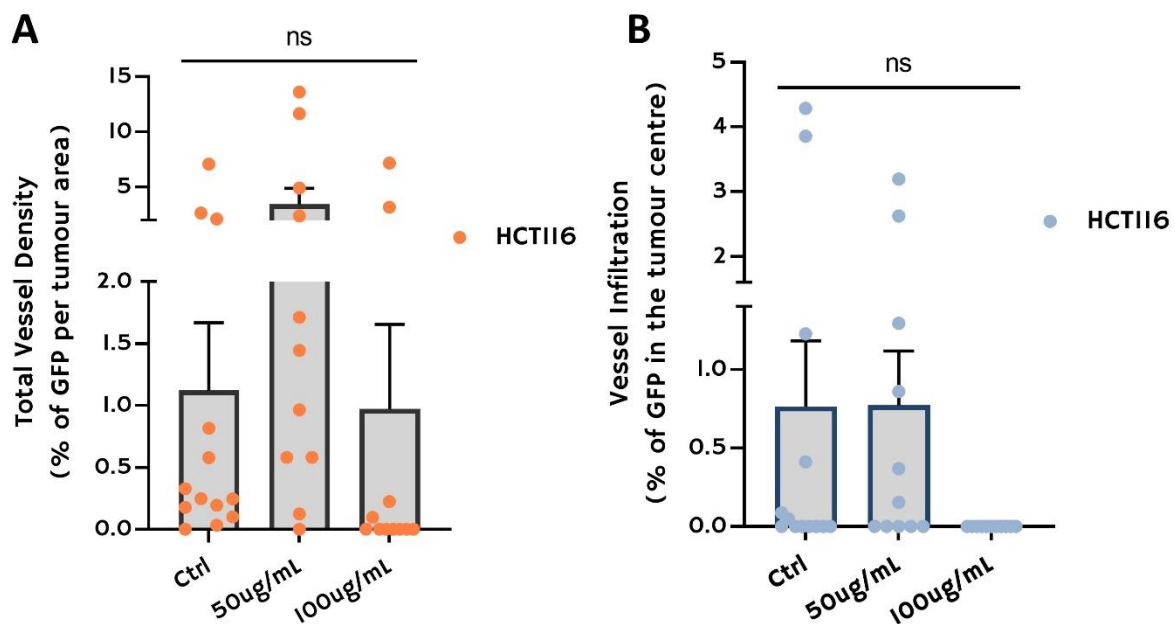


Figure 4.13: Angiogenesis quantification in zebrafish HCT116 xenografts. Total vessel density (A) and vessel infiltration (B) were quantified. Vessel density was assessed throughout z projections of corresponding images using ImageJ Z Projection tool and the percentage of eGFP fluorescent per tumor was quantified. To analyze vessel infiltration, the superficial slices of the tumor were not considered and the percentage of eGFP fluorescent per tumor core was quantified. All outcomes are expressed as means \pm SEM. Each dot on the graphic represents one zebrafish xenograft. Statistical analysis was performed using an unpaired t-test. Statistical results: (ns) >0.05 .

According to our results, we found that deflamin does not seem to interfere with the angiogenesis in tumors of the CRC cell line HCT116. However, and despite the lack of regulation of the formation of new blood vessels, there is a trend towards lower vessel infiltration in samples with higher concentration of deflamin, 100 μ g/mL.

As previously described one of the main principles applicable to all tumors is its ability to generate a blood vascular supply, promoting tumor growth and evasion through the supply of nutrients and formation of new blood vessels around and inside the tumoral mass. Neo angiogenesis at primary tumor sites is a key element of cancer spread and progression [128], and is thought to occur after an “angiogenic switch” is triggered. At this point the cancer colony reaches a size where perfusion is necessary to provide nutrients and oxygen for growth [128]. Thus, the process of new vessel formation could present targets for inhibition of tumor recurrence and metastasis [128].

It has also been shown that MMPs are well known to be key enzymes for tumor invasion and metastasis, as they act both as positive and negative regulators of angiogenesis [49]. Several pro-angiogenic factors, such as vascular endothelial growth factor (VEGF), basic fibroblast growth factors (bFGF), TGF- α and TGF- β , are induced or activated by these enzymes, triggering the angiogenic switch during carcinogenesis and facilitating vascular remodeling and neovascularization [55,56]. Some angiogenic factors require proteolytic cleavage for their full activity, raising the attractive idea of indirectly interfering with angiogenic factors by targeting their activating proteases [129], namely MMP-2, MMP-9 and MMP-14[40].

As previously verified *in vitro*, deflamin showed an inhibitory action on the migration and gelatinolytic activity of gelatinases mainly in the lines HT29, SW480 and HCT116 [50,59]. Considering that gelatinases actively participate in the initial process of tumor growth, through the remodeling of the ECM and formation of new blood vessels, through the bioavailability of pro-angiogenic and growth factors [55,56,129], and that deflamin could exert an inhibitory action on the activity of gelatinases in zebrafish, we hypothesized that deflamin, by inhibiting gelatinases, could be promoting the inhibition of new vessel formation in the primary tumor. However, this inhibition was not found, at least significantly, for the formation of new vessels but a trend was seen in the inhibition of blood vessel infiltration.

These results can be explained by diverse reasons. First, 72h after starting treatment, the animals were sacrificed and analyzed. If tumor-infiltrating angiogenesis takes longer to be expressed or seen, it would be necessary to prolong the experimental time. Second, angiogenesis is a process that is not only controlled by MMPs, but by many other factors, which are also regulated by other cellular pathways.

In the past decades, a plethora of angiogenic factors have been identified that directly or indirectly induce proliferation and differentiation of endothelial cells ^[129]. Of the polypeptide factors, VEGF-A is a prototypic pro-angiogenic factor and a major regulator of physiological and pathological angiogenesis ^[129]. Although many elements may influence the VEGF pathway, hypoxia remains the main factor that regulates angiogenesis, inducing VEGF-A expression through transcription factor hypoxia inducible factor-1 (HIF-1) and HIF-2 ^[130]. Fibroblast growth factor (FGF)-1 and -2 and platelet-derived growth factor (PDGF)-B and C are also important positive regulators of angiogenesis, as they induce endothelial cell proliferation and migration by their direct interaction with their specific receptors expressed on endothelial cells ^[129]. Angiopoietins also contribute to angiogenesis by cooperating with other angiogenic factors in modulating the activation status of endothelial cells by binding to the Tie-2 tyrosine kinase receptor expressed by endothelial cells ^[129].

Although some of these pro-angiogenic factors are controlled, in part, by MMPs, the inhibitory activity of deflamin on MMP-2 and MMP-9 may not be sufficient to inhibit the formation of new blood vessels, since there are other pathways that positively regulate pro-angiogenic factors. However, there may be some inhibitory action of deflamin that prevents the vessels from infiltrating the tumor mass. This lack of vessels within the tumor mass does not allow the exchange of nutrients, oxygen, and waste products by a population of clustered cells, for which the simple diffusion of these substances on their external surfaces is not adequate. This mechanism may also explain, albeit in part, the increased apoptotic rate observed on tumors of this CRC cell line in zebrafish ^[63].

4.3.2. Degraded collagen analysis in wild-type zebrafish model

Despite intensive investigation, the processes that convert mechanical signals into biochemical responses are still not fully understood. In assays performed with zebrafish, MMP-2 or MMP-9 labeling was not performed, nor was a zymography performed to verify the activity of both molecules *in vivo*. However, this strategy may be important to verify and better understand the mechanisms through which deflamin interacts with the tumor in the process of growth, ECM degradation, vessel formation, as well as migration and promotion of apoptosis.

Since previous studies by the *Lima et al.* group demonstrate the inhibitory effect of deflamin on gelatinases ^[59], especially MMP-9, it is of great interest to understand whether the targets of these enzymes, in particular type IV collagen, are also affected, and how, by the presence of deflamin.

To determine a potential effect of deflamin on degradation of type IV collagen and extracellular matrix remodeling, the wild-type zebrafish model (AB) was used. The cells were fluorescently labeled with dtTomato and an immunofluorescence was performed, using DAPI to label cell nuclei and CHP (collagen hybridizing peptide) to detect the degraded collagen (figure 4.14). Using this model, our analyzes allowed us to determine the degraded collagen area as a percentage of GFP per tumor area.

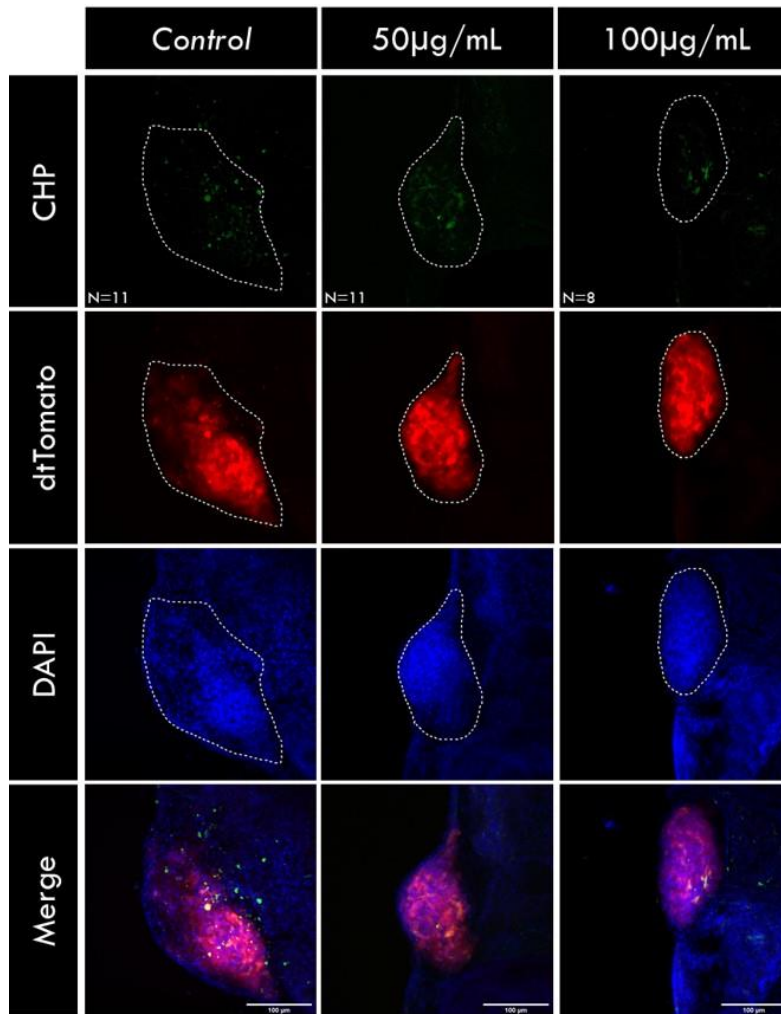


Figure 4.14: Zebrafish CHP analysis in HCT116 xenografts. Human cancer cell line HCT116 was fluorescently labeled with dtTomato (in red) and injected into the PVS of 2dpf AB zebrafish larvae. Zebrafish xenografts were treated *in vivo* with deflamin (50µg/mL and 100µg/mL) and compared with untreated controls. The collagen hybridizing peptide (CHP) was imaged by confocal microscopy (in green). The number of zebrafish analyzed is indicated in the representative images. Scale bars represent 100µm.

According to the analysis of the results, there is no significant difference between the control group and the 50µg/mL group ($p=0,4279$). However, there is a significant difference between the control and the 100µg/mL group ($p= 0,0168$), indicating that deflamin might have an inhibitory action regulating the degradation of type IV collagen (figure 4.15).

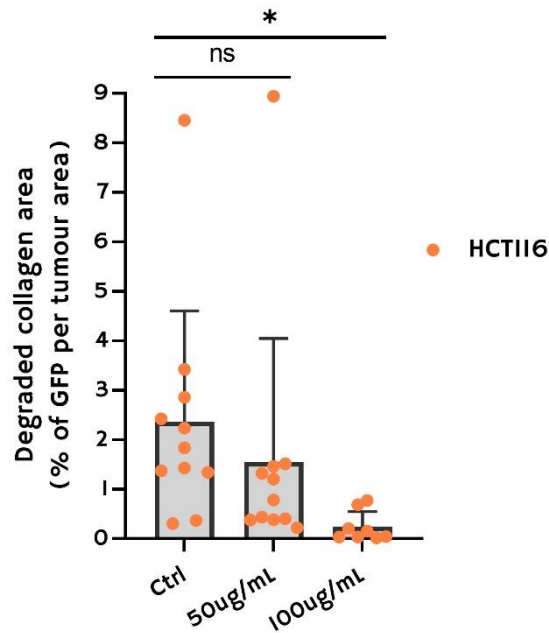


Figure 4.15: Degraded collagen quantification in zebrafish HCT116 xenografts. Degraded collagen was assessed throughout z projections of corresponding images using ImageJ Z Projection tool and the percentage of eGFP fluorescent per tumor area was quantified. All outcomes are expressed as means \pm SEM. Each dot on the graphic represents one zebrafish xenograft. Statistical analysis was performed using an unpaired t-test. Statistical results: (*ns*) >0.05 , $*p \leq 0.05$.

As described above, extracellular matrix (ECM) remodeling is one of the most important processes for malignant progression, allowing cancer cells to migrate and metastasize to other organs. In this context, disruption of the tightly controlled production, degradation, and remodeling of the major components, disorganizes the ECM, promoting abnormal cell behavior, tumor-associated angiogenesis, and inflammation, and finally leads to generation and progression of cancer microenvironment^[30,40]. Remodeling of the ECM is characterized by the increased synthesis and deposition of collagens and upregulation of matrix metalloproteinases (MMPs)^[11,30]. These enzymes process matrix components, such as collagens, leading to the production and release of bioactive fragments mainly from non-fibrillar collagens^[30].

MMP-2 and MMP-9 have been implicated to play a role in colon cancer progression and metastasis, due to their ability to degrade type IV collagen, which is a major component of the basement membrane (BM) ^[10]. Type IV collagen provides a scaffold in the BM with other macromolecules, such as laminins, proteoglycans, fibronectin, entactin, and play an important role in cell adhesion, migration, differentiation, and growth ^[131,132]. The degradation of this type of collagen provides a permissive microenvironment for invasiveness phenotype of cancer ^[132].

Bearing in mind that MMP-2 and MMP-9 are described as actively participating in the process of remodeling of the extracellular matrix, through the degradation of its main components ^[10,125], it is expected that, by inhibiting gelatinases, an inhibition of ECM remodeling occurs as well as less degradation of its main targets, namely type IV collagen. Therefore, we hypothesized that deflamin could exert an inhibitory action on the activity of gelatinases in zebrafish and, consequently, could be promoting the inhibition of degradation of type IV collagen on the primary tumor.

According to the results obtained, an inhibition of collagen degradation is verified, represented by a lower percentage of GFP per tumor area. By inhibiting these metalloproteinases, they become less bioavailable in the ECM and, therefore, there is less degradation of their substrates, namely type IV collagen. Since there is less degradation of ECM substrates, there is a greater spatial limitation for cell growth and development, two fundamental factors for tumor growth and apoptosis. Previously obtained results demonstrate, in fact, that the presence of deflamin in the medium leads to a higher apoptotic rate and lower tumor growth ^[63].

Although there are already some studies regarding deflamin and its anti-tumor action in CRC cell lines *in vitro*, there is still a great deal of research needed to prove this inhibitory activity. In assays performed with this model of zebrafish, MMP-2 or MMP-9 labeling was also not performed, nor was a zymography performed to verify the activity of both molecules *in vivo*. This can prove to be extremely important as there are several mechanisms and cellular pathways that can lead to the same end. Thus, reinforcing that the results obtained with zebrafish are a direct consequence of the action of deflamin on gelatinases can be considered an important strategy to better determine the mechanisms of action of deflamin.

5. Conclusion and future perspectives

Over the past decade, health care has been facing some main challenges for cancer therapy, such as maximizing the effectiveness and specificity of the treatment, as well as minimizing the toxicity and resistance of the therapeutic regimens.

The increment of MMPs activity is detected in a wide range of cancers and implicated in their invasive and metastatic potential, being, therefore, considered important targets for both diagnostic and therapeutic purposes. During the recent years a substantial amount of research has been made, attempting to develop synthetic, low-molecular-weight inhibitors of MMPs for the potential treatment of diseases in which they play a major role. Yet, technical difficulties, side effects and dose-dependent toxicity have greatly limited the development in the clinical practice of specific anti-MMP drugs. By contrast, interesting results have been obtained with natural compounds with anti-inflammatory and anti-tumoral activity.

Currently, studies on molecules of natural origin have shown promise in inhibiting MMPs, especially MMP-9, in inflammatory and oncogenic pathological processes. One of these molecules is deflamin, a natural compound extracted from white lupine seeds (*Lupinus albus*) that has high affinity and inhibitory activity on MMP-9 activity. In this sense, this work aimed to better explore the activity of deflamin, using 3D cellular and zebrafish models in order to better understand its mechanisms of action.

This work demonstrates that cell viability, as well as apoptosis, were not affected by the presence of deflamin in the medium, suggesting that deflamin does not exert direct cytotoxic effects on the cell lines studied, thus proving its safety as a potential therapeutic strategy against CRC. For the *in vitro* analysis with spheroid models, deflamin showed an inhibitory activity of the invasive process for the HT29, HCT116 and SW480 cell lines ($p=0,0464$; $p=0,0482$ and $p=,0130$, respectively), but it was shown not to affect cell proliferation for HCT116 and SW480 lines ($p=0,8571$ and $p=0,1850$, respectively), which reinforces its inhibitory activity on invasion, previously described in 2D cell cultures.

After the *in vitro* studies, we analyzed deflamin in *in vivo* models of zebrafish, to verify its activity on the tumor. Although deflamin does not affect the formation of new blood vessels, there is a trend observed for lower infiltration of blood vessels in the center of the tumor mass in fish from the treated group (100µg/mL) when compared to the control group ($p=0,1093$). In addition, deflamin was shown to be effective in reducing tumor degraded collagen in treated individuals compared to controls ($p=0,0168$), thus indicating less remodeling of the extracellular matrix.

In general, the results obtained corroborate previous studies, showing that deflamin inhibits the invasive activity in 3D models, as well as the remodeling of the extracellular matrix in *in vivo* models. Evidently, further studies are needed in order to consolidate our results. In this work no approaches were made regarding the effects of deflamin on the gelatinolytic activity of MMP-9 and MMP-2. This is extremely important since it is necessary to prove that the reported effects are a consequence of the action of deflamin on matrix metalloproteinases, and not on other potential targets.

In future studies, investigate the cyto- and genotoxicity effects of deflamin is necessary, and how it might have implications for clinical studies, as there are very few studies regarding the toxicity of deflamin. Deepening existing data, as well as proving the results already obtained, has the potential to reveal a new nutritional therapeutic approach, with major implications for the health and well-being of CRC patients. Additionally, a nutritional fortification of foods with deflamin has been proposed, which could be a strategy to prevent inflammatory bowel diseases associated with colorectal cancer.

6. References

1. Globocan. (2020). Colorectal Cancer Incidence in The World. *The Global Cancer Observatory*, 419, 1–2.
2. Arnold, M., Sierra, M. S., Laversanne, M., Soerjomataram, I., Jemal, A., & Bray, F. (2017). Global patterns and trends in colorectal cancer incidence and mortality. *Gut*, 66(4), 683–691. <https://doi.org/10.1136/gutjnl-2015-310912>
3. Gandomani, H. S., Yousefi, S. M., Aghajani, M., Mohammadian-Hafshejani, A., Tarazoj, A. A., Pouyesh, V., & Salehiniya, H. (2017). Colorectal cancer in the world: incidence, mortality and risk factors. *Biomedical Research and Therapy*, 4(10), 1656. <https://doi.org/10.15419/bmrat.v4i10.372>
4. Levin, B., Lieberman, D. A., McFarland, B., Smith, R. A., Brooks, D., Andrews, K. S., Dash, C., Giardiello, F. M., Glick, S., Levin, T. R., Pickhardt, P., Rex, D. K., Thorson, A., & Winawer, S. J. (2008). Screening and Surveillance for the Early Detection of Colorectal Cancer and Adenomatous Polyps, 2008: A Joint Guideline from the American Cancer Society, the US Multi-Society Task Force on Colorectal Cancer, and the American College of Radiology. *CA: A Cancer Journal for Clinicians*, 58(3), 130–160. <https://doi.org/10.3322/ca.2007.0018>
5. Ouakrim, D. A., Pizot, C., Boniol, M., Malvezzi, M., Boniol, M., Negri, E., Bota, M., Jenkins, M. A., Bleiberg, H., & Autier, P. (2015). Trends in colorectal cancer mortality in Europe: Retrospective analysis of the WHO mortality database. *The BMJ*, 351, 1–10. <https://doi.org/10.1136/bmj.h4970>
6. Arvelo, F., Sojo, F., & Cotte, C. (2015). Biology of colorectal cancer. *Ecancermedicalscience*, 9, 1–20. <https://doi.org/10.3332/ecancer.2015.520>
7. Granados-romero, J. J., Valderrama-treviño, A. I., Contreras-flores, E. H., Barrera-mera, B., & Enríquez, M. H. (2017). Colorectal cancer : a review Review Article Colorectal cancer : a review. *International Journal of Research in Medical Sciences*, 5(October), 4667–4676.
8. Rawla, P., Sunkara, T., & Barsouk, A. (2019). Epidemiology of colorectal cancer: Incidence, mortality, survival, and risk factors. *Przegląd Gastroenterologiczny*, 14(2), 89–103. <https://doi.org/10.5114/pg.2018.81072>
9. Puppa, G., Sonzogni, A., Colombari, R., & Pelosi, G. (2010). TNM staging system of colorectal carcinoma: A critical appraisal of challenging issues. *Archives of Pathology and Laboratory Medicine*, 134(6), 837–852. <https://doi.org/10.5858/134.6.837>
10. Salem, N., Kamal, I., Al-Maghrabi, J., Abuzenadah, A., Peer-Zada, A. A., Qari, Y., Al-Ahwal, M., Al-Qahtani, M., & Buhmeida, A. (2016). High expression of matrix metalloproteinases: MMP-2 and MMP-9 predicts poor survival outcome in colorectal carcinoma. *Future Oncology*, 12(3), 323–331. <https://doi.org/10.2217/fon.15.325>
11. Said, A. H., Raufman, J. P., & Xie, G. (2014). The role of matrix metalloproteinases in colorectal cancer. *Cancers*, 6(1), 366–375. <https://doi.org/10.3390/cancers6010366>
12. Jögi, A., Vaapil, M., Johansson, M., & Pählman, S. (2012). Cancer cell differentiation heterogeneity and aggressive behavior in solid tumors. *Uppsala Journal of Medical Sciences*, 117(2), 217–224. <https://doi.org/10.3109/03009734.2012.659294>
13. Hanahan, D., & Weinberg, R. A. (2011). Hallmarks of cancer: The next generation. *Cell*, 144(5), 646–674. <https://doi.org/10.1016/j.cell.2011.02.013>

14. Hanahan, D., & Weinberg, R. A. (2000). The Hallmarks of Cancer. *Cell*, *100*(4), 57–70.
15. De Rosa, M., Pace, U., Rega, D., Costabile, V., Duraturo, F., Izzo, P., & Delrio, P. (2015). Genetics, diagnosis and management of colorectal cancer (Review). *Oncology Reports*, *34*(3), 1087–1096. <https://doi.org/10.3892/or.2015.4108>
16. Yamagishi, H., Kuroda, H., Imai, Y., & Hiraishi, H. (2016). Molecular pathogenesis of sporadic colorectal cancers. *Chinese Journal of Cancer*, *35*(1), 1–8. <https://doi.org/10.1186/s40880-015-0066-y>
17. Fearon, E. F., & Vogelstein, B. (1990). A genetic model for Colorectal Tumorigenesis. *Cell*, *61*, 759–767.
18. Tariq, K., & Ghias, K. (2016). Colorectal cancer carcinogenesis: a review of mechanisms. *Cancer Biology and Medicine*, *13*(1), 120–135. <https://doi.org/10.28092/j.issn.2095-3941.2015.0103>
19. Carethers, J. M., & Jung, B. H. (2015). Genetics and Genetic Biomarkers in Sporadic Colorectal Cancer. *Gastroenterology*, *149*(5), 1177–1190.e3. <https://doi.org/10.1053/j.gastro.2015.06.047>
20. Mundade, R., Imperiale, T. F., Prabhu, L., Loehrer, P. J., & Lu, T. (2014). Genetic pathways, prevention, and treatment of sporadic colorectal cancer. *Oncoscience*, *1*(6), 400–406. <https://doi.org/10.18632/oncoscience.59>
21. Armelao, F., & De Pretis, G. (2014). Familial colorectal cancer: A review. *World Journal of Gastroenterology*, *20*(28), 9292–9298. <https://doi.org/10.3748/wjg.v20.i28.9292>
22. Burt, R. (2007). Inheritance of colorectal cancer. *Drug Discovery Today: Disease Mechanisms*, *4*(4), 293–300. <https://doi.org/10.1016/j.ddmec.2008.05.004>
23. Axelrad, J. E., Lichtiger, S., & Yajnik, V. (2016). Inflammatory bowel disease and cancer: The role of inflammation, immunosuppression, and cancer treatment. *World Journal of Gastroenterology*, *22*(20), 4794–4801. <https://doi.org/10.3748/wjg.v22.i20.4794>
24. Dulai, P. S., Sandborn, W. J., & Gupta, S. (2016). Colorectal cancer and dysplasia in inflammatory bowel disease: A review of disease Epidemiology, Pathophysiology, and Management. *Cancer Prevention Research*, *9*(12), 887–894. <https://doi.org/10.1158/1940-6207.CAPR-16-0124>
25. Wang, Z.-H., & Fang, J.-Y. (2014). Colorectal Cancer in Inflammatory Bowel Disease: Epidemiology, Pathogenesis and Surveillance. *Gastrointestinal Tumors*, *1*(3), 146–154. <https://doi.org/10.1159/000365309>
26. Pedersen, N., Duricova, D., Elkjaer, M., Gamborg, M., Munkholm, P., & Jess, T. (2010). Risk of extra-intestinal cancer in inflammatory bowel disease: Meta-analysis of population-based cohort studies. *American Journal of Gastroenterology*, *105*(7), 1480–1487. <https://doi.org/10.1038/ajg.2009.760>
27. Herszenyi, L., Miheller, P., & Tulassay, Z. (2007). Carcinogenesis in inflammatory bowel disease. *Digestive Diseases*, *25*(3), 267–269. <https://doi.org/10.1159/000103898>
28. Herszenyi, L., Barabás, L., Miheller, P., & Tulassay, Z. (2014). Colorectal cancer in patients with inflammatory bowel disease: The true impact of the risk. *Digestive Diseases*, *33*(1), 52–57. <https://doi.org/10.1159/000368447>

29. Vogelstein, B., Papadopoulos, N., Velculescu, V. E., Zhou, S., Diaz, L. A., & Kinzler, K. W. (2013). Cancer genome landscapes. *Science*, *340*(6127), 1546–1558. <https://doi.org/10.1126/science.1235122>
30. Giussani, M., Triulzi, T., Sozzi, G., & Tagliabue, E. (2019). Tumor Extracellular Matrix Remodeling: New Perspectives as a Circulating Tool in the Diagnosis and Prognosis of Solid Tumors. *Cells*, *8*(2), 81. <https://doi.org/10.3390/cells8020081>
31. Peddareddigari, V. G., Wang, D., & Dubois, R. N. (2010). The tumor microenvironment in colorectal carcinogenesis. *Cancer Microenvironment*, *3*(1), 149–166. <https://doi.org/10.1007/s12307-010-0038-3>
32. Giraldo, N. A., Sanchez-Salas, R., Peske, J. D., Vano, Y., Becht, E., Petitprez, F., Validire, P., Ingels, A., Cathelineau, X., Fridman, W. H., & Sautès-Fridman, C. (2019). The clinical role of the TME in solid cancer. *British Journal of Cancer*, *120*(1), 45–53. <https://doi.org/10.1038/s41416-018-0327-z>
33. Murdoch, C., Muthana, M., Coffelt, S. B., & Lewis, C. E. (2008). The role of myeloid cells in the promotion of tumour angiogenesis. *Nature Reviews Cancer*, *8*(8), 618–631. <https://doi.org/10.1038/nrc2444>
34. Haabeth, O. A. W., Lorvik, K. B., Hammarström, C., Donaldson, I. M., Haraldsen, G., Bogen, B., & Corthay, A. (2011). Inflammation driven by tumour-specific Th1 cells protects against B-cell cancer. *Nature Communications*, *2*(1). <https://doi.org/10.1038/ncomms1239>
35. Pyonteck, S. M., Akkari, L., Schuhmacher, A. J., Bowman, R. L., Sevenich, L., Quail, D. F., Olson, O. C., Quick, M. L., Huse, J. T., Teijeiro, V., Setty, M., Leslie, C. S., Oei, Y., Pedraza, A., Zhang, J., Brennan, C. W., Sutton, J. C., Holland, E. C., Daniel, D., & Joyce, J. A. (2013). CSF-1R inhibition alters macrophage polarization and blocks glioma progression. *Nature Medicine*, *19*(10), 1264–1272. <https://doi.org/10.1038/nm.3337>
36. Hanahan, D., & Folkman, J. (1996). Patterns and emerging mechanisms of the angiogenic switch during tumorigenesis. *Cell*, *86*(3), 353–364. [https://doi.org/10.1016/S0092-8674\(00\)80108-7](https://doi.org/10.1016/S0092-8674(00)80108-7)
37. Kazerounian, S., Yee, K. O., & Lawler, J. (2008). Thrombospondins: From structure to therapeutics - Thrombospondins in cancer. *Cellular and Molecular Life Sciences*, *65*(5), 700–712. <https://doi.org/10.1007/s00018-007-7486-z>
38. Kanta, J. (2015). Collagen matrix as a tool in studying fibroblastic cell behavior. *Cell Adhesion and Migration*, *9*(4), 308–316. <https://doi.org/10.1080/19336918.2015.1005469>
39. Lu, P., Takai, K., Weaver, V. M., & Werb, Z. (2011). Extracellular Matrix degradation and remodeling in development and disease. *Cold Spring Harbor Perspectives in Biology*, *3*(12), 1–24. <https://doi.org/10.1101/cshperspect.a005058>
40. Jabłońska-Trypuć, A., Matejczyk, M., & Rosochacki, S. (2016). Matrix metalloproteinases (MMPs), the main extracellular matrix (ECM) enzymes in collagen degradation, as a target for anticancer drugs. *Journal of Enzyme Inhibition and Medicinal Chemistry*, *31*, 177–183. <https://doi.org/10.3109/14756366.2016.1161620>
41. Lu, P., Weaver, V. M., & Werb, Z. (2012). The extracellular matrix: A dynamic niche in cancer progression. *Journal of Cell Biology*, *196*(4), 395–406. <https://doi.org/10.1083/jcb.201102147>

42. Crotti, S., Piccoli, M., Rizzolio, F., Giordano, A., Nitti, D., & Agostini, M. (2017). Extracellular Matrix and Colorectal Cancer: How Surrounding Microenvironment Affects Cancer Cell Behavior? *Journal of Cellular Physiology*, 232(5), 967–975. <https://doi.org/10.1002/jcp.25658>
43. Trédan, O., Galmarini, C. M., Patel, K., & Tannock, I. F. (2007). Drug resistance and the solid tumor microenvironment. *Journal of the National Cancer Institute*, 99(19), 1441–1454. <https://doi.org/10.1093/jnci/djm135>
44. Krstic, J., & Santibanez, J. F. (2014). Transforming growth factor-beta and matrix metalloproteinases: Functional interactions in tumor stroma-infiltrating myeloid cells. *The Scientific World Journal*, 2014. <https://doi.org/10.1155/2014/521754>
45. Gilkes, D. M., Semenza, G. L., & Wirtz, D. (2014). Hypoxia and the extracellular matrix: Drivers of tumour metastasis. *Nature Reviews Cancer*, 14(6), 430–439. <https://doi.org/10.1038/nrc3726>
46. Panyathep, A., Chewonarin, T., Taneyhill, K., Vinitketkumnuen, U., & Surh, Y. J. (2013). Inhibitory Effects of Dried Longan (*Euphoria longana* Lam.) Seed Extract on Invasion and Matrix Metalloproteinases of Colon Cancer Cells. *Journal of Agricultural and Food Chemistry*, 61(15), 3631–3641. <https://doi.org/10.1021/jf3052863>
47. Herszényi, L., Hritz, I., Lakatos, G., Varga, M. Z., & Tulassay, Z. (2012). The Behavior of matrix metalloproteinases and their inhibitors in colorectal cancer. *International Journal of Molecular Sciences*, 13(10), 13240–13263. <https://doi.org/10.3390/ijms131013240>
48. Van Wart, H. E., & Birkedal-Hansen, H. (1990). The cysteine switch: A principle of regulation of metalloproteinase activity with potential applicability to the entire matrix metalloproteinase gene family. *Proceedings of the National Academy of Sciences of the United States of America*, 87(14), 5578–5582. <https://doi.org/10.1073/pnas.87.14.5578>
49. Gialeli, C., Theocharis, A. D., & Karamanos, N. K. (2011). Roles of matrix metalloproteinases in cancer progression and their pharmacological targeting. *FEBS Journal*, 278(1), 16–27. <https://doi.org/10.1111/j.1742-4658.2010.07919.x>
50. Mota, J. (2016). Deflamin bioactivities : a novel inhibitory protein of MMP-9 from lupinus albus (Master Thesis Dissertation) [Medical School–Faculdade de Ciências Médicas (NMS-FCM), Lisbon, Portugal, 2016]. In *Health Physics* (Vol. 80, Issue 4). <https://doi.org/10.1097/00004032-200104000-00006>
51. Szarvas, T., Vom Dorp, F., Ergün, S., & Rübber, H. (2011). Matrix metalloproteinases and their clinical relevance in urinary bladder cancer. *Nature Reviews Urology*, 8(5), 241–254. <https://doi.org/10.1038/nrurol.2011.44>
52. Kessenbrock, K., Plaks, V., & Werb, Z. (2010). Matrix Metalloproteinases: Regulators of the Tumor Microenvironment. *Cell*, 141(1), 52–67. <https://doi.org/10.1016/j.cell.2010.03.015>
53. Alvim, M. (2020). *Deflamin in Lupinus mutabilis (Master Thesis Dissertation)*. Instituto Superior de Agronomia, Universidade de Lisboa.
54. Baker, A. H., Edwards, D. R., & Murphy, G. (2002). Metalloproteinase inhibitors: Biological actions and therapeutic opportunities. *Journal of Cell Science*, 115(19), 3719–3727. <https://doi.org/10.1242/jcs.00063>
55. Zitka, O., Kukucka, J., Krizkova, S., Huska, D., Adam, V., Masarik, M., Prusa, R., & Kizek, R.

- (2010). Matrix Metalloproteinases. *Current Medicinal Chemistry*, 17(31), 3751–3768.
56. Quintero-Fabián, S., Arreola, R., Becerril-Villanueva, E., Torres-Romero, J. C., Arana-Argáez, V., Lara-Riegos, J., Ramírez-Camacho, M. A., & Alvarez-Sánchez, M. E. (2019). Role of Matrix Metalloproteinases in Angiogenesis and Cancer. *Frontiers in Oncology*, 9(December), 1–21. <https://doi.org/10.3389/fonc.2019.01370>
 57. Kryczka, J., Stasiak, M., Dzikis, L., Mik, M., Dziki, A., & Cierniewski, C. S. (2012). Matrix metalloproteinase-2 cleavage of the $\beta 1$ integrin ectodomain facilitates colon cancer cell motility. *Journal of Biological Chemistry*, 287(43), 36556–36566. <https://doi.org/10.1074/jbc.M112.384909>
 58. Mook, O. R. F., Frederiks, W. M., & Van Noorden, C. J. F. (2004). The role of gelatinases in colorectal cancer progression and metastasis. *Biochimica et Biophysica Acta - Reviews on Cancer*, 1705(2), 69–89. <https://doi.org/10.1016/j.bbcan.2004.09.006>
 59. Mota, J., Figueira, M. E., Ferreira, R. B., & Lima, A. (2021). An Up-Scalable and Cost-Effective Methodology for Isolating a Polypeptide Matrix Metalloproteinase-9 Inhibitor from *Lupinus albus* Seeds. *Foods*, 10(7), 1663. <https://doi.org/10.3390/foods10071663>
 60. Canete-Soler, R., Litzky, L., Lubensky, I., & Muschel, R. J. (1994). Localization of the 92 kd gelatinase mRNA in squamous cell and adenocarcinomas of the lung using in situ hybridization. *American Journal of Pathology*, 144(3), 518–527.
 61. Winer, A., Adams, S., & Mignatti, P. (2018). Matrix metalloproteinase inhibitors in cancer therapy: Turning past failures into future successes. *Molecular Cancer Therapeutics*, 17(6), 1147–1155. <https://doi.org/10.1158/1535-7163.MCT-17-0646>
 62. Fingleton, B. (2006). Matrix Metalloproteinases as Valid Clinical Target. *Current Pharmaceutical Design*, 13(3), 333–346. <https://doi.org/10.2174/138161207779313551>
 63. Basso, B. (2019). *In vitro and in vivo activities of an MMP-9 inhibitory protein isolated from Lupinus albus seeds against colon adenocarcinoma (Master Thesis Dissertation)*. Faculdade de Medicina de Lisboa, Universidade de Lisboa.
 64. Rasmussen, H. S., & McCann, P. P. (1997). Matrix metalloproteinase inhibition as a novel anticancer strategy: A review with special focus on Batimastat and Marimastat. *Pharmacology and Therapeutics*, 75(1), 69–75. [https://doi.org/10.1016/S0163-7258\(97\)00023-5](https://doi.org/10.1016/S0163-7258(97)00023-5)
 65. Rosenbaum, E., Zahurak, M., Sinibaldi, V., Carducci, M. A., Pili, R., Laufer, M., DeWeese, T. L., & Eisenberger, M. A. (2005). Marimastat in the treatment of patients with biochemically relapsed prostate cancer: A prospective randomized, double-blind, phase I/II trial. *Clinical Cancer Research*, 11(12), 4437–4443. <https://doi.org/10.1158/1078-0432.CCR-04-2252>
 66. Vandenbroucke, R. E., & Libert, C. (2014). Is there new hope for therapeutic matrix metalloproteinase inhibition? *Nature Reviews Drug Discovery*, 13(12), 904–927. <https://doi.org/10.1038/nrd4390>
 67. Lombard, M. A., Wallace, T. L., Kubicek, M. F., Petzold, G. L., Mitchell, M. A., Hendges, S. K., & Wilks, J. W. (1998). Synthetic Matrix Metalloproteinase Inhibitors and Tissue Inhibitor of Metalloproteinase (TIMP)-2, but not TIMP-1, Inhibit Shedding of Tumor Necrosis Factor- α Receptors in a Human Colon Adenocarcinoma (Colo 205) Cell Line. *Cancer Research*, 58(17), 4001 LP – 4007. <http://cancerres.aacrjournals.org/content/58/17/4001.abstract>

68. Peterson, J. T. (2004). Matrix metalloproteinase inhibitor development and the remodeling of drug discovery. *Heart Failure Reviews*, 9(1), 63–79. <https://doi.org/10.1023/B:HREV.0000011395.11179.af>
69. Levin, M., Udi, Y., Solomonov, I., & Sagi, I. (2017). Next generation matrix metalloproteinase inhibitors — Novel strategies bring new prospects. *Biochimica et Biophysica Acta - Molecular Cell Research*, 1864(11), 1927–1939. <https://doi.org/10.1016/j.bbamcr.2017.06.009>
70. Aune, D., De Stefani, E., Ronco, A., Boffetta, P., Deneo-Pellegrini, H., Acosta, G., & Mendilaharsu, M. (2009). Legume intake and the risk of cancer: A multisite case-control study in Uruguay. *Cancer Causes and Control*, 20(9), 1605–1615. <https://doi.org/10.1007/s10552-009-9406-z>
71. Wang, Y., Wang, Z., Fu, L., Chen, Y., & Fang, J. (2013). Legume Consumption and Colorectal Adenoma Risk: A Meta-Analysis of Observational Studies. *PLoS ONE*, 8(6), 6–12. <https://doi.org/10.1371/journal.pone.0067335>
72. Zhu, B., Sun, Y., Qi, L., Zhong, R., & Miao, X. (2015). Dietary legume consumption reduces risk of colorectal cancer: Evidence from a meta-analysis of cohort studies. *Scientific Reports*, 5, 27–33. <https://doi.org/10.1038/srep08797>
73. Tayyem, R. F., Bawadi, H. A., Shehadah, I., Agraib, L. M., Al-Awwad, N. J., Heath, D. D., & Bani-Hani, K. E. (2016). Consumption of Whole Grains, Refined Cereals, and Legumes and Its Association with Colorectal Cancer among Jordanians. *Integrative Cancer Therapies*, 15(3), 318–325. <https://doi.org/10.1177/1534735415620010>
74. Aranda-Olmedo, I., & Rubio, L. A. (2020). Dietary legumes, intestinal microbiota, inflammation and colorectal cancer. *Journal of Functional Foods*, 64(July 2019), 103707. <https://doi.org/10.1016/j.jff.2019.103707>
75. Xu, B., & Chang, S. K. C. (2012). Comparative study on antiproliferation properties and cellular antioxidant activities of commonly consumed food legumes against nine human cancer cell lines. *Food Chemistry*, 134(3), 1287–1296. <https://doi.org/10.1016/j.foodchem.2012.02.212>
76. Giovannucci, E. (2001). Insulin, insulin-like growth factors and colon cancer: A review of the evidence. *Journal of Nutrition*, 131(11 SUPPL.). <https://doi.org/10.1093/jn/131.11.3109s>
77. Yang, G., Shu, X. O., Li, H., Chow, W. H., Cai, H., Zhang, X., Gao, Y. T., & Zheng, W. (2009). Prospective cohort study of soy food intake and colorectal cancer risk in women. *American Journal of Clinical Nutrition*, 89(2), 577–583. <https://doi.org/10.3945/ajcn.2008.26742>
78. Clemente, A., & Del Carmen Arques, M. (2014). Bowman-Birk inhibitors from legumes as colorectal chemopreventive agents. *World Journal of Gastroenterology*, 20(30), 10305–10315. <https://doi.org/10.3748/wjg.v20.i30.10305>
79. Lima, A. I. G., Mota, J., Monteiro, S. A. V. S., & Ferreira, R. M. S. B. (2016). Legume seeds and colorectal cancer revisited: Protease inhibitors reduce MMP-9 activity and colon cancer cell migration. *Food Chemistry*, 197, 30–38. <https://doi.org/10.1016/j.foodchem.2015.10.063>
80. Papandreou, C., Becerra-Tomás, N., Bulló, M., Martínez-González, M. Á., Corella, D., Estruch, R., Ros, E., Arós, F., Schroder, H., Fitó, M., Serra-Majem, L., Lapetra, J., Fiol, M., Ruiz-Canela, M., Sorli, J. V., & Salas-Salvadó, J. (2019). Legume consumption and risk of all-cause, cardiovascular, and cancer mortality in the PREDIMED study. *Clinical Nutrition*, 38(1), 348–356. <https://doi.org/10.1016/j.clnu.2017.12.019>

81. Michels, K. B., Giovannucci, E., Chan, A. T., Singhania, R., Fuchs, C. S., & Willett, W. C. (2006). Fruit and vegetable consumption and colorectal adenomas in the nurses' health study. *Cancer Research*, 66(7), 3942–3953. <https://doi.org/10.1158/0008-5472.CAN-05-3637>
82. Lajolo, F. M., & Genovese, M. I. (2002). Nutritional significance of lectins and enzyme inhibitors from legumes. *Journal of Agricultural and Food Chemistry*, 50(22), 6592–6598. <https://doi.org/10.1021/jf020191k>
83. Karthik, L., Manohar, R., Elamparithi, K., & Gunasekaran, K. (2019). Purification, characterization and functional analysis of a serine protease inhibitor from the pulps of *Cicer arietinum* L. (Chick Pea). *Indian Journal of Biochemistry and Biophysics*, 56(2), 117–124.
84. Clemente, A., & Domoney, C. (2006). Biological Significance of Polymorphism in Legume Protease Inhibitors from the Bowman-Birk Family. *Current Protein & Peptide Science*, 7(3), 201–216. <https://doi.org/10.2174/138920306777452349>
85. Kouris-Blazos, A., & Belski, R. (2016). Health benefits of legumes and pulses with a focus on Australian sweet lupins. *Asia Pacific Journal of Clinical Nutrition*, 25(1), 1–17. <https://doi.org/10.6133/apjcn.2016.25.1.23>
86. Prusinski, J. (2017). White lupin (*Lupinus albus* L.) - Nutritional and health values in human nutrition - A review. *Czech Journal of Food Sciences*, 35(2), 95–105. <https://doi.org/10.17221/114/2016-CJFS>
87. La, V. D., Bergeron, C., Gafner, S., & Grenier, D. (2009). Grape Seed Extract Suppresses Lipopolysaccharide-Induced Matrix Metalloproteinase (MMP) Secretion by Macrophages and Inhibits Human MMP-1 and -9 Activities. *Journal of Periodontology*, 80(11), 1875–1882. <https://doi.org/10.1902/jop.2009.090251>
88. Spoerlein, C., Mahal, K., Schmidt, H., & Schobert, R. (2013). Effects of chrysin, apigenin, genistein and their homoleptic copper(II) complexes on the growth and metastatic potential of cancer cells. *Journal of Inorganic Biochemistry*, 127, 107–115. <https://doi.org/10.1016/j.jinorgbio.2013.07.038>
89. Bourguet, E., Hornebeck, W., Sapi, J., Jean-Paul, A., & Moroy, G. (2012). Pharmacomodulation of Broad Spectrum Matrix Metalloproteinase Inhibitors Towards Regulation of Gelatinases. *Enzyme Inhibition and Bioapplications*. <https://doi.org/10.5772/35412>
90. Ndinguri, M. W., Bhowmick, M., Tokmina-Roszyk, D., Robichaud, T. K., & Fields, G. B. (2012). Peptide-based selective inhibitors of matrix metalloproteinase-mediated activities. *Molecules*, 17(12), 14230–14248. <https://doi.org/10.3390/molecules171214230>
91. Breslin, S., & O'Driscoll, L. (2013). Three-dimensional cell culture: The missing link in drug discovery. *Drug Discovery Today*, 18(5–6), 240–249. <https://doi.org/10.1016/j.drudis.2012.10.003>
92. Anton, D., Burckel, H., Josset, E., & Noel, G. (2015). Three-dimensional cell culture: A breakthrough in vivo. *International Journal of Molecular Sciences*, 16(3), 5517–5527. <https://doi.org/10.3390/ijms16035517>
93. Costa, E. C., Moreira, A. F., de Melo-Diogo, D., Gaspar, V. M., Carvalho, M. P., & Correia, I. J. (2016). 3D tumor spheroids: an overview on the tools and techniques used for their analysis. *Biotechnology Advances*, 34(8), 1427–1441. <https://doi.org/10.1016/j.biotechadv.2016.11.002>

94. Stadler, M., Scherzer, M., Walter, S., Holzner, S., Pudenko, K., Riedl, A., Unger, C., Kramer, N., Weil, B., Neesen, J., Hengstschläger, M., & Dolznig, H. (2018). Exclusion from spheroid formation identifies loss of essential cell-cell adhesion molecules in colon cancer cells. *Scientific Reports*, 8(1), 1–16. <https://doi.org/10.1038/s41598-018-19384-0>
95. Mehta, G., Hsiao, A. Y., Ingram, M., Luker, G. D., & Takayama, S. (2012). Opportunities and challenges for use of tumor spheroids as models to test drug delivery and efficacy. *Journal of Controlled Release*, 164(2), 192–204. <https://doi.org/10.1016/j.jconrel.2012.04.045>
96. Haycock, J. W. (n.d.). *Chapter 1 and Techniques*. 695, 1–15. <https://doi.org/10.1007/978-1-60761-984-0>
97. Hill, D., Chen, L., Snaar-Jagalska, E., & Chaudhry, B. (2018). Embryonic zebrafish xenograft assay of human cancer metastasis. *F1000Research*, 7. <https://doi.org/10.12688/f1000research.16659.2>
98. Costa, B., Estrada, M. F., Mendes, R. V., & Fior, R. (2020). Zebrafish Avatars towards Personalized Medicine-A Comparative Review between Avatar Models. *Cells*, 9(2). <https://doi.org/10.3390/cells9020293>
99. Burstein, H. J., Mangu, P. B., Somerfield, M. R., Schrag, D., Samson, D., Holt, L., Zelman, D., & Ajani, J. A. (2011). American Society of Clinical Oncology clinical practice guideline update on the Use of chemotherapy sensitivity and resistance assays. *Journal of Clinical Oncology*, 29(24), 3328–3330. <https://doi.org/10.1200/JCO.2011.36.0354>
100. Hason, M., & Bartůněk, P. (2019). Zebrafish models of cancer-new insights on modeling human cancer in a non-mammalian vertebrate. *Genes*, 10(11), 1–30. <https://doi.org/10.3390/genes10110935>
101. Gomez-Cuadrado, L., Tracey, N., Ma, R., Qian, B., & Brunton, V. G. (2017). Mouse models of metastasis: Progress and prospects. *DMM Disease Models and Mechanisms*, 10(9), 1061–1074. <https://doi.org/10.1242/dmm.030403>
102. Lieschke, G. J., & Currie, P. D. (2007). Animal models of human disease: Zebrafish swim into view. *Nature Reviews Genetics*, 8(5), 353–367. <https://doi.org/10.1038/nrg2091>
103. Fior, R., Póvoa, V., Mendes, R. V., Carvalho, T., Gomes, A., Figueiredo, N., & Ferreira, F. R. (2017). Single-cell functional and chemosensitive profiling of combinatorial colorectal therapy in zebrafish xenografts. *Proceedings of the National Academy of Sciences of the United States of America*, 114(39), E8234–E8243. <https://doi.org/10.1073/pnas.1618389114>
104. Zhao, C., Wang, X., Zhao, Y., Li, Z., Lin, S., Wei, Y., & Yang, H. (2011). A novel xenograft model in zebrafish for high-resolution investigating dynamics of neovascularization in tumors. *PLoS ONE*, 6(7), 1–9. <https://doi.org/10.1371/journal.pone.0021768>
105. Howe, K., Clark, M. D., Torroja, C. F., Torrance, J., Berthelot, C., Muffato, M., Collins, J. E., Humphray, S., McLaren, K., Matthews, L., McLaren, S., Sealy, I., Caccamo, M., Churcher, C., Scott, C., Barrett, J. C., Koch, R., Rauch, G. J., White, S., ... Stemple, D. L. (2013). The zebrafish reference genome sequence and its relationship to the human genome. *Nature*, 496(7446), 498–503. <https://doi.org/10.1038/nature12111>
106. Veinotte, C. J., Dellaire, G., & Berman, J. N. (2014). Hooking the big one: The potential of zebrafish xenotransplantation to reform cancer drug screening in the genomic era. *DMM Disease Models and Mechanisms*, 7(7), 745–754. <https://doi.org/10.1242/dmm.015784>

107. Kirchberger, S., Sturtzel, C., Pascoal, S., & Distel, M. (2017). Quo natus, Danio?—Recent Progress in Modeling Cancer in Zebrafish. *Frontiers in Oncology*, 7(AUG). <https://doi.org/10.3389/fonc.2017.00186>
108. Nguyen-Chi, M., Laplace-Builhe, B., Travnickova, J., Luz-Crawford, P., Tejedor, G., Phan, Q. T., Duroux-Richard, I., Levraud, J. P., Kissa, K., Lutfalla, G., Jorgensen, C., & Djouad, F. (2015). Identification of polarized macrophage subsets in zebrafish. *ELife*, 4(JULY 2015), 1–14. <https://doi.org/10.7554/eLife.07288>
109. Lawson, N. D., & Weinstein, B. M. (2002). In vivo imaging of embryonic vascular development using transgenic zebrafish. *Developmental Biology*, 248(2), 307–318. <https://doi.org/10.1006/dbio.2002.0711>
110. Brown, H. K., Schiavone, K., Tazzyman, S., Heymann, D., & Chico, T. J. A. (2017). Zebrafish xenograft models of cancer and metastasis for drug discovery. *Expert Opinion on Drug Discovery*, 12(4), 379–389. <https://doi.org/10.1080/17460441.2017.1297416>
111. Rebelo de Almeida, C., Mendes, R. V., Pezzarossa, A., Gago, J., Carvalho, C., Alves, A., Nunes, V., Brito, M. J., Cardoso, M. J., Ribeiro, J., Cardoso, F., Ferreira, M. G., & Fior, R. (2020). Zebrafish xenografts as a fast screening platform for bevacizumab cancer therapy. *Communications Biology*, 3(1). <https://doi.org/10.1038/s42003-020-1015-0>
112. Letrado, P., De Miguel, I., Lamberto, I., Díez-Martínez, R., & Oyarzabal, J. (2018). Zebrafish: Speeding up the cancer drug discovery process. *Cancer Research*, 78(21), 6048–6058. <https://doi.org/10.1158/0008-5472.CAN-18-1029>
113. 3Helix. (2021). 3Helix_CHP_User_Guide. In *Main* (Vol. 900200, Issue 90).
114. Mahmood, T., & Yang, P. C. (2012). Western blot: Technique, theory, and trouble shooting. *North American Journal of Medical Sciences*, 4(9), 429–434. <https://doi.org/10.4103/1947-2714.100998>
115. Ernst, O., & Zor, T. (2010). Linearization of the Bradford protein assay. *Journal of Visualized Experiments*, 38, 1–6. <https://doi.org/10.3791/1918>
116. Promega Corporation. (2018). Apo-ONE® Homogeneous Caspase-3/7 Assay. *Promega*, 1–15.
117. O'Brien, J., Wilson, I., Orton, T., & Pognan, F. (2000). Investigation of the Alamar Blue (resazurin) fluorescent dye for the assessment of mammalian cell cytotoxicity. *European Journal of Biochemistry*, 267(17), 5421–5426. <https://doi.org/10.1046/j.1432-1327.2000.01606.x>
118. ThermoFisher Scientific. (n.d.). *AlamarBlue Assays for Cell Viability*. https://www.thermofisher.com/pt/en/home/life-science/cell-analysis/fluorescence-microplate-assays/microplate-assays-cell-viability/alamarblue-assay-cell-viability.html?ef_id=CjwKCAjw_tWRBhAwEiwALxFPobuAF483Jsqc8GGdiOvuH2I8lki4KytDCGt_6uKvMMtokRTjT0H_fBoCz
119. Elegheert, J., Behiels, E., Bishop, B., Scott, S., Woolley, R. E., Griffiths, S. C., Byrne, E. F. X., Chang, V. T., Stuart, D. I., Jones, E. Y., Siebold, C., & Aricescu, A. R. (2018). Lentiviral transduction of mammalian cells for fast, scalable and high-level production of soluble and membrane proteins. *Nature Protocols*, 13(12), 2991–3017. <https://doi.org/10.1038/s41596-018-0075-9>
120. Lee, C. S., Ryan, E. J., & Doherty, G. A. (2014). Gastro-intestinal toxicity of chemotherapeutics in

- colorectal cancer: The role of inflammation. *World Journal of Gastroenterology*, 20(14), 3751–3761. <https://doi.org/10.3748/wjg.v20.i14.3751>
121. Ribatti, D., Tamma, R., & Annese, T. (2020). Epithelial-Mesenchymal Transition in Cancer: A Historical Overview. *Translational Oncology*, 13(6), 100773. <https://doi.org/10.1016/j.tranon.2020.100773>
 122. Nitulescu, G. M., Van De Venter, M., Nitulescu, G., Ungurianu, A., Juzenas, P., Peng, Q., Olaru, O. T., Grădinaru, D., Tsatsakis, A., Tsoukalas, D., Spandidos, D. A., & Margina, D. (2018). The Akt pathway in oncology therapy and beyond (Review). *International Journal of Oncology*, 53(6), 2319–2331. <https://doi.org/10.3892/ijo.2018.4597>
 123. Guo, Y., Pan, W., Liu, S., Shen, Z., Xu, Y., & Hu, L. (2020). ERK/MAPK signalling pathway and tumorigenesis (Review). *Experimental and Therapeutic Medicine*, 1997–2007. <https://doi.org/10.3892/etm.2020.8454>
 124. Breslin, S., & O’Driscoll, L. (2013). Three-dimensional cell culture: The missing link in drug discovery. *Drug Discovery Today*, 18(5–6), 240–249. <https://doi.org/10.1016/j.drudis.2012.10.003>
 125. Huang, H. (2018). Matrix metalloproteinase-9 (MMP-9) as a cancer biomarker and MMP-9 biosensors: Recent advances. *Sensors (Switzerland)*, 18(10), 5–7. <https://doi.org/10.3390/s18103249>
 126. Dios-Figueroa, G. T., Aguilera-Marquez, J. D. R., Camacho-Villegas, T. A., & Lugo-Fabres, P. H. (2021). 3d cell culture models in covid-19 times: A review of 3d technologies to understand and accelerate therapeutic drug discovery. *Biomedicines*, 9(6). <https://doi.org/10.3390/biomedicines9060602>
 127. Tevis, K. M., Colson, Y. L., & Grinstaff, M. W. (2017). Embedded Spheroids as Models of the Cancer Microenvironment. *Advanced Biosystems*, 1(10). <https://doi.org/10.1002/adbi.201700083>
 128. Brown, H. K., Schiavone, K., Tazzyman, S., Heymann, D., & Chico, T. J. A. (2017). Zebrafish xenograft models of cancer and metastasis for drug discovery. *Expert Opinion on Drug Discovery*, 12(4), 379–389. <https://doi.org/10.1080/17460441.2017.1297416>
 129. Baeriswyl, V., & Christofori, G. (2009). The angiogenic switch in carcinogenesis. *Seminars in Cancer Biology*, 19(5), 329–337. <https://doi.org/10.1016/j.semcancer.2009.05.003>
 130. Battaglin, F., Puccini, A., Intini, R., Schirripa, M., Ferro, A., Bergamo, F., Lonardi, S., Zagonel, V., Lenz, H. J., & Loupakis, F. (2018). The role of tumor angiogenesis as a therapeutic target in colorectal cancer. *Expert Review of Anticancer Therapy*, 18(3), 251–266. <https://doi.org/10.1080/14737140.2018.1428092>
 131. Sudhakar, A., & Kalluri, R. (2010). Molecular mechanisms of angiostasis. *Encyclopedia of the Eye*, 52–59. <https://doi.org/10.1016/B978-0-12-374203-2.00128-7>
 132. Tanjore, H., & Kalluri, R. (2006). The role of type IV collagen and basement membranes in cancer progression and metastasis. *American Journal of Pathology*, 168(3), 715–717. <https://doi.org/10.2353/ajpath.2006.051321>
 133. *BioRenderApp*. (n.d.). <https://app.biorender.com/>

134. Winkler, J., Abisoye-Ogunniyan, A., Metcalf, K. J., & Werb, Z. (2020). Concepts of extracellular matrix remodelling in tumour progression and metastasis. *Nature Communications*, *11*(1), 1–19. <https://doi.org/10.1038/s41467-020-18794-x>
135. Benjamin, M. M., & Khalil, R. A. (2012). Matrix metalloproteinase inhibitors as investigative tools in the pathogenesis and management of vascular disease. In *Exs* (Vol. 103). https://doi.org/10.1007/978-3-0348-0364-9_7
136. Ortiz-Martinez, M., Winkler, R., & García-Lara, S. (2014). Preventive and therapeutic potential of peptides from cereals against cancer. *Journal of Proteomics*, *111*, 165–183. <https://doi.org/10.1016/j.jprot.2014.03.044>

